P-06-245

Oskarshamn site investigation

Difference flow logging of borehole KLX13A

Subarea Laxemar

Juha Väisäsvaara, Janne Pekkanen
PRG-Tec Oy

June 2007

Svensk Kärnbränslehantering AB
Swedish Nuclear Fuel
and Waste Management Co
Box 5864
SE-102 40 Stockholm Sweden
Tel 08-459 84 00
+46 8 459 84 00
Fax 08-661 57 19
+46 8 661 57 19

ISSN 1651-4416
SKB P-06-245

Oskarshamn site investigation

Difference flow logging of borehole KLX13A

Subarea Laxemar

Juha Väisäsvaara, Janne Pekkanen
PRG-Tec Oy

June 2007

Keywords: Laxemar, Hydrogeology, Hydraulic tests, Difference flow measurements, Flow logging, Pumping test, Transmissivity.

Abstract

Difference flow logging is a swift method for the determination of the transmissivity and the hydraulic head in borehole sections and fractures/fracture zones in core drilled boreholes. This report presents the main principles of the methods as well as the results of the measurements carried out in borehole KLX13A at Oskarshamn, Sweden, in September and October 2006, using Posiva Flow Log. Posiva Flow Log is a multipurpose measurement instrument developed by PRG-Tec Oy for the use of Posiva Oy. The primary aim of the measurements was to determine the position and flow rate of flow yielding fractures in borehole KLX13A.

The first flow logging measurements were done with a 5 m test section by moving the measurement tool in 0.5 m steps. This method was used to flow log the entire measurable part of the borehole during natural (un-pumped) as well as pumped conditions. The flow measurements were repeated at the location of detected flow anomalies using a 1 m long test section, which was moved in 0.1 m steps.

Length calibration was made based on length marks milled into the borehole wall at accurately determined positions along the borehole. The length marks were detected by caliper and single-point resistance measurements using sensors connected to the flow logging tool.

A high-resolution absolute pressure sensor was used to measure the total pressure along the borehole. These measurements were carried out together with the flow measurements.

The electric conductivity (EC) and temperature of borehole water were also measured. The EC measurements were used to study the occurrence of saline water in the borehole during natural as well as pumped conditions. The EC of fracture-specific water was also measured (0.5 m test section) for a selection of fractures.

The recovery of the groundwater level in the borehole was measured after the pumping of the borehole was stopped.

Sammanfattning

Differensflödesloggning är en snabb metod för bestämning av transmissivitet och hydraulisk tryckhöjd i borrhålssektioner och sprickor/sprickzoner i kärnborrhål. Denna rapport presenterar huvudprinciperna för metoden och resultat av mätningar utförda i borrhål KLX13A i Oskarshamn, Sverige, i september och oktober 2006 med Posiva flödesloggningsmetod. Det primära syftet med mätningarna var att bestämma läget och flödet för vattenförande sprickor i borrhål KLX13A.

Flödet till eller från en 5 m lång testsektion (som förflyttades successivt med 0,5 m) mättes i borrhål KLX13A under såväl naturliga (icke-pumpade) som pumpade förhållanden. Flödesmätningarna upprepades vid lägena för de detekterade flödesanomalierna med en 1 m lång testsektion som förflyttades successivt med 0,1 m.

Längdkalibrering gjordes baserad på längdmärkena som frästs in i borrhålsväggen vid noggrant bestämda positioner längs borrhålet. Längdmärkena detekterades med caliper-mätningar och med punktresistansmätningar med hjälp av sensorer anslutna på flödesloggningssonden.

En högupplösande absoluttryckgivare användes för att mäta det absoluta totala trycket längs borrhålet. Dessa mätningar utfördes tillsammans med flödesmätningarna.

Elektrisk konduktivitet och temperatur på borrhålsvattnet mättes också. EC-mätningarna användes för att studera förekomsten av saltvatten i borrhålet under såväl naturliga som pumpade förhållanden. Sprickspecifikt (0,5 m lång testsektion) EC mättes även vid utvalda sprickor.

Återhämtningen av grundvattennivån mättes efter att pumpningen i hålet avslutades.

Contents

1 Introduction

This document reports the results acquired by flow logging the borehole KLX13A at Oskarshamn, Sweden. The work was carried out in accordance with Activity Plan AP PS 400-06-080. The controlling documents for performing according to this activity plan are listed in Table 1-1. The list of the controlling documents excludes the assignment-specific quality plans. Both the Activity Plan and the method descriptions are SKB's internal controlling documents.

The difference flow logging in the core drilled borehole KLX13A at Oskarshamn was conducted between September 21 and October 1, 2006. KLX13A is 595.85 m long and its inclination at the ground level is 82.25° from the horizontal plane. The borehole was drilled using a telescopic drilling technique, where the c. 0–100 m interval was percussion drilled and the remaining part was core drilled. The 0 m–11.75 m interval of the percussion drilled section was cased with cement. The inner diameter of the casing and the percussion drilled section is approximately 200 mm. The diameter of the core drilled section is 76 mm. There is a conical steel guide at 96.11 m–101.21 m. The values given above are values on the axis parallel to the borehole. We call this the borehole length axis.

The location of KLX13A in the subarea of Laxemar in Oskarshamn is illustrated in Figure 1-1.

The field work and the subsequent data interpretation were conducted by PRG-Tec Oy as Posiva Oy's subcontractor. The Posiva Flow Log/Difference Flow Method has previously been employed in Posiva's site characterisation programme in Finland as well as at the Äspö Hard Rock Laboratory at Simpevarp, Sweden.

Table 1-1. SKB's internal controlling documents for the activities concerning this report.

Activity plan	**Number**	**Version**
Difference flow logging in borehole KLX13A	AP PS 400-06-080	1.0
Method descriptions	**Number**	**Version**
Method description for difference flow logging	SKB MD 322.010	1.0
Instruktion för rengöring av borrhålsutrustning och viss markbaserad utrustning	SKB MD 600.004	1.0
Instruktion för längdkalibrering vid undersökningar i kärnborrhål	SKB MD 620.010	2.0
Instruktion för analys av injektions- och enhålspumptester	SKB MD 320.004	1.0

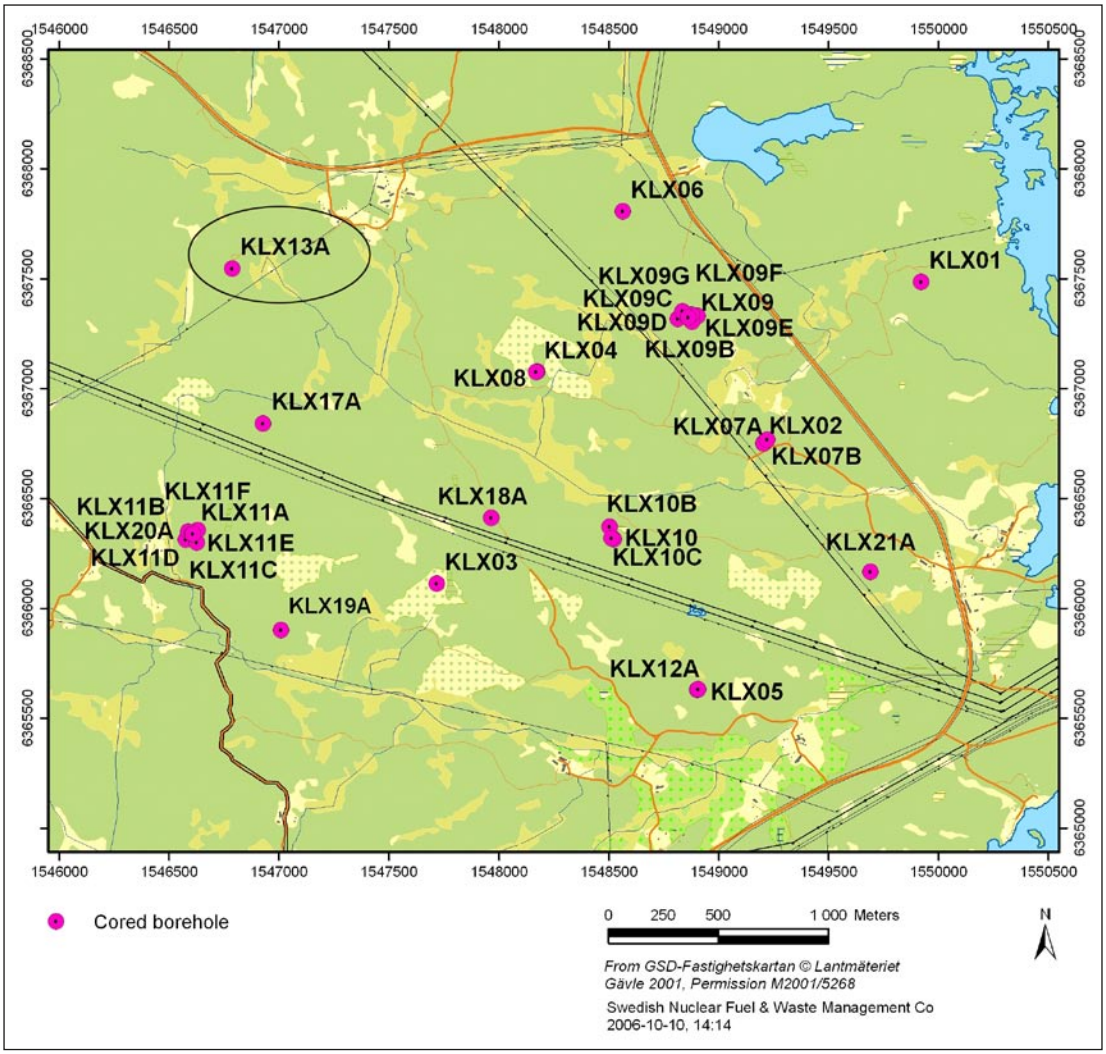

Figure 1-1. *Site map showing the location of borehole KLX13A situated in the subarea of Laxemar.*

2 Objective and scope

The main objective of the difference flow logging in KLX13A was to identify water-conductive sections/fractures. Secondly, the measurements aimed at a hydrogeological characterisation, which includes the inspection of the prevailing water flow balance in the borehole and the hydraulic properties (transmissivity and undisturbed hydraulic head) of the tested sections. Based on the results of these investigations, a more detailed characterisation of flow anomalies along the borehole, e.g. an estimate of the conductive fracture frequency (CFF), may be obtained.

Besides difference flow logging, the measurement programme also included supporting measurements, performed in order to gain a better understanding of the overall hydrogeochemical conditions. The data gathered in these measurements consisted of the single-point resistance of the borehole wall and the electric conductivity of the borehole water. The electric conductivity of a number of selected high-transmissive fractures in the borehole was also measured. Furthermore, the recovery of the groundwater level after pumping was registered and interpreted hydraulically.

A high-resolution absolute pressure sensor was used to measure the total pressure along the borehole. These measurements were carried out together with the flow measurements. The results are used in the calculation of the hydraulic head along the borehole.

Single-point resistance measurements were also combined with caliper (borehole diameter) measurements to detect depth marks milled into the borehole wall at accurately determined positions. This procedure allowed for the length calibration of the other measurements that were conducted.

3 Principles of measurement and interpretation

3.1 Measurements

Unlike traditional types of borehole flowmeters, the Difference Flowmeter measures the flow rate into or out of limited sections of the borehole instead of measuring the total cumulative flow rate along the borehole. The advantage of measuring the flow rate in isolated sections is a better detection of the incremental changes of flow along the borehole, which are generally very small and can easily be missed using traditional types of flowmeters.

Rubber discs at both ends of the downhole tool are used to isolate the flow rate in the test section from the flow rate in the rest of the borehole, see Figure 3-1. The flow inside the test section goes through its own tube and passes through the area where the flow sensors are located. The flow along the borehole outside the isolated test section passes through the test section by means of a bypass pipe and is discharged at the upper end of the downhole tool. This entire structure is called the flow guide.

The Difference Flowmeter can be used in two modes, a sequential mode and an overlapping mode. In the sequential mode, the measurement increment is as long as the section length. It is used for determining the transmissivity and the hydraulic head /Öhberg and Rouhiainen 2000/. In the overlapping mode, the measurement increment is shorter than the section length. It is mostly used to determine the location of hydraulically conductive fractures and to classify them with regards to their flow rates.

The Difference Flowmeter measures the flow rate into or out of the test section by means of thermistors, which track both the dilution (cooling) of a thermal pulse and the transfer of a thermal pulse with moving water. In the sequential mode, both methods are used, whereas in the overlapping mode, only the thermal dilution method is used because it is faster than thermal pulse method.

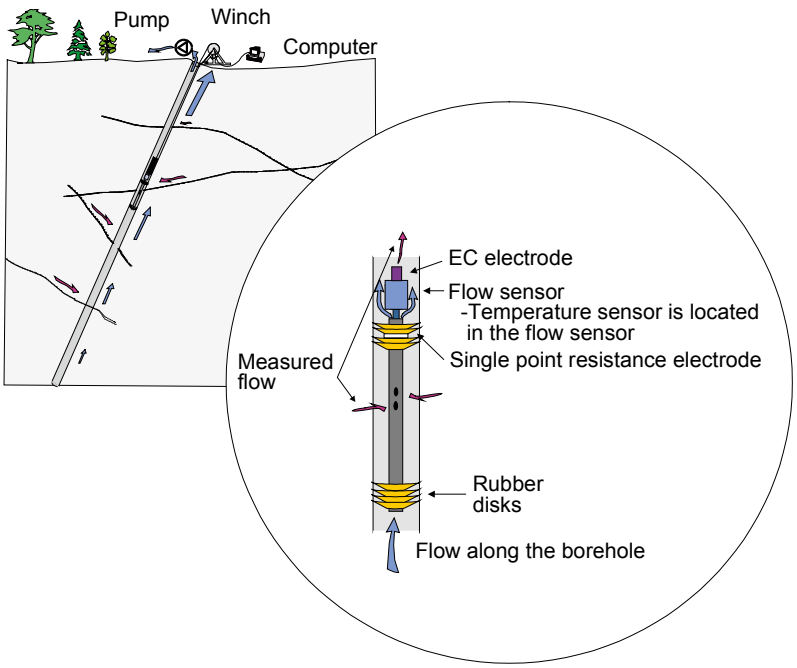

Figure 3-1. *Schematic of the downhole equipment used in the Difference Flowmeter.*

Besides incremental changes of flow, the downhole tool of the Difference Flowmeter can also be used to measure:

- The electric conductivity (EC) of the borehole water and fracture-specific water. The electrode for the EC measurements is located on the top of the flow sensor, Figure 3-1.
- The single-point resistance (SPR) of the borehole wall (grounding resistance). The electrode of the Single-point resistance tool is located in between the uppermost rubber discs, see Figure 3-1. This method is used for high-resolution depth/length determination of fractures and geological structures.
- The diameter of the borehole (caliper). The caliper tool, combined with SPR, is used for the detection of the depth/length marks milled into the borehole wall. This enables an accurate depth/length calibration of the flow measurements.
- The prevailing water pressure profile in the borehole. The pressure sensor is located inside the electronics tube and connected through a tube to the borehole water, Figure 3-2.
- Temperature of the borehole water. The temperature sensor is placed in the flow sensor, Figure 3-1.

All of the above measurements were performed in KLX13A.

The principles of difference flow measurements are described in Figures 3-3 and 3-4. The flow sensor consists of three thermistors, see Figure 3-3a. The central thermistor, A, is used both as a heating element and for the registration of temperature changes, Figures 3-3b and c. The side thermistors, B1 and B2, serve to detect the moving thermal pulse, Figure 3-3d, caused by the constant power heating in A, Figure 3-3b.

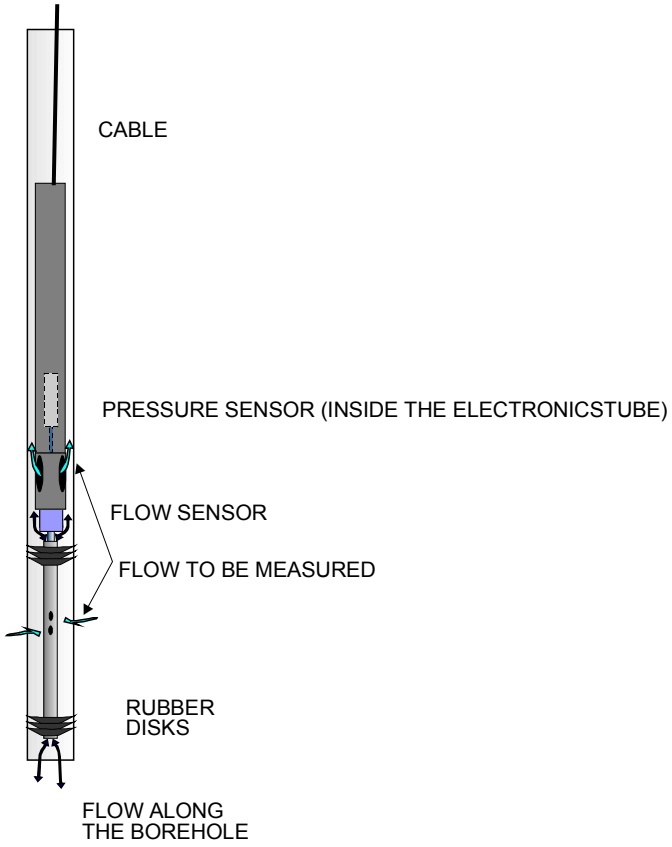

Figure 3-2. *The absolute pressure sensor is located inside the electronics tube and connected through a tube to the borehole water.*

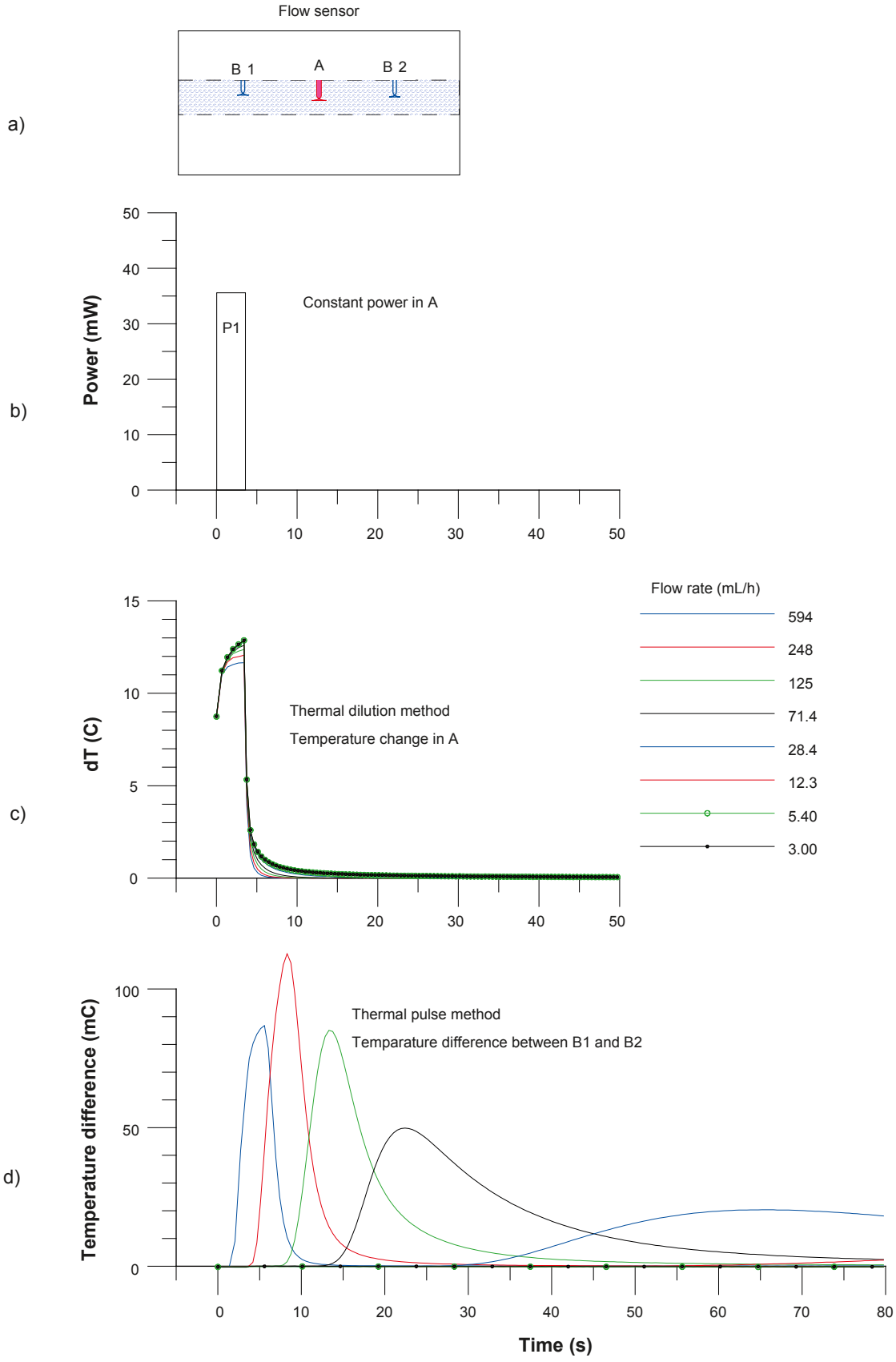

Figure 3-3. *Flow measurement, flow rate < 600 mL/h.*

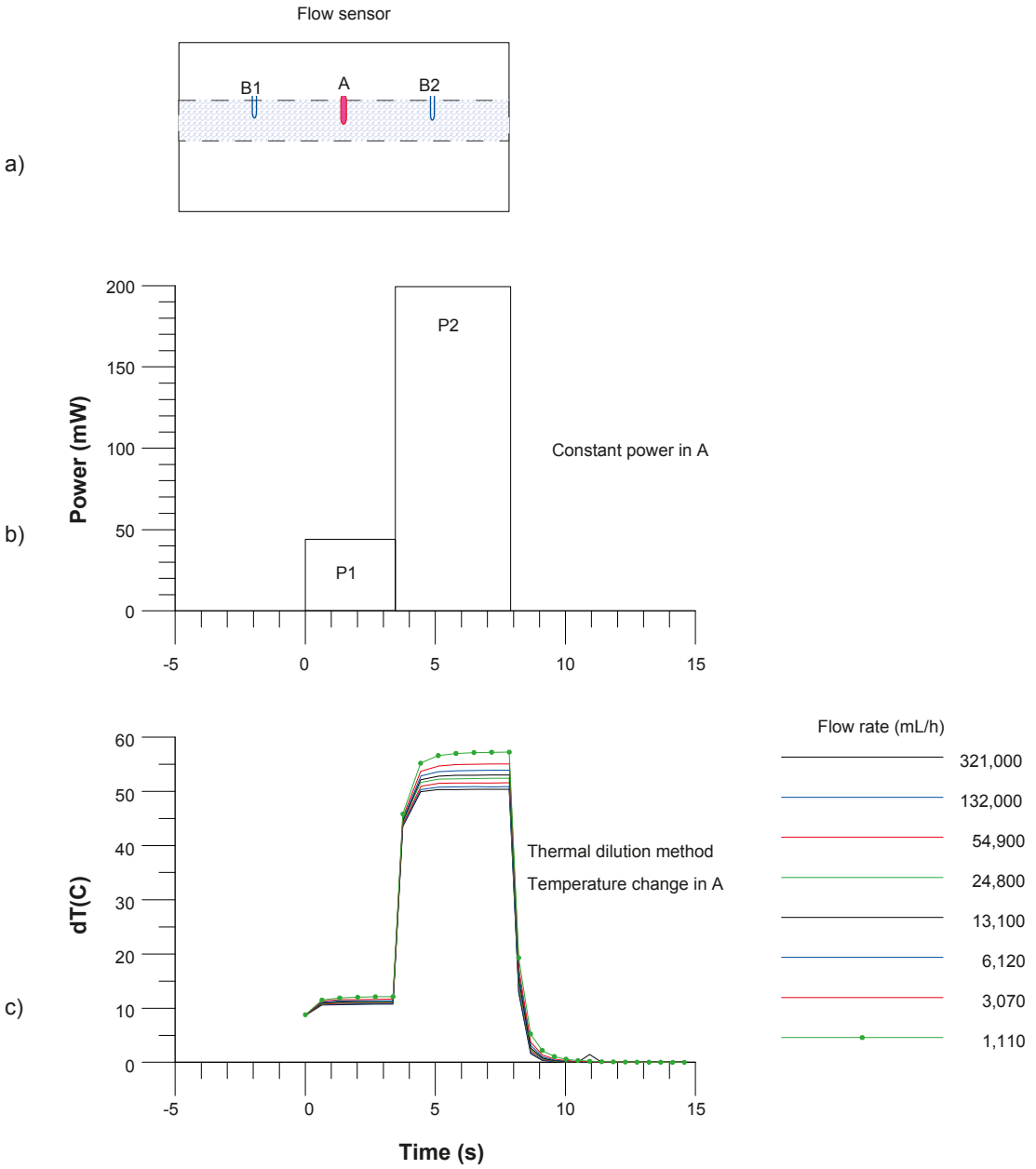

Figure 3-4. *Flow measurement, flow rate > 600 mL/h.*

Flow rate is measured during the constant power (P_1) heating (Figure 3-3b). If the flow rate exceeds 600 mL/h, the constant power heating is increased (to P_2), Figure 3-4b, and the thermal dilution method is applied.

If the flow rate during the constant power heating (Figure 3-3b) falls below 600 mL/h, the measurement continues by monitoring transient thermal dilution (Figure 3-3c) and thermal pulse response (Figure 3-3d). When applying the thermal pulse method, thermal dilution is also measured. The same heat pulse is used for both methods.

The flow is measured when the tool is at rest. After the tool is transferred to a new position, there is a waiting time (the duration of which can be adjusted according to the prevailing circumstances) before the heat pulse (Figure 3-3b) is applied. The waiting time after the constant power thermal pulse can also be adjusted, but it is normally 10 s for thermal dilution and 300 s for the thermal pulse method. The measurement range of each method is given in Table 3-1.

Table 3-1. Ranges of flow measurement.

Method	Range of measurement (mL/h)
Thermal dilution P1	30–6,000
Thermal dilution P2	600–300,000
Thermal pulse	6–600

The lower end limits of the thermal dilution and the thermal pulse methods in Table 3-1 are theoretical lowest measurable values. Depending on the borehole conditions these limits may not always prevail. Examples of disturbing conditions are suspended drilling debris in the borehole water, gas bubbles in the water and high flow rates (above about 30 L/min) along the borehole. If the disturbing conditions are significant, a practical measurement limit is calculated for each set of data.

3.2 Interpretation

The interpretation of data is based on Thiem's or Dupuit's formula that describes a steady state and two dimensional radial flow into the borehole /Marsily, 1986/:

$$h_s - h = Q/(T \cdot a) \qquad 3\text{-}1$$

where

h is the hydraulic head in the vicinity of the borehole and h_s at the radius of influence (R),

Q is the flow rate into the borehole,

T is the transmissivity of the test section,

a is a constant depending on the assumed flow geometry.

For cylindrical flow, the constant a is:

$$a = 2 \cdot \pi / \ln(R/r_0) \qquad 3\text{-}2$$

where

r_0 is the radius of the well and

R is the radius of influence, i.e. the zone inside which the effect of the pumping is felt.

If flow rate measurements are carried out using two levels of hydraulic head in the borehole, i.e. natural or pump-induced hydraulic heads, then the undisturbed (natural) hydraulic head and transmissivity of the tested borehole sections can be calculated. Two equations can be written directly from equation 3-1:

$$Q_{s0} = T_s \cdot a \cdot (h_s - h_0) \qquad 3\text{-}3$$

$$Q_{s1} = T_s \cdot a \cdot (h_s - h_1) \qquad 3\text{-}4$$

where

h_0 and h_1 are the hydraulic heads in the borehole at the test level,

Q_{s0} and Q_{s1} are the measured flow rates in the test section,

T_s is the transmissivity of the test section and

h_s is the undisturbed hydraulic head of the tested zone far from the borehole.

Since, in general, very little is known about the flow geometry, cylindrical flow without any skin zones is assumed. Cylindrical flow geometry is also justified because the borehole is at a constant head and there are no strong pressure gradients along the borehole, except at its ends.

The radial distance R to the undisturbed hydraulic head h_s is not known and must be assumed. Here a value of 500 is selected for the quotient R/r_0.

The hydraulic head and the test section transmissivity can be deduced from the two measurements:

$$h_s = (h_0 - b \cdot h_1)/(1 - b) \quad 3\text{-}5$$

$$T_s = (1/a)\,(Q_{s0} - Q_{s1})/(h_1 - h_0) \quad 3\text{-}6$$

where

$b = Q_{s0}/Q_{s1}$

Transmissivity (T_f) and the hydraulic head (h_f) of individual fractures can be calculated provided that the flow rates of individual fractures are known. Similar assumptions as above have to be used (a steady state cylindrical flow regime without skin zones).

$$h_f = (h_0 - b \cdot h_1)/(1 - b) \quad 3\text{-}7$$

$$T_f = (1/a)\,(Q_{f0} - Q_{f1})/(h_1 - h_0) \quad 3\text{-}8$$

where
Q_{f0} and Q_{f1} are the flow rates at a fracture and
h_f and T_f are the hydraulic head (far away from borehole) and the transmissivity of a fracture, respectively.

Since the actual flow geometry and the skin effects are unknown, transmissivity values should be considered only as an indication of the orders of magnitude. As the calculated hydraulic heads do not depend on geometrical properties but only on the ratio of the flows measured at different heads in the borehole, they should be less sensitive to unknown fracture geometries. A discussion of potential uncertainties in the calculation of transmissivity and the hydraulic head is provided in /Ludvigson et al. 2002/.

Transmissivity of the entire borehole can be evaluated in several ways using the data of the pumping phase and of the recovery phase. For the pumping phase the assumptions above (cylindrical and steady state flow) lead to Dupuit's formula /Marsily 1986/:

$$T = \frac{Q}{s 2\pi} \ln\left(\frac{R}{r_0}\right) \quad 3\text{-}9$$

where
s is drawdown and
Q is the pumping rate at the end of the pumping phase.

In the Moye's formula /Moye 1967/ it is assumed that the steady state flow is cylindrical near the borehole (to distance r = L/2, where L is the section under test) and spherical further away:

$$T = \frac{Q}{s 2\pi} \cdot \left[1 + \ln\left(\frac{L}{2r_0}\right)\right] \quad 3\text{-}10$$

where L is length of test section (m), in this case the water filled, uncased part of the borehole.

4 Equipment specifications

The Posiva Flow Log/Difference Flowmeter monitors the flow of groundwater into or out from a borehole by means of a flow guide (,which uses rubber discs to isolate the flow). The flow guide thereby defines the test section to be measured without altering the hydraulic head. Groundwater flowing into or out from the test section is guided to the flow sensor. The flow is measured using the thermal pulse and/or thermal dilution methods. Measured values are transferred into a computer in digital form.

Type of instrument:	Posiva Flow Log/Difference Flowmeter.
Borehole diameters:	56 mm, 66 mm and 76 mm.
Length of test section:	A variable length flow guide is used.
Method of flow measurement:	Thermal pulse and/or thermal dilution.
Range and accuracy of measurement:	See Table 4-1.
Additional measurements:	Temperature, Single-point resistance, Electric conductivity of water, Caliper, Water pressure.
Winch:	Mount Sopris Wna 10, 0.55 kW, 220V/50Hz. Steel wire cable 1,500 m, four conductors, Gerhard-Owen cable head.
Length determination:	Based on a marked cable and a digital length counter.
Logging computer:	PC, Windows XP.
Software:	In-house developed software using MS Visual Basic.
Total power consumption:	1.5–2.5 kW depending on the pumps.
Calibrated:	August 2006.
Calibration of cable length:	Using length marks in the borehole.

Range and accuracy of sensors is presented in Table 4-1.

Table 4-1. Range and accuracy of sensors.

Sensor	Range	Accuracy
Flow	6 – 300,000 mL/h	± 10% curr.value
Temperature (middle thermistor)	0 – 50°C	0.1°C
Temperature difference (between outer thermistors)	–2 – +2°C	0.0001°C
Electric conductivity of water (EC)	0.02 – 11 S/m	± 5% curr.value
Single-point resistance	5 – 500,000 Ω	± 10% curr.value
Groundwater level sensor	0 – 0.1 MPa	± 1% fullscale
Absolute pressure sensor	0 – 20 MPa	± 0.01% fullscale

5 Performance

5.1 Execution of the field work

The commission was performed according to Activity Plan AP PS 400-06-080 (SKB internal controlling document) following the SKB Method Description 322.010, Version 1.0 (Method description for difference flow logging). Prior to the measurements, the downhole tools and the measurement cable were disinfected. Every clock was synchronized to the official Swedish time. The activity schedule of the borehole measurements is presented in Table 5-1. The items and activities in Table 5-1 are the same as in the Activity Plan.

Logging cables, wires, and pipe strings are exposed to stretching when lowered into a vertical or sub-vertical borehole. This will introduce a certain error in defining the position of a test tool connected to the end of a logging cable. Immediately after the completion of the drilling operations in borehole KLX13A, length marks were milled into the borehole wall at certain intervals to be used for length calibration of various logging tools. By using the known positions of the length marks, logging cables etc can be calibrated in order to obtain an accurate length correction of the testing tool.

Table 5-1. Flow logging and testing in KLX13A. Activity schedule.

Item	Activity	Explanation	Date
8	Dummy logging	Borehole stability/risk evaluation.	2006-09-21–2006-09-23
9	Calibration	SKB Caliper and SPR. Logging without the lower rubber discs, no pumping.	2006-09-23–2006-09-24
10	EC- and temp-logging of the borehole fluid	Logging without the lower rubber discs, no pumping.	2006-09-25
11	Telescopic part of borehole flow logging	Logging without the lower rubber discs, no pumping.	Not measured
12	Combined overlapping/sequential flow logging	Section length L_w=5 m, step length dL=0.5 m, no pumping.	2006-09-24–2006-09-25
13	Overlapping flow logging	Section length L_w=5 m, step length dL=0.5 m, pumping (includes 1 day waiting after the pumping was started).	2006-09-26–2006-09-27
14	Overlapping flow logging	Section length L_w=1 m, step length dL=0.1 m, pumping.	2006-09-27–2006-09-29
15	Fracture-specific EC-measurements in pre-selected fractures	Section length L_w=0.5 m, pumping, in pre-selected fractures.	2006-09-29–2006-09-30
16	EC- and temp- logging of the borehole fluid	Logging without the lower rubber discs, pumping.	2006-09-30
17	Recovery transient	Measurement of water level and absolute pressure in the borehole after the pumping was stopped. The measurement was continued between 2006-10-01 and 2006-10-08 by SKB.	2006-09-30–2006-10-01

Each length mark consists of two 20 mm wide tracks in the borehole wall. The distance between the tracks is 100 mm. The upper track defines a reference level. An inevitable condition for a successful length calibration is that all length marks, or at least the major part of them, are detectable. The Difference Flowmeter system uses caliper measurements in combination with single-point resistance measurements for this purpose. These methods also reveal parts of the borehole widened for some reason (fracture zones, breakouts etc). The length calibration (Item 9) of KLX13A was performed before any other measurements were started. The only exception was the dummy logging (Item 8) of the borehole, which is done in order to assure that the measurement tools do not get stuck in the borehole. Item 8 was conducted four times, because on the first three times stones (one or two each time) that were slightly larger than the limit for starting the measurements were found. On the fourth time there were no stones larger than the limit and the measurements were started.

The caliper/SPR-measurements in the measurement schedule were followed by measurements of the electric conductivity (EC) and temperature of the borehole water (Item 10) during natural (un-pumped) conditions.

The telescopic part of the borehole (Item 11) was not flow logged, because of a misunderstanding.

The combined overlapping/sequential flow logging (Item 12) was carried out in the borehole with a 5 m section length and in 0.5 m length increments (step length). The measurements were performed during natural (un-pumped) conditions. Every tenth flow measurement (sequential mode) had a longer measurement time than normally in the overlapping mode. This was done in order to ensure the direction of the flow (into the borehole or out of it).

Pumping was started on September 25. After a waiting time of c. 23 hours, overlapping flow logging (Item 13) was conducted using the same section and step lengths as before.

The overlapping flow logging was then continued by re-measuring previously detected flow anomalies with a 1 m section length and a 0.1 m step length (Item 14).

The fracture-specific EC of water from some selected fractures (Item 15) was also measured.

The EC of borehole water (Item 16) was measured while the borehole was still pumped. After this, the pump was stopped and the recovery of the groundwater level was monitored (Item 17).

5.2 Nonconformities

The measurement of flow rate along the borehole was included in the Activity Plan for KLX13A (Item 11). The aim of it is to check the flow balance in the borehole when the borehole is at rest. Unfortunately it was unintentionally left out of the measurements by PRG-Tec Oy due to insufficient checking of the correct version of the Activity Plan.

All head and transmissivity calculations have been done on revised elevation data (Z-coordinates). Borehole coordinates that formed the basis for this revision of ground water head data were retrieved from SKB Sicada 2007-03-07 EG154 (provided by SKB in file Krökdata_korrigerade_070307_KLX03-KLX29 utom KLX15,HLX13,15,26-28,32, 36-38,43.xls) /Stenberg and Håkansson 2007/.

6 Results

6.1 Length calibration

6.1.1 Caliper and SPR measurement

Accurate length measurements are difficult to conduct in long boreholes, i.e. the accurate position of the measurement equipment is difficult to determine. The main cause of inaccuracy is the stretching of the logging cable. The stretching depends on the tension on the cable, which in turn depends, among other things, on the inclination of the borehole and the roughness (friction properties) of the borehole wall. The cable tension is higher when the borehole is measured upwards. The cables, especially new cables, may also stretch out permanently.

Length marks on the borehole wall can be used to minimise the length errors. The length marks are initially detected with the SKB caliper tool. The length scale is first corrected according to the length marks. Single-point resistance is recorded simultaneously with the caliper logging. All flow measurement sequences can then be length corrected by synchronising the SPR results (SPR is recorded during all the measurements except during borehole EC measurements) with the original caliper/SPR-measurement.

The procedure of the length correction was the following:

- The caliper/SPR-measurements (Item 9) were initially length corrected in relation to the known length marks, Appendix 1.23, black curve. Corrections between the length marks were obtained by linear interpolation.
- The SPR curve of Item 9 was then compared with the SPR curves of Items 12, 13, 14 and 15 to obtain relative length errors of these measurement sequences.
- All SPR curves could then be synchronized, as can be seen in Appendices 1.2–1.22.

The results of the caliper and single-point resistance measurements from all measurements in the entire borehole are presented in Appendix 1.1. The five SPR-curves are plotted together with the caliper-data. These measurements correspond to Items 9, 12, 13, 14 and 15 in Table 5-1.

The caliper tool outputs a low voltage value when the borehole diameter is below 77 mm and a high value when the borehole diameter is over 77 mm.

Zoomed results of the caliper and SPR data are presented in Appendices 1.2–1.22. The detected length marks are listed in Table 6-1. All the marks except the 500 m mark were detected by the caliper tool. On the other hand, all the length marks were detected in the single-point resistance measurements. However, the SPR-anomaly is complicated due to the four rubber discs used at the upper end of the section, two at each side of the resistance electrode. If only one length mark is detected, the decision whether it is the lower or the upper mark is made based on the shape of the SPR-anomaly. The SPR-anomaly at the length marks has a distinctive shape, which can usually be recognized. In this case there were no partially recognized length marks. Appendix 1 also illustrates many natural anomalies (for example Appendices 1.4 and 1.6), which can help in synchronizing the results.

The aim of the plots in Appendices 1.2–1.22 is to verify the accuracy of the length correction. The curves in these plots are the length corrected results.

The magnitude of the length correction along the borehole is presented in Appendix 1.23. The negative values of the error represent the situation where the logging cable has been extended, i.e. the cable is longer than the nominal length marked on it.

Table 6-1. Detected length marks.

Length marks given by SKB (m)	Length marks detected by caliper	Length marks detected by SPR
110	both	yes
150	both	yes
200	both	yes
250	both	yes
300	both	yes
350	both	yes
400	both	yes
450	both	yes
500	–	yes
550	both	yes
581	both	yes

6.1.2 Estimated error in the location of detected fractures

In spite of the length correction described above, there can still be length errors due to the following reasons:

1. The point interval in the overlapping mode flow measurements is 0.1 m. This could cause an error of ± 0.05 m.
2. The length of the test section is not exact. The specified section length denotes the distance between the nearest upper and lower rubber discs. Effectively, the section length can be larger. At the upper end of the test section there are four rubber discs. The distance between them is 5 cm. This will cause rounded flow anomalies: a flow may be detected already when a fracture is situated between the upper rubber discs. These phenomena can cause an error of ± 0.05 m when the short step length (0.1 m) is used.
3. There could sometimes be a need for the corrections between the length marks to be other than linear. This could cause an error of ± 0.1 m in the caliper/SPR-measurement (Item 9).
4. SPR curves may be imperfectly synchronized. This could cause an error of ± 0.1 m

In the worst case, the errors from sources 1, 2, 3 and 4 are summed and the total estimated error between the length marks would be ± 0.3 m.

The situation is slightly better near the length marks. In the worst case, the errors from sources 1, 2 and 4 are summed and the total estimated error would be ± 0.2 m.

Knowing the location accurately is important when different measurements are compared, for instance flow logging and borehole TV. In a case like that the situation may not be as severe as in the worst case above, since some of the length errors are systematic and the error is nearly constant in fractures that are close to each other. However, the error caused by source 1 is random.

Fractures nearly parallel with the borehole may also be problematic. Fracture location may be difficult to define accurately in such cases.

The errors given above are estimations and are based on the experiences and observations from earlier measurements.

6.2 Electric conductivity and temperature

6.2.1 Electric conductivity and temperature of borehole water

The electric conductivity of the borehole water was initially measured when the borehole was at rest, i.e. at natural, un-pumped conditions. The measurement was performed downwards and upwards, see Appendix 2.1.

The EC measurement was repeated during pumping (after a pumping period of about six days), see Appendix 2.1, green curves.

The temperature of the borehole water was measured simultaneously with the EC measurements. The EC values are temperature corrected to 25°C to make them more comparable with other EC measurements /Heikkonen et al. 2002/. The temperature results in Appendix 2.2 have the same length axis as the EC results in Appendix 2.1.

The length calibration of the borehole electric conductivity measurements is not as accurate as in other measurements, because single-point resistance is not registered. The length correction of the SPR/caliper-measurement was applied to the borehole EC measurements, black curve in Appendix 1.23.

6.2.2 Electric conductivity of fracture-specific water

The flow direction is always from the fractures into the borehole if the borehole is pumped with a sufficiently large drawdown. This enables the determination of electric conductivity from fracture-specific water. Both electric conductivity and temperature of flowing water from the fractures were measured.

The fractures detected in the flow measurements can be measured for electric conductivity later. These fracture-specific measurements begin near the fracture, which has been chosen for inspection. The tool is first moved stepwise closer to the fracture until the detected flow is larger than a predetermined limit. At this point the tool is stopped. The measurement is continued at the given position allowing the fracture-specific water to enter the section. The waiting time for the EC measurement can be automatically calculated from the measured flow rate. The aim is to flush the water volume within the test section sufficiently to gain accurate results. The measuring computer is programmed so that the water in the test section will be replaced approximately three times over. After the set of stationary measurements the tool is once again moved stepwise past the fracture for a short distance. The electric conductivity is also measured between the steps before and after the set of stationary measurements.

The test section in these measurements was 0.5 m long and the tool was moved in 0.1 m steps. The water volume in a half metre long test section is 1.8 L. The results are presented in Appendix 14. The blue symbol represents the conductivity value when the tool was moved and the red symbol is used for the set of stationary measurements.

Borehole lengths at the upper and lower ends of the section, fracture locations as well as the final EC values are listed in Table 6-2.

The electric conductivity of the entire borehole in pumped and un-pumped conditions is illustrated in Appendix 2.1 along with the fracture specific results.

Table 6-2. Fracture-specific EC.

Upper end of section (m)	Lower end of section (m)	Fractures measured (m)	EC (S/m) at 25°C
544.64	545.14	545.0	0.31
465.94	466.44	466.3	0.21
387.17	387.67	387.5	0.11
374.17	374.67	374.4	0.10
227.98	228.48	228.2	0.09
122.01	122.51	122.3	0.05

6.3 Pressure measurements

Absolute pressure was registered with the other measurements in Items 10–17. The pressure sensor measures the sum of hydrostatic pressure in the borehole and air pressure. Air pressure was also registered separately, Appendix 13.2. The hydraulic head along the borehole is determined in the following way. First, the monitored air pressure at the site is subtracted from the measured absolute pressure by the pressure sensor. The hydraulic head (h) at a certain elevation (z) is then calculated according to the following expression /Freeze and Cherry 1979/:

$$h = (p_{abs} - p_b)/(\rho_{fw}\, g) + z \qquad (6\text{-}1)$$

where

h is the hydraulic head (metres above sea level) according to the RHB 70 reference system,

p_{abs} is absolute pressure (Pa),

p_b is barometric (air) pressure (Pa),

ρ_{fw} is unit density 1,000 kg/m^3

g is standard gravity 9.80665 m/s^2 and

z is the elevation of measurement (metres above sea level) according to the RHB 70 reference system.

A tool-specific offset of 2.30 kPa is subtracted from absolute pressure raw data.

Exact z-coordinates are important in head calculations, 10 cm error in z-coordinate means 10 cm error in the head. All head and transmissivity calculations have been done on revised elevation data (Z-coordinates). Borehole coordinates that formed the basis for this revision of groundwater head data were retrieved from SKB Sicada 2007-03-07 EG154 (provided by SKB in file Krökdata_korrigerade_070307_KLX03-KLX29 utom KLX15,HLX13,15,26-28, 32, 36-38,43.xls) /Stenberg and Håkansson 2007/.

The calculated head values are presented in a graph in Appendix 13.1.

6.4 Flow logging

6.4.1 General comments on results

The flow results are presented together with the single-point resistance results (right hand side) and the caliper plot (in the middle), see Appendices 3.1–3.26. Single-point resistance is usually lower in value on a fracture where a flow is detected. There are also many other resistance anomalies from other fractures and geological features. The electrode of the Single-point resistance tool is located in between the upper rubber discs. Thus, the locations of the resistance anomalies of leaky fractures coincide with the lower end of the flow anomalies in the data plot.

The flow logging was first performed with a 5 m section length and with 0.5 m length increments, see Appendices 3.1–3.26. The method (overlapping flow logging) gives the length and the thickness of conductive zones with a length resolution of 0.5 m. To obtain quick results, only the thermal dilution method is used for flow determination.

Under natural conditions or if the borehole isn't pumped using a sufficient drawdown the flow direction may be into the borehole or out from it. The direction of small flows (< 100 mL/h) cannot be detected in the normal overlapping mode (thermal dilution method). Therefore the measurement time was longer (so that the thermal pulse method could be used) at every 5 m interval in both 5 m section measurements. In the 1 m section measurements the thermal pulse method was also used, if it was deemed necessary based on the 5 m section measurements in pumped conditions. The thermal pulse method was only used to detect the flow direction.

The test section length determines the width of a flow anomaly of a single fracture in the plots. If the distance between flow yielding fractures is less than the section length, the anomalies will overlap, resulting in a stepwise flow data plot. Overlapping flow logging was therefore repeated in the vicinity of identified flow anomalies using a 1 m long test section and 0.1 m length increments, see Appendices 3.1–3.26 (violet curve).

The positions (borehole length) of the detected fractures are shown on the caliper scale. They are interpreted on the basis of the flow curves and therefore represent flowing fractures. A long line represents the location of a leaky fracture; a short line denotes that the existence of a leaky fracture is uncertain. A short line is used if the flow rate is less than 30 mL/h or the flow anomalies are overlapping or unclear because of noise.

The coloured triangles in the illustrations show the magnitudes of the measured flows. The triangles have same colour than the corresponding curves.

The table in Appendix 10 were used to calculate conductive fracture frequency (CFF). The number of conductive fractures was counted on the same 5 metre sections as in Appendix 7. The number of conductive fractures was sorted in six columns depending on their flow rate. The total conductive fracture frequency is presented graphically, see Appendix 11.

The basic data for KLX13A measurements is presented in Appendix 6 and the explanations to the tables in Appendices 6–8 in Appendix 9.

6.4.2 Transmissivity and hydraulic head of borehole sections

The entire borehole between 94.33 m and 589.58 m was flow logged with a 5 m section length and with 0.5 m length increments. The results of the measurements with a 5 m section length are presented in tables, see Appendix 7. Only the results with 5 m length increments are used. All borehole sections are shown in Appendices 3.1–3.26. Secup and Seclow in Appendix 7 are the distances along the borehole from the reference level (top of the casing tube) to the upper end of the test section and to the lower end of the test section, respectively. The Secup and Seclow values for the two sequences (measurements at un-pumped and pumped conditions) are not exactly identical, due to a minor difference in the cable stretching. The difference between these two sequences was small. Secup and Seclow given in Appendix 7 are calculated as the average of these two values.

Pressure was measured and calculated as described in Section 6.3. h_{0FW} and h_{1FW} in Appendix 7 represent heads determined without and with pumping, respectively. The head in the borehole and calculated heads of borehole sections are given on the RHB 70 scale.

The flow results in Appendix 7 (Q_0 and Q_1), representing the flow rates derived from measurements during un-pumped and pumped conditions, are presented side by side to make

comparison easier. Flow rates are positive if the flow direction is from the bedrock into the borehole and vice versa. With the borehole at rest, 44 sections were detected as flow yielding, 33 of which had a flow direction from the borehole into the bedrock (negative flow). During pumping, all 62 detected flows were directed towards the borehole.

It is possible to detect the existence of flow anomalies below the measurement limit (30 mL/h = $8.33 \cdot 10^{-9}$ m^3/s), even though the exact numerical values below the limit are uncertain. Some of the section flow rates in the natural conditions were below this limit (see Appendix 7).

The flow data is presented as a plot, see Appendix 4.1. The left hand side of each diagram represents flow from the borehole into the bedrock for the respective test sections, whereas the right hand side represents the opposite. If the measured flow was zero (below the measurement limit), it is not visible in the logarithmic scale of the appendices.

The lower and upper measurement limits of the flow are also presented in the plots (Appendix 4.1) and in the tables (Appendix 7). There are theoretical and practical lower limits of flow, see Section 6.4.4.

The hydraulic head and transmissivity (T_D) of borehole sections can be calculated from the flow data using the method described in Chapter 3. The hydraulic head of sections is presented in the plots if none of the two flow values at the same length is equal to zero. Transmissivity is presented if none or just one of the flows is equal to zero, see Appendix 4.2. The measurement limits of transmissivity are also shown in Appendix 4.2 and in Appendix 7. All the measurement limit values of transmissivity are based on the actual pressure difference in the borehole (h_{0FW} and h_{1FW} in Appendix 7).

The sum of detected flows without pumping (Q_0) was $-3.71 \cdot 10^{-5}$ m^3/s (–133,700 mL/h). This sum should normally be zero if all the flows in the borehole are correctly measured, the borehole is not pumped, the water level is constant, the salinity distribution in the borehole is stabilized and the fractures are at steady state pressure. In this case the sum is not close to zero. Based on the EC and temperature results in Appendices 2.1 and 2.2 it seems possible that there are three possibly significant fractures at approximately 54 m, 74 m and 89 m. The effect of these fractures on the flow balance is unknown. It should also be noted that the borehole was not measured below 589.58 m.

6.4.3 Transmissivity and hydraulic head of fractures

An attempt was made to evaluate the magnitude of fracture-specific flow rates. The results for a 1 m section length and 0.1 m length increments were used for this purpose. The first step in this procedure is to identify the locations of individual flowing fractures and then evaluate their flow rates.

In cases where the fracture distance is less than one metre, it may be difficult to evaluate the flow rate. There are such cases for instance in Appendix 3.2. In these cases a stepwise increase or decrease in the flow data plot equals the flow rate of a specific fracture (filled triangles in the Appendices).

Since the 1 m section was not used in un-pumped conditions, the results for the 5 m section were used instead. The fracture locations are important when evaluating the flow rate in un-pumped conditions. The fracture locations are known on the basis of the 1 m section measurements. It is not a problem to evaluate the flow rate in un-pumped conditions when the distance between flowing fractures is more than 5 m. The evaluation may, however, be problematic when the distance between fractures is less than 5 m. In this case an increase or decrease of a flow anomaly at the fracture location determines the flow rate. However, this evaluation is used conservatively, i.e. only in the clearest of cases, and no flow value is usually

evaluated for un-pumped conditions at densely fractured parts of bedrock. If the flow for a specific fracture cannot be determined conclusively, the flow rate is marked with "–" and the value 0 is used in the transmissivity calculation, see Appendix 8. The flow direction is evaluated as well. The results of the evaluation are plotted in Appendix 3, blue filled triangle.

Some fracture-specific results were classified to be "uncertain". The basis for this classification is either a minor flow rate (< 30 mL/h) or unclear fracture anomalies. Anomalies are considered unclear if the distance between them is less than one metre or their nature is unclear because of noise.

The total amount of detected flowing fractures was 155, but only 17 could be defined without pumping. These 17 fractures could be used for head estimation and all 155 were used for transmissivity estimations, Appendix 8. The transmissivity and hydraulic head of fractures are plotted in Appendix 5.

Fracture-specific transmissivities were compared with the transmissivities of borehole sections in Appendix 12. All fracture-specific transmissivities within each 5 m interval were first summed together to make them comparable with the measurements with a 5 m section length. The results are, in most cases, consistent between the two types of measurements. The decrease of flow as a function of pumping time can be seen in most fractures. The measurements with a 1 m section were carried out later than with a 5 m section (during pumping) and therefore the flow rate and transmissivity are generally smaller.

6.4.4 Theoretical and practical limits of flow measurements and transmissivity

The theoretical minimum of the measurable flow rate in the overlapping method (thermal dilution method only) is about 30 mL/h. The thermal pulse method can also be used. Its theoretical lower limit is about 6 mL/h. In this borehole the thermal pulse method was only used to detect the flow direction, not the flow rate. The upper limit of the flow measurements is 300,000 mL/h. These limits are determined on the basis of flow calibration. It is assumed that a flow can be reliably detected between the upper and lower theoretical limits in favorable borehole conditions.

In practice, the minimum measurable flow rate might, however, be much higher. Borehole conditions may be such that the base level of flow (noise level) is higher than assumed. The noise level can be evaluated on such intervals of the borehole where there are no flowing fractures or other structures. The noise level may vary along the borehole.

There are several known reasons for increased noise levels:

1) Rough borehole wall.
2) Solid particles in the water such as clay or drilling mud.
3) Gas bubbles in the water.
4) High flow rate along the borehole.

A rough borehole wall always causes a high noise level, not only in the flow results but also in the single-point resistance results. The flow curve and the SPR curves are typically spiky when the borehole wall is rough.

Drilling mud in the borehole water usually increases the noise level. Typically this kind of noise is seen both in un-pumped and pumped conditions.

Pumping causes the pressure drop in the borehole water and in the water in the fractures near the borehole. This may lead to the release of dissolved gas and increase the amount of gas bubbles in the water. Some fractures may produce more gas than others. Sometimes the noise level is larger just above certain fractures (when the borehole is measured upwards). The reason for this is assumed to be gas bubbles. The bubbles may cause a decrease of the average density of water and therefore also decrease the measured head in the borehole.

The effect of a high flow rate along the borehole can often be seen above high flowing fractures. Any minor leak at the lower rubber discs is directly measured as increased noise.

A high noise level in a flow masks the "real" flow if it is smaller than the noise. Real flows are totally invisible if they are about ten times smaller than the noise and they are registered correctly if they are about ten times larger than the noise. Based on experience, real flows between 1/10 times the noise level and 10 times the noise level are summed with the noise. Therefore the noise level could be subtracted from the measured flow to get the real flow. This correction has not been done so far because it is unclear whether it is applicable in each case.

The practical minimum of the measurable flow rate is evaluated and presented in Appendices 3.1–3.26 using a grey dashed line (Lower limit of flow rate). The practical minimum level of the measurable flow is always evaluated in pumped conditions since this measurement is the most important for transmissivity calculations. The limit is an approximation. It is evaluated to obtain a limit below which there may be fractures or structures that remain undetected.

The noise level in KLX13A was near 30 mL/h. In some places anomalies below the theoretical limit of the thermal dilution method (30 mL/h) could be detected. The noise line (grey dashed line) was never drawn below 30 mL/h, because the values of flow rate measured below 30 mL/h are uncertain.

In some boreholes the upper limit of flow measurement (300,000 mL/h) may be exceeded. Such fractures or structures hardly remain undetected (as the fractures below the lower limit). High flow fractures can be measured separately at a smaller drawdown. In KLX13A the flow values never exceeded the upper limit.

The practical minimum of measurable flow rate is also presented in Appendix 7 (Q-lower limit P). It is taken from the plotted curve in Appendix 3 (Lower limit of flow rate). The practical minimum of measurable transmissivity can be evaluated using Q-lower limit and the actual head difference at each measurement location, see Appendix 7 (T_D-$measl_{LP}$). The theoretical minimum measurable transmissivity (T_D-$measl_{LT}$) is evaluated using a Q value of 30 mL/h (minimum theoretical flow rate with the thermal dilution method). The upper measurement limit of transmissivity can be evaluated using the maximum flow rate (300,000 mL/h) at the actual head difference as above, see Appendix 7 (T_D-$measl_U$).

All three flow limits are also plotted with measured flow rates, see Appendix 4.1. Theoretical minimum and maximum values are 30 mL/h and 300,000 mL/h, respectively.

The three transmissivity limits are also presented graphically, see Appendix 4.2.

Similar flow and transmissivity limits are not given for the fracture-specific results, Appendices 5 and 8. Approximately the same limits would also be valid for these results. The limits for fracture-specific results are more difficult to define. For instance, it may be difficult to see a small flow rate near (< 1 m) a high flowing fracture. The situation is similar for the upper flow limit. If there are several high flowing fractures less than one metre apart from each other, the upper flow limit depends on the sum of flows, which must be below 300,000 mL/h.

6.4.5 Transmissivity of the entire borehole

The pumping phase for the logging and its subsequent recovery is utilized to evaluate the transmissivity of the entire borehole. This is done with the two steady state methods, described in Chapter 3.

For Dupuit's formula (equation 3-9) R/r_0 is chosen to be 500, Q was 39 L/min and s (drawdown) was 10.02 m. Transmissivity calculated with Dupuit's formula is $6.42 \cdot 10^{-5}$ m^2/s.

In Moye's formula (equation 3-10) the length of the test section L is 584.1 m (595.85 m–11.75 m) and the borehole diameter $2r_0$ is 0.076 m. Transmissivity calculated with Moye's formula is $1.03 \cdot 10^{-4}$ m^2/s.

6.5 Groundwater level and pumping rate

The groundwater level and the pumping rate are illustrated in Appendix 13.2. The borehole was pumped between September 25 and September 30 with a drawdown of approximately 10.0 m. The pump intake was at level 3.3 m (metres above sea level, RHB 70). The groundwater level sensor (pressure transducer) was at 3.0 m (metres above sea level, RHB 70).

The groundwater recovery was measured after the pumping period between September 30 and October 1, Appendix 13.3. The measurement was done with two sensors, the water level sensor (pressure sensor) and the absolute pressure sensor located in the flowmeter tool at the borehole length of 23.76 m. The measurement was continued by SKB between October 1 and 8.

Table 6-3. Transmissivity of the entire borehole KLX13A.

Method	Transmissivity (m^2/s)
Dupuit	$6.42 \cdot 10^{-5}$
Moye	$1.03 \cdot 10^{-4}$

7 Summary

In this study, the Posiva Flow Log/Difference Flow Method has been used to determine the location and flow rate of flowing fractures or structures in borehole KLX13A at Oskarshamn. Measurements were carried out both when the borehole was at rest and during pumping. A 5 m section length with 0.5 m length increments was used initially. The detected flow anomalies were re-measured with a 1 m section length using a 0.1 m measurement interval.

Length calibration was made using the length marks on the borehole wall. The length marks were detected by caliper and in single-point resistance logging. The latter method was also performed simultaneously with the flow measurements, and thus all flow results could be length calibrated by synchronizing the single-point resistance logs.

The distribution of saline water along the borehole was logged by electric conductivity and temperature measurements of the borehole water. In addition, electric conductivity was measured in selected flowing fractures.

The water level in the borehole during pumping and its recovery after the pump was turned off were also measured.

The total amount of detected flowing fractures was 155. Transmissivity and hydraulic head were calculated for borehole sections and fractures for the depth range of 94.33 m–589.58 m. The highest transmissivity ($2.0 \cdot 10^{-6}$ m^2/s) was detected in a fracture at the length of 385.1 m. High-transmissive fractures were also found at 122.3 m, 387.5 m and 450.8 m. The lowest identified flowing fracture was at the approximate length of 582.9 m.

References

Freeze R A, Cherry J A, 1979. Groundwater. Prentice Hall, Inc., United States of America.

Heikkonen J, Heikkinen E, Mäntynen M, 2002. Mathematical modelling of temperature adjustment algorithm for groundwater electrical conductivity on basis of synthetic water sample analysis. Helsinki, Posiva Oy. Working report 2002-10 (in Finnish).

Ludvigson J-E, Hansson K, Rouhiainen P, 2002. Methodology study of Posiva difference flowmeter in borehole KLX02 at Laxemar. SKB R-01-52, Svensk Kärnbränslehantering AB.

Marsily G, 1986. Quantitative Hydrogeology, Groundwater Hydrology for Engineers. Academic Press, Inc., London.

Moye D G, 1967. Diamond Drilling for Foundation Exploration. Civil Engineering Trans., April, (2150), pp. 95–100.

Stenberg L, Håkansson N, 2007. Revision of borehole deviation measurements in Oskarshamn. SKB P-07-54, Svensk Kärnbränslehantering AB (in preparation).

Öhberg A, Rouhiainen P, 2000. Posiva groundwater flow measuring techniques. Helsinki, Posiva Oy. Report POSIVA 2000-12.

Appendices

Appendix 1.1

Laxemar, borehole KLX13A
SPR and Caliper results after length correction

SPR+Caliper (downwards), 2006-09-23 - 2006-09-24
SPR without pumping (upwards) (L = 5 m), 2006-09-24 - 2006-09-25
SPR with pumping (upwards) (L = 5 m), 2006-09-26 - 2006-09-27
SPR with pumping (upwards) (L = 1 m), 2006-09-27 - 2006-09-29
SPR with pumping (upwards during fracture-EC) (L = 0.5 m), 2006-09-29 - 2006-09-30

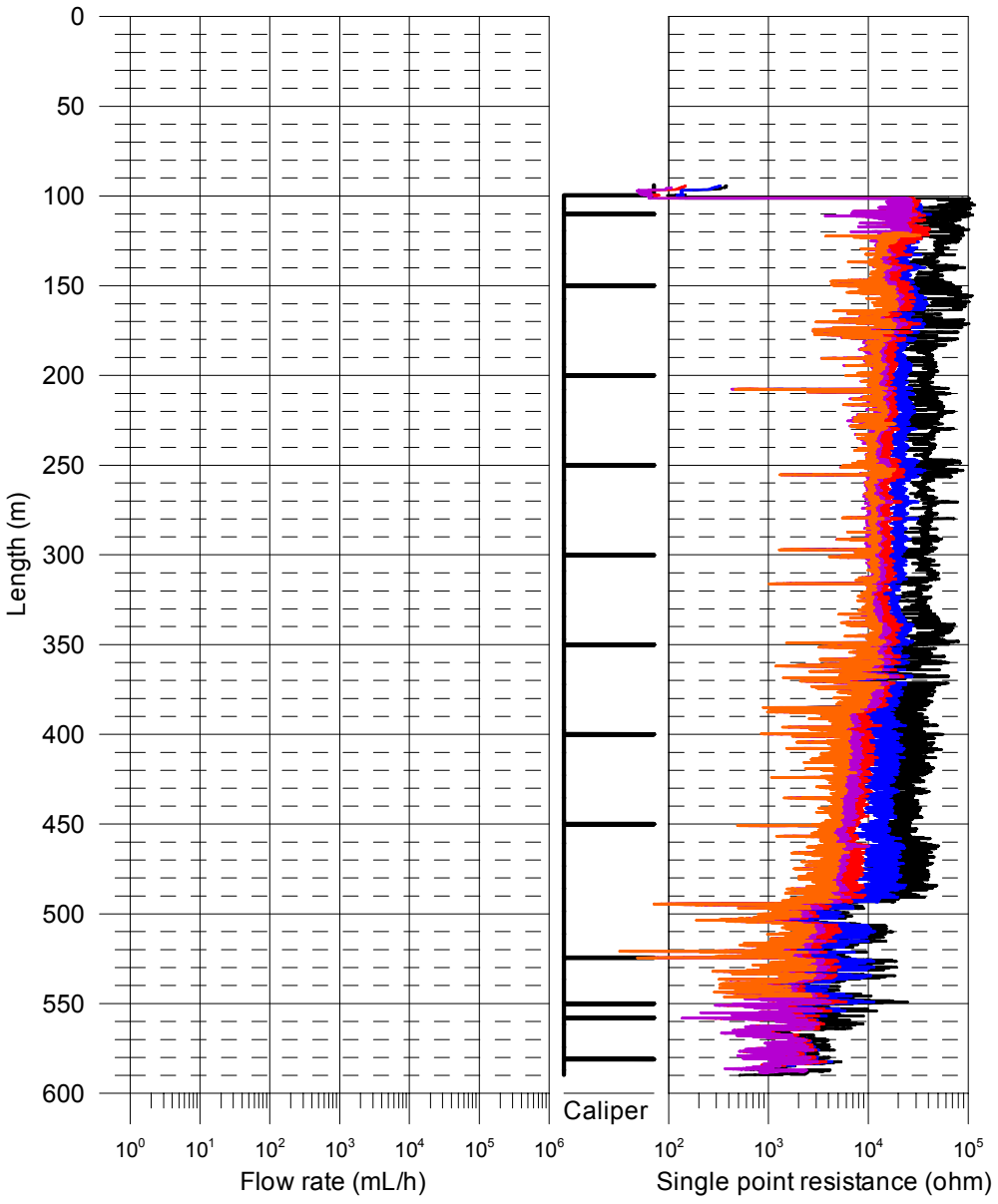

Appendix 1.2

Laxemar, borehole KLX13A
SPR and Caliper results after length correction

SPR+Caliper (downwards), 2006-09-23 - 2006-09-24
SPR without pumping (upwards) (L = 5 m), 2006-09-24 - 2006-09-25
SPR with pumping (upwards) (L = 5 m), 2006-09-26 - 2006-09-27
SPR with pumping (upwards) (L = 1 m), 2006-09-27 - 2006-09-29
SPR with pumping (upwards during fracture-EC) (L = 0.5 m), 2006-09-29 - 2006-09-30

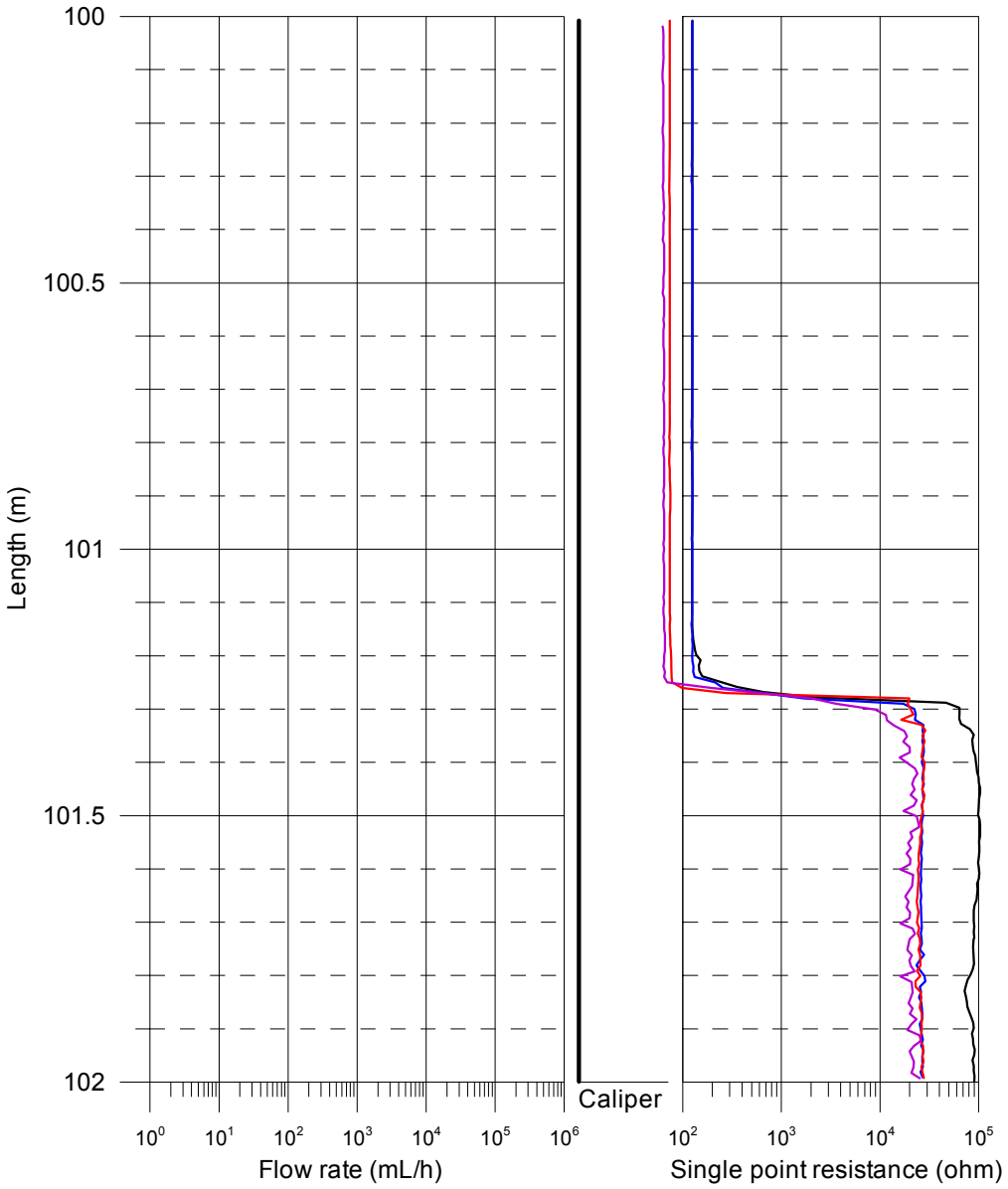

Appendix 1.3

Laxemar, borehole KLX13A
SPR and Caliper results after length correction

SPR+Caliper (downwards), 2006-09-23 - 2006-09-24
SPR without pumping (upwards) (L = 5 m), 2006-09-24 - 2006-09-25
SPR with pumping (upwards) (L = 5 m), 2006-09-26 - 2006-09-27
SPR with pumping (upwards) (L = 1 m), 2006-09-27 - 2006-09-29
SPR with pumping (upwards during fracture-EC) (L = 0.5 m), 2006-09-29 - 2006-09-30

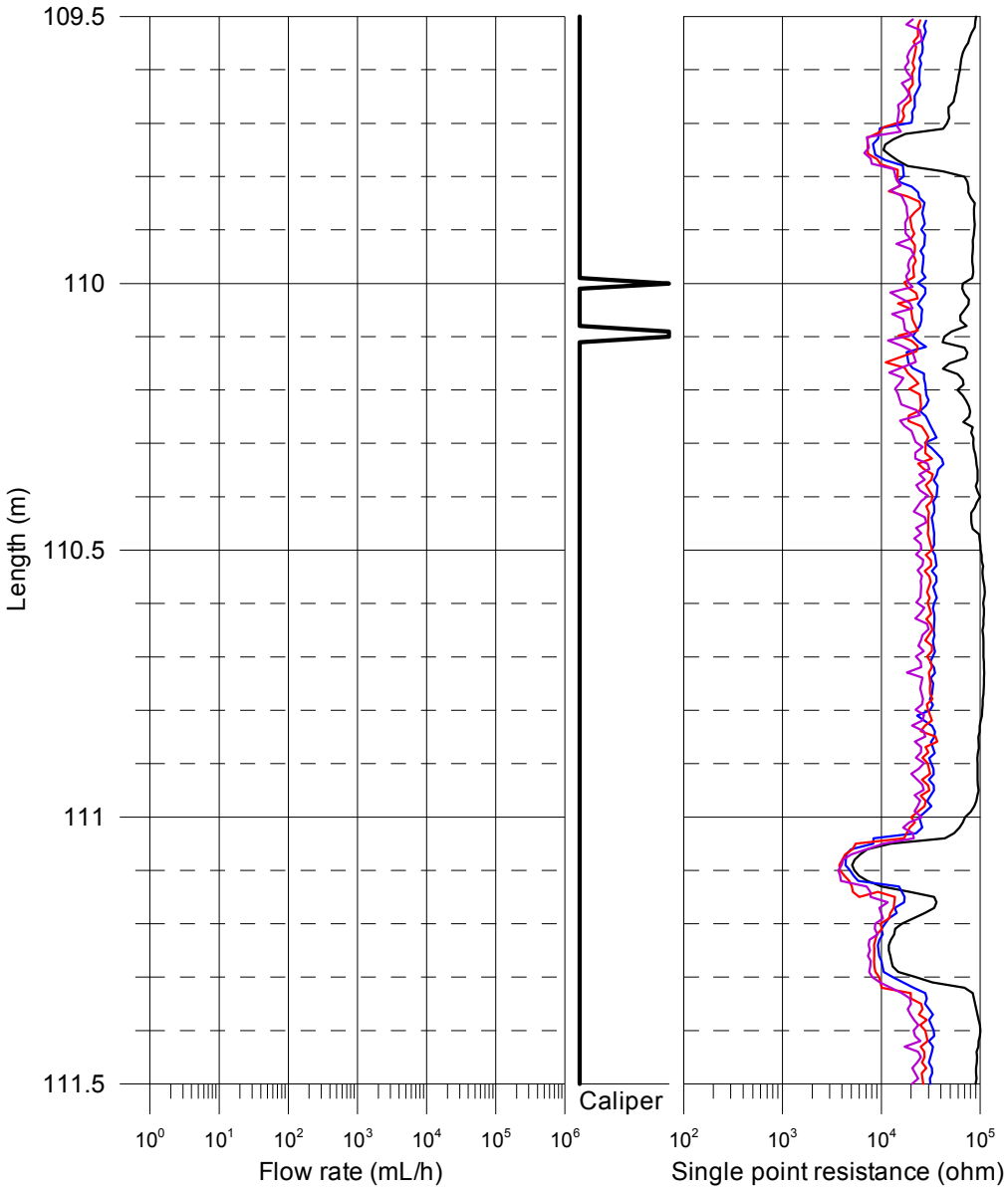

Appendix 1.4

Laxemar, borehole KLX13A
SPR and Caliper results after length correction

SPR+Caliper (downwards), 2006-09-23 - 2006-09-24
SPR without pumping (upwards) (L = 5 m), 2006-09-24 - 2006-09-25
SPR with pumping (upwards) (L = 5 m), 2006-09-26 - 2006-09-27
SPR with pumping (upwards) (L = 1 m), 2006-09-27 - 2006-09-29
SPR with pumping (upwards during fracture-EC) (L = 0.5 m), 2006-09-29 - 2006-09-30

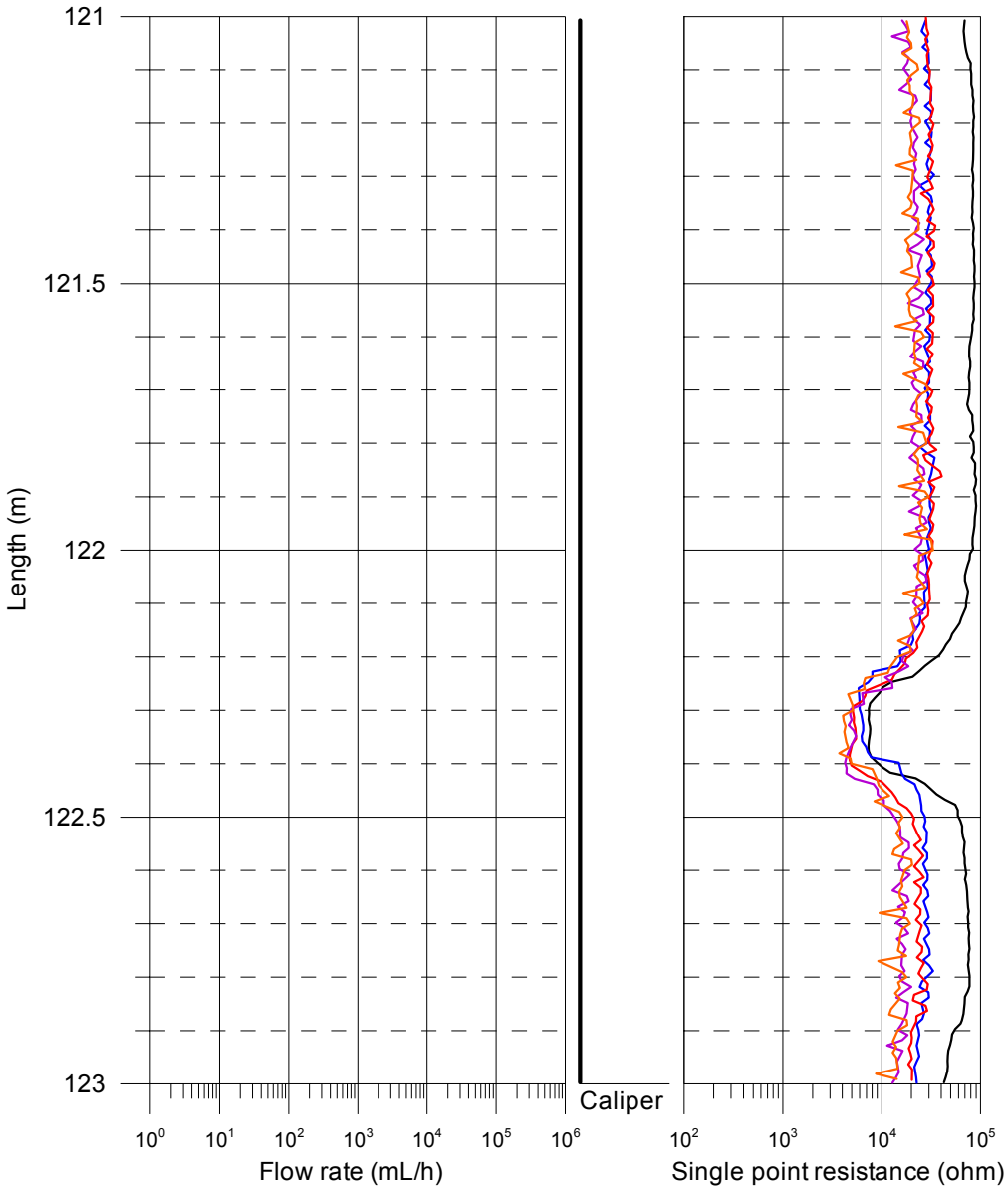

Appendix 1.5

Laxemar, borehole KLX13A
SPR and Caliper results after length correction

SPR+Caliper (downwards), 2006-09-23 - 2006-09-24
SPR without pumping (upwards) (L = 5 m), 2006-09-24 - 2006-09-25
SPR with pumping (upwards) (L = 5 m), 2006-09-26 - 2006-09-27
SPR with pumping (upwards) (L = 1 m), 2006-09-27 - 2006-09-29
SPR with pumping (upwards during fracture-EC) (L = 0.5 m), 2006-09-29 - 2006-09-30

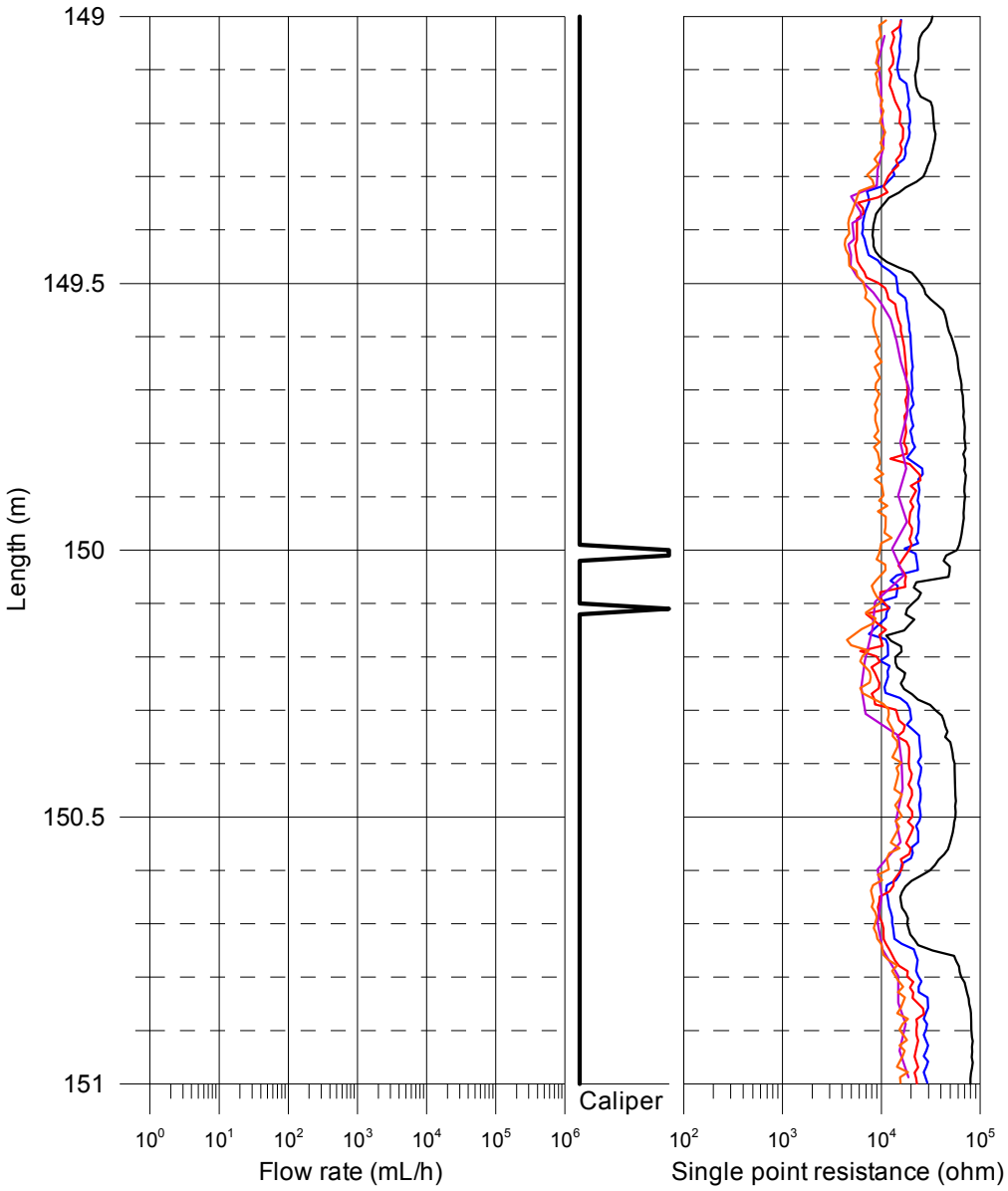

Appendix 1.6

Laxemar, borehole KLX13A
SPR and Caliper results after length correction

SPR+Caliper (downwards), 2006-09-23 - 2006-09-24
SPR without pumping (upwards) (L = 5 m), 2006-09-24 - 2006-09-25
SPR with pumping (upwards) (L = 5 m), 2006-09-26 - 2006-09-27
SPR with pumping (upwards) (L = 1 m), 2006-09-27 - 2006-09-29
SPR with pumping (upwards during fracture-EC) (L = 0.5 m), 2006-09-29 - 2006-09-30

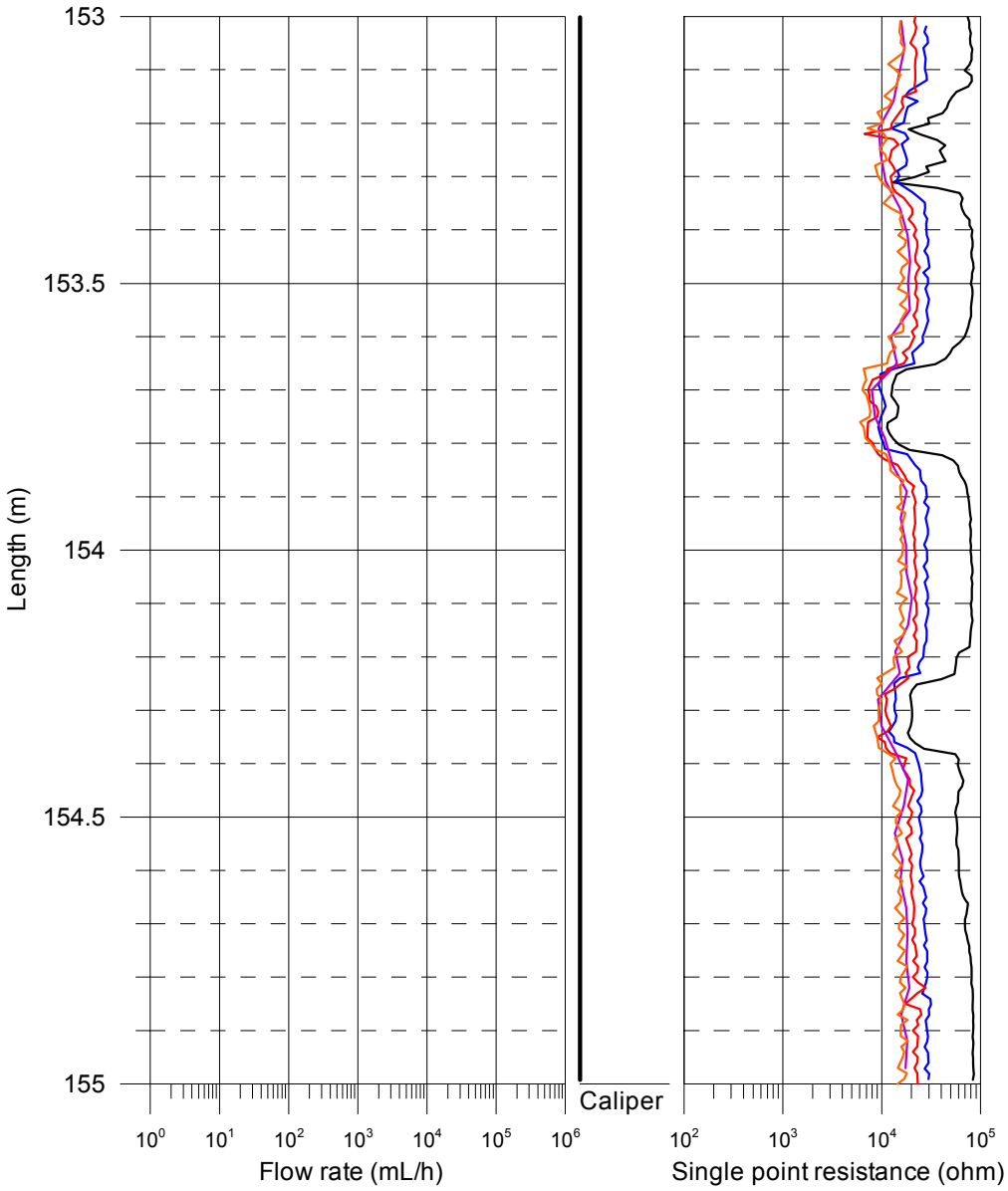

Appendix 1.7

Laxemar, borehole KLX13A
SPR and Caliper results after length correction

SPR+Caliper (downwards), 2006-09-23 - 2006-09-24
SPR without pumping (upwards) (L = 5 m), 2006-09-24 - 2006-09-25
SPR with pumping (upwards) (L = 5 m), 2006-09-26 - 2006-09-27
SPR with pumping (upwards) (L = 1 m), 2006-09-27 - 2006-09-29
SPR with pumping (upwards during fracture-EC) (L = 0.5 m), 2006-09-29 - 2006-09-30

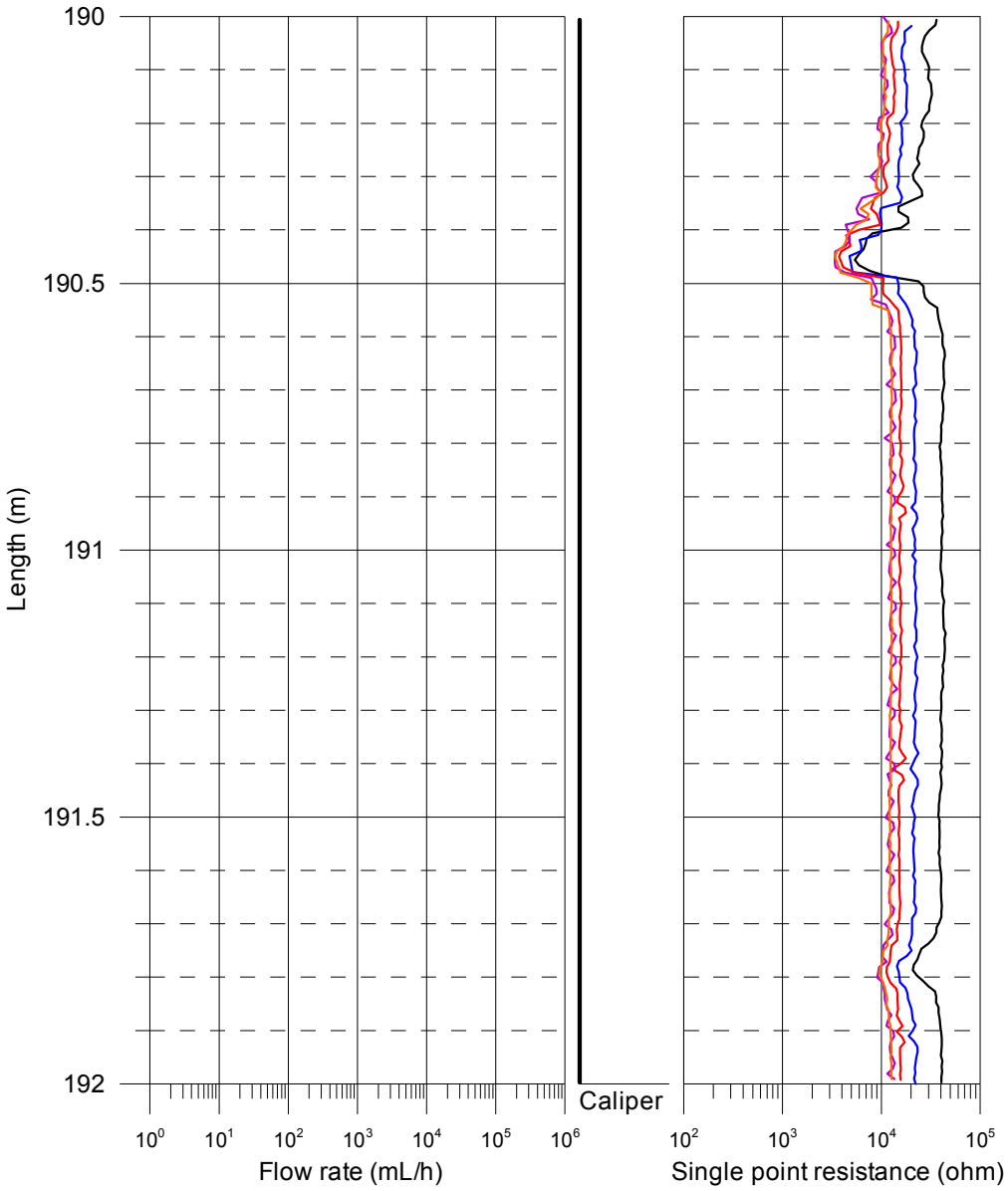

Appendix 1.8

Laxemar, borehole KLX13A
SPR and Caliper results after length correction

SPR+Caliper (downwards), 2006-09-23 - 2006-09-24
SPR without pumping (upwards) (L = 5 m), 2006-09-24 - 2006-09-25
SPR with pumping (upwards) (L = 5 m), 2006-09-26 - 2006-09-27
SPR with pumping (upwards) (L = 1 m), 2006-09-27 - 2006-09-29
SPR with pumping (upwards during fracture-EC) (L = 0.5 m), 2006-09-29 - 2006-09-30

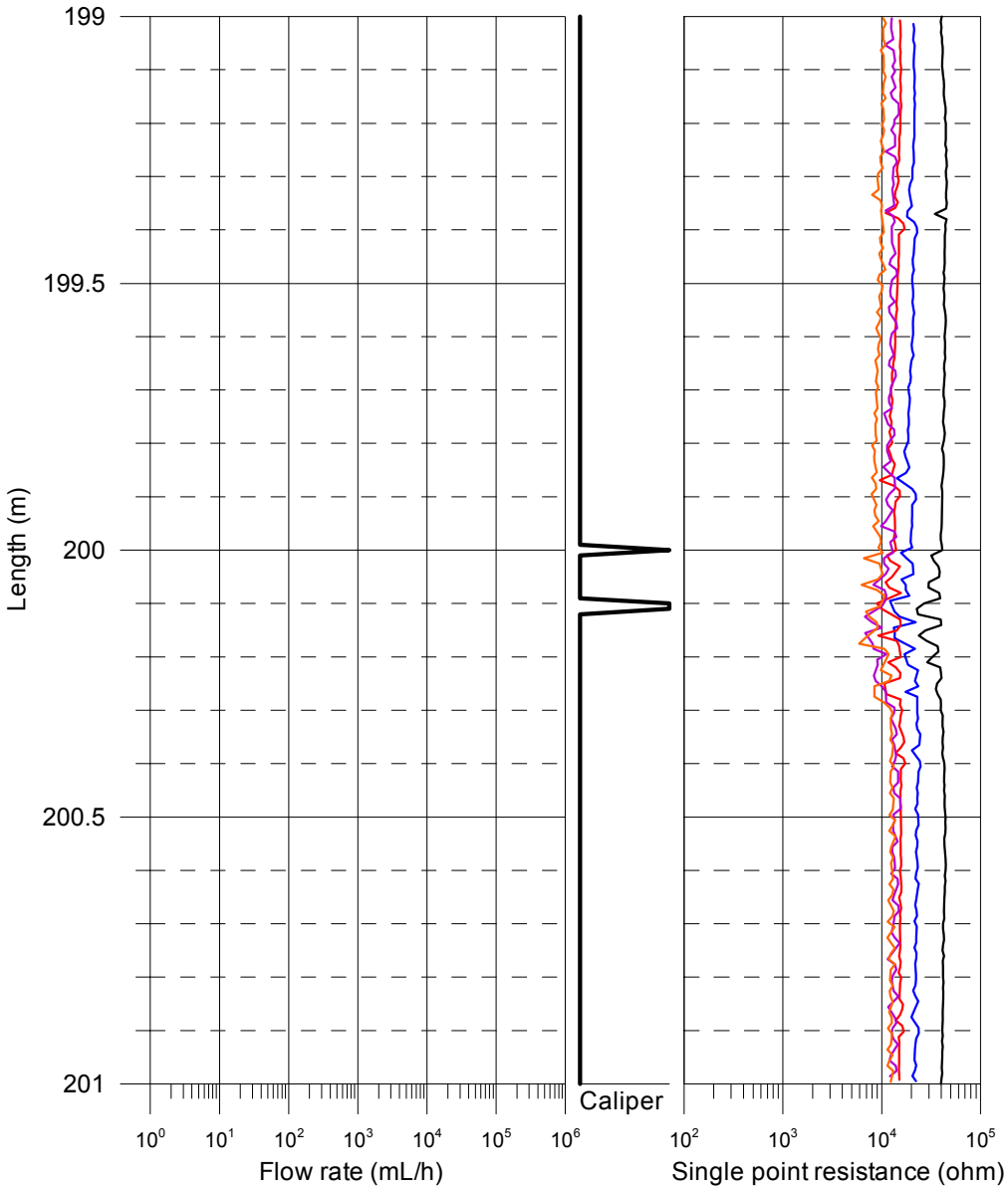

Appendix 1.9

Laxemar, borehole KLX13A
SPR and Caliper results after length correction

SPR+Caliper (downwards), 2006-09-23 - 2006-09-24
SPR without pumping (upwards) (L = 5 m), 2006-09-24 - 2006-09-25
SPR with pumping (upwards) (L = 5 m), 2006-09-26 - 2006-09-27
SPR with pumping (upwards) (L = 1 m), 2006-09-27 - 2006-09-29
SPR with pumping (upwards during fracture-EC) (L = 0.5 m), 2006-09-29 - 2006-09-30

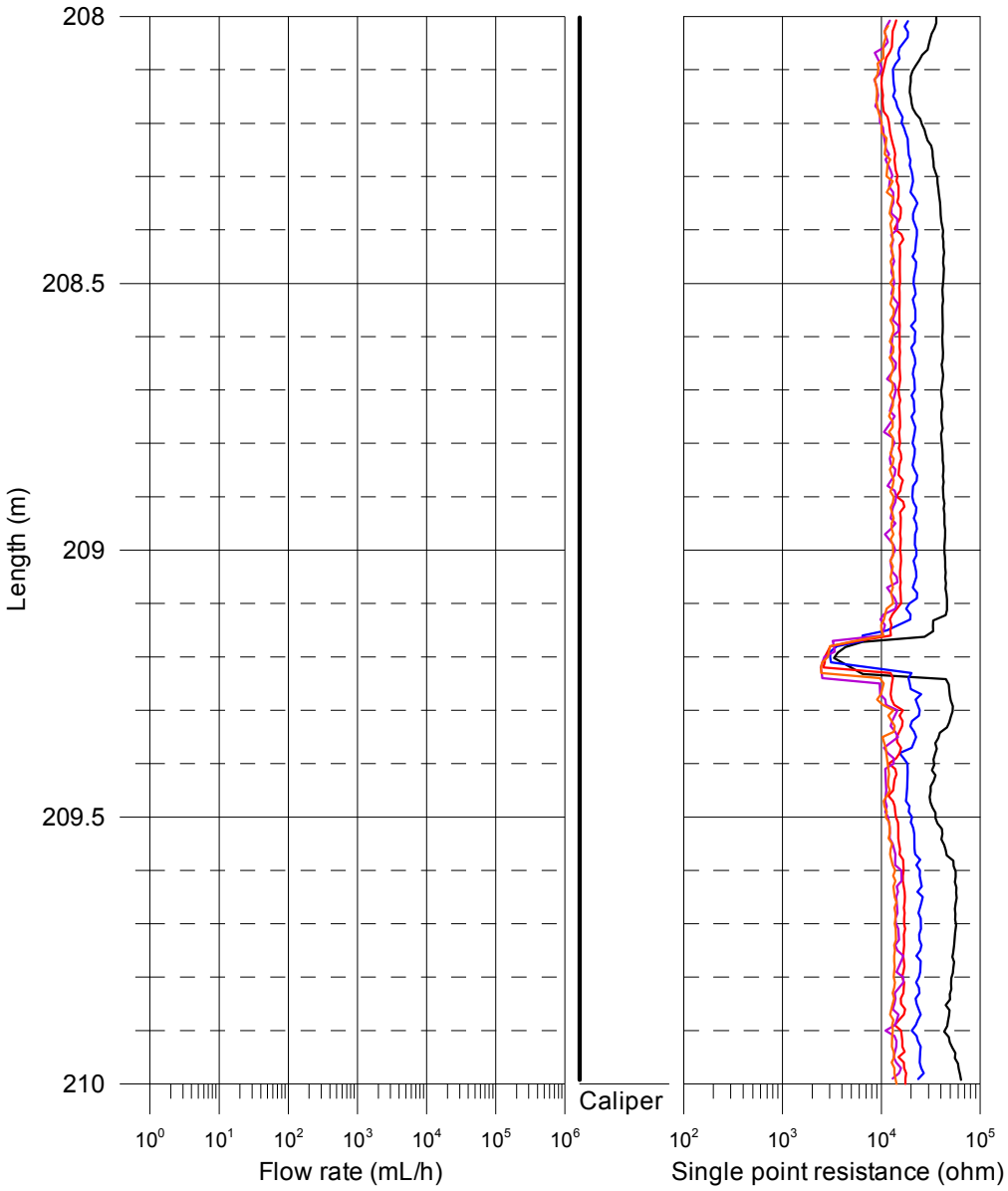

Appendix 1.10

Laxemar, borehole KLX13A
SPR and Caliper results after length correction

SPR+Caliper (downwards), 2006-09-23 - 2006-09-24
SPR without pumping (upwards) (L = 5 m), 2006-09-24 - 2006-09-25
SPR with pumping (upwards) (L = 5 m), 2006-09-26 - 2006-09-27
SPR with pumping (upwards) (L = 1 m), 2006-09-27 - 2006-09-29
SPR with pumping (upwards during fracture-EC) (L = 0.5 m), 2006-09-29 - 2006-09-30

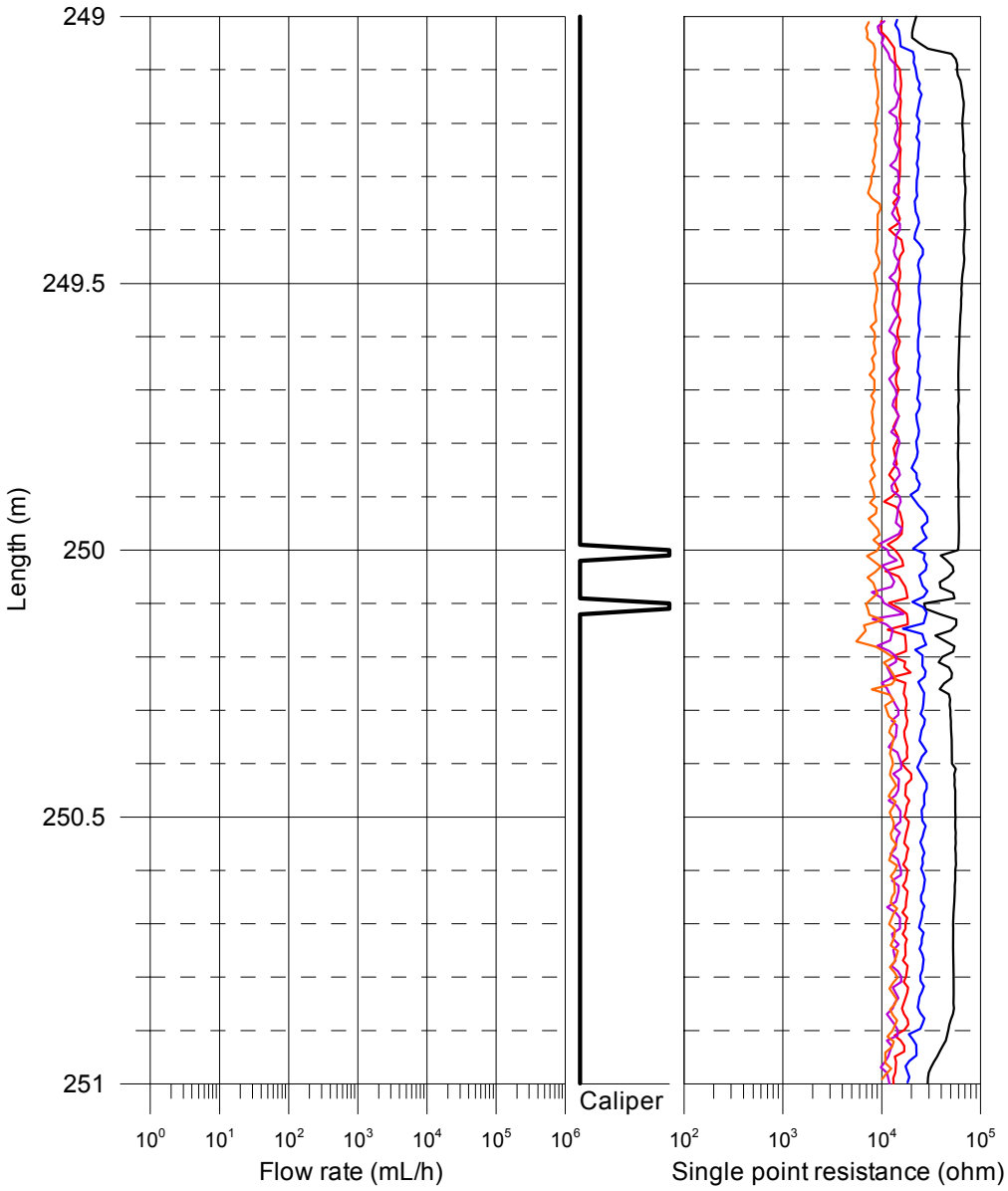

Appendix 1.11

Laxemar, borehole KLX13A
SPR and Caliper results after length correction

SPR+Caliper (downwards), 2006-09-23 - 2006-09-24
SPR without pumping (upwards) (L = 5 m), 2006-09-24 - 2006-09-25
SPR with pumping (upwards) (L = 5 m), 2006-09-26 - 2006-09-27
SPR with pumping (upwards) (L = 1 m), 2006-09-27 - 2006-09-29
SPR with pumping (upwards during fracture-EC) (L = 0.5 m), 2006-09-29 - 2006-09-30

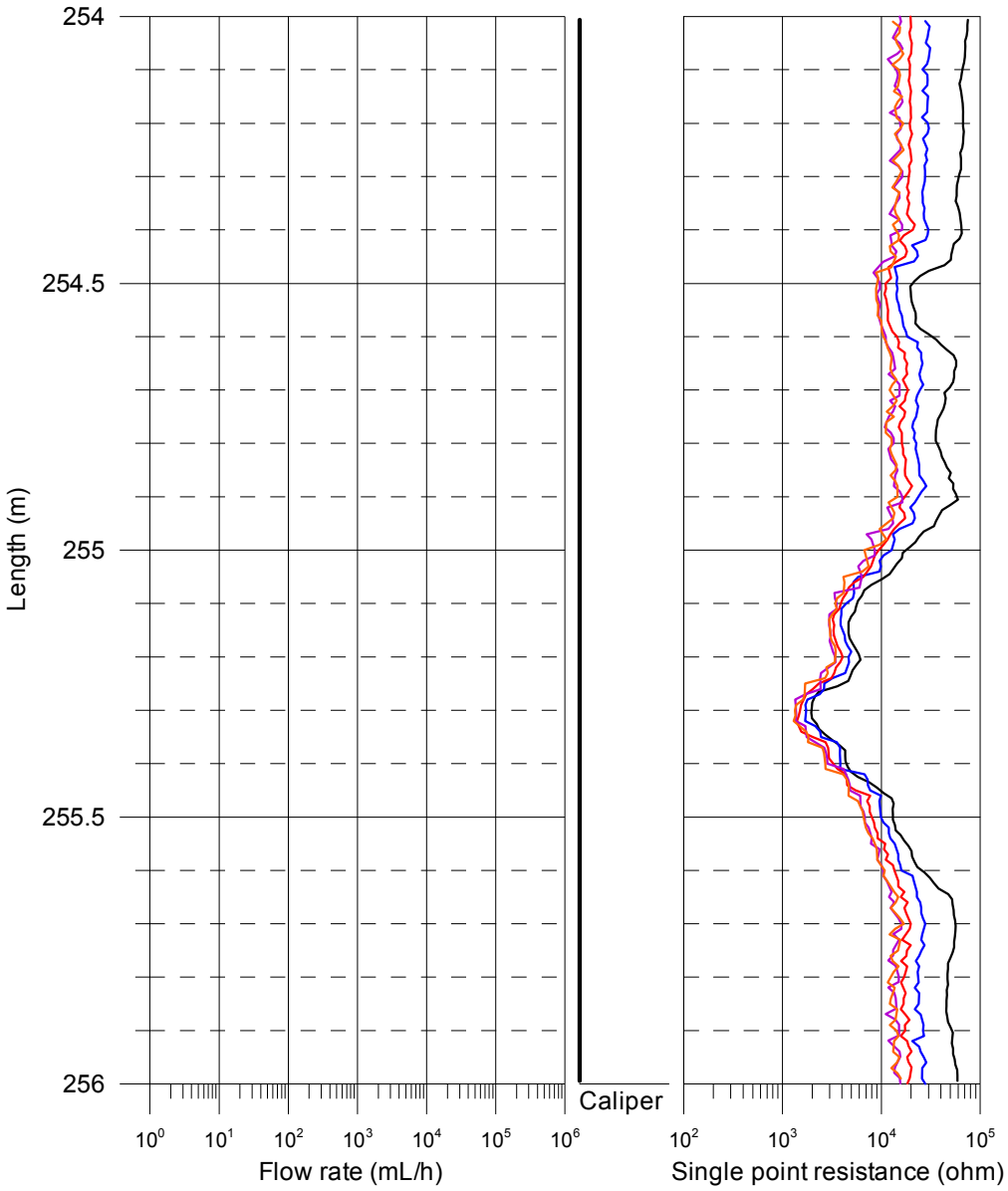

Appendix 1.12

Laxemar, borehole KLX13A
SPR and Caliper results after length correction

SPR+Caliper (downwards), 2006-09-23 - 2006-09-24
SPR without pumping (upwards) (L = 5 m), 2006-09-24 - 2006-09-25
SPR with pumping (upwards) (L = 5 m), 2006-09-26 - 2006-09-27
SPR with pumping (upwards) (L = 1 m), 2006-09-27 - 2006-09-29
SPR with pumping (upwards during fracture-EC) (L = 0.5 m), 2006-09-29 - 2006-09-30

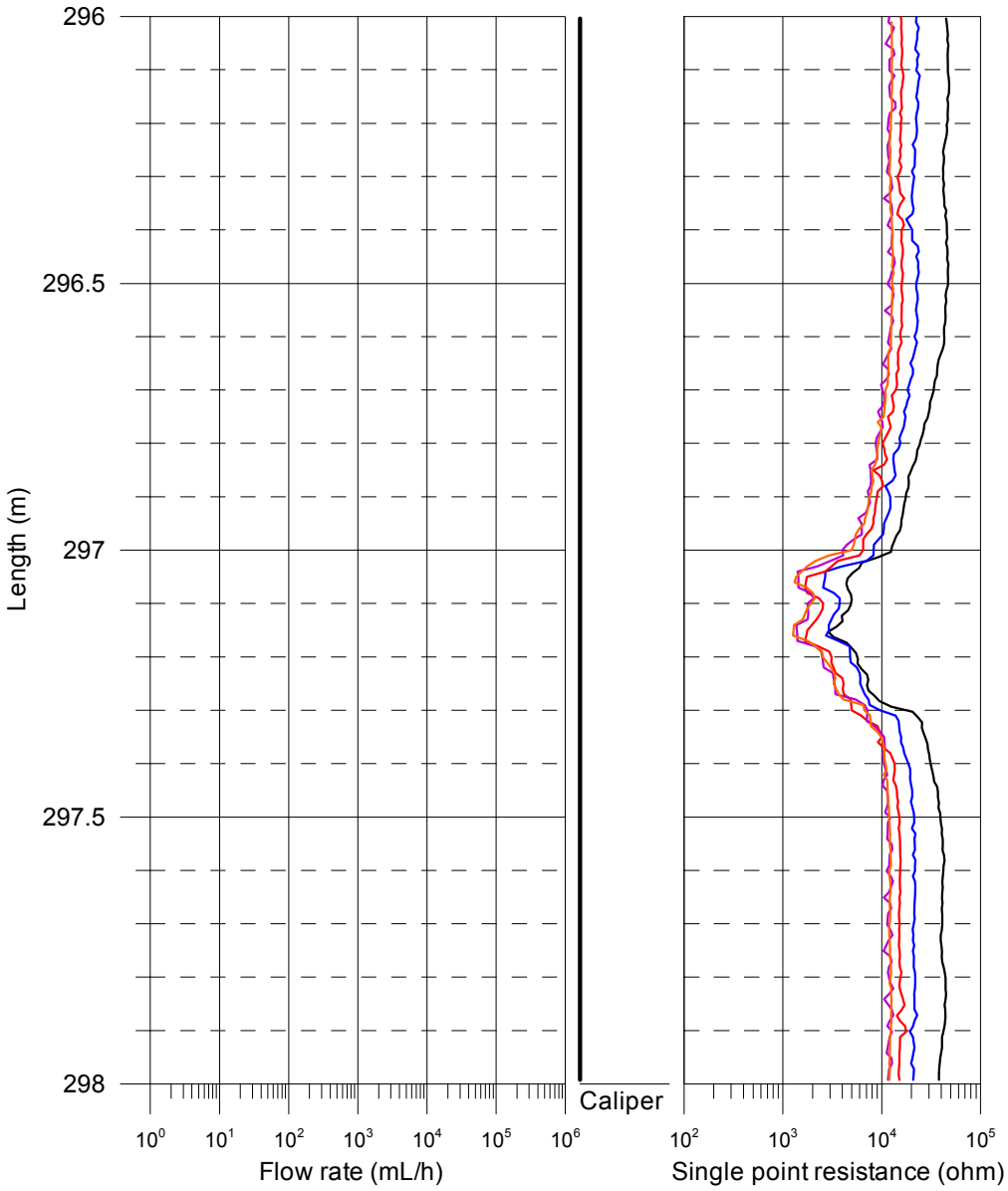

Appendix 1.13

Laxemar, borehole KLX13A
SPR and Caliper results after length correction

SPR+Caliper (downwards), 2006-09-23 - 2006-09-24
SPR without pumping (upwards) (L = 5 m), 2006-09-24 - 2006-09-25
SPR with pumping (upwards) (L = 5 m), 2006-09-26 - 2006-09-27
SPR with pumping (upwards) (L = 1 m), 2006-09-27 - 2006-09-29
SPR with pumping (upwards during fracture-EC) (L = 0.5 m), 2006-09-29 - 2006-09-30

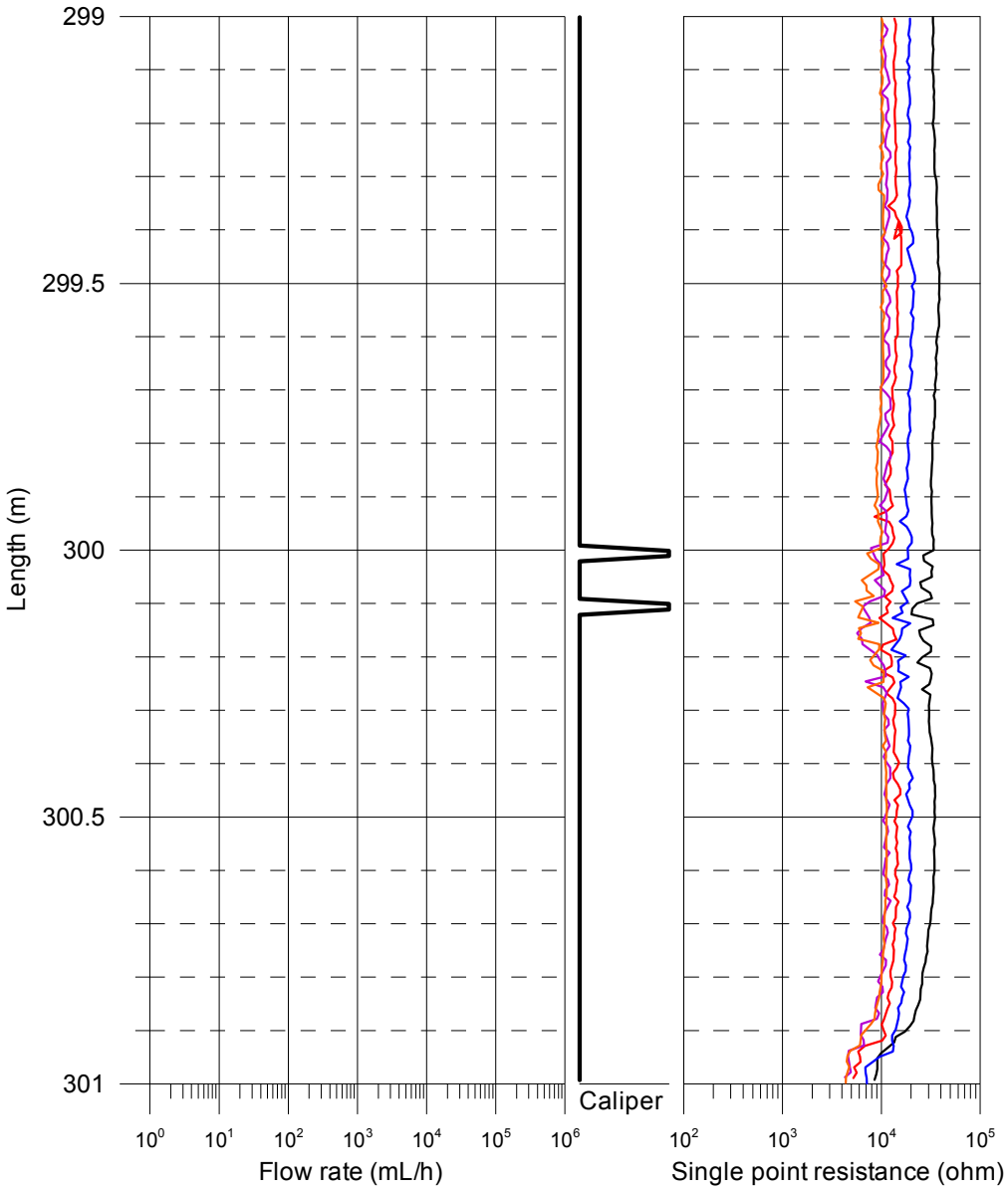

Appendix 1.14

Laxemar, borehole KLX13A
SPR and Caliper results after length correction

SPR+Caliper (downwards), 2006-09-23 - 2006-09-24
SPR without pumping (upwards) (L = 5 m), 2006-09-24 - 2006-09-25
SPR with pumping (upwards) (L = 5 m), 2006-09-26 - 2006-09-27
SPR with pumping (upwards) (L = 1 m), 2006-09-27 - 2006-09-29
SPR with pumping (upwards during fracture-EC) (L = 0.5 m), 2006-09-29 - 2006-09-30

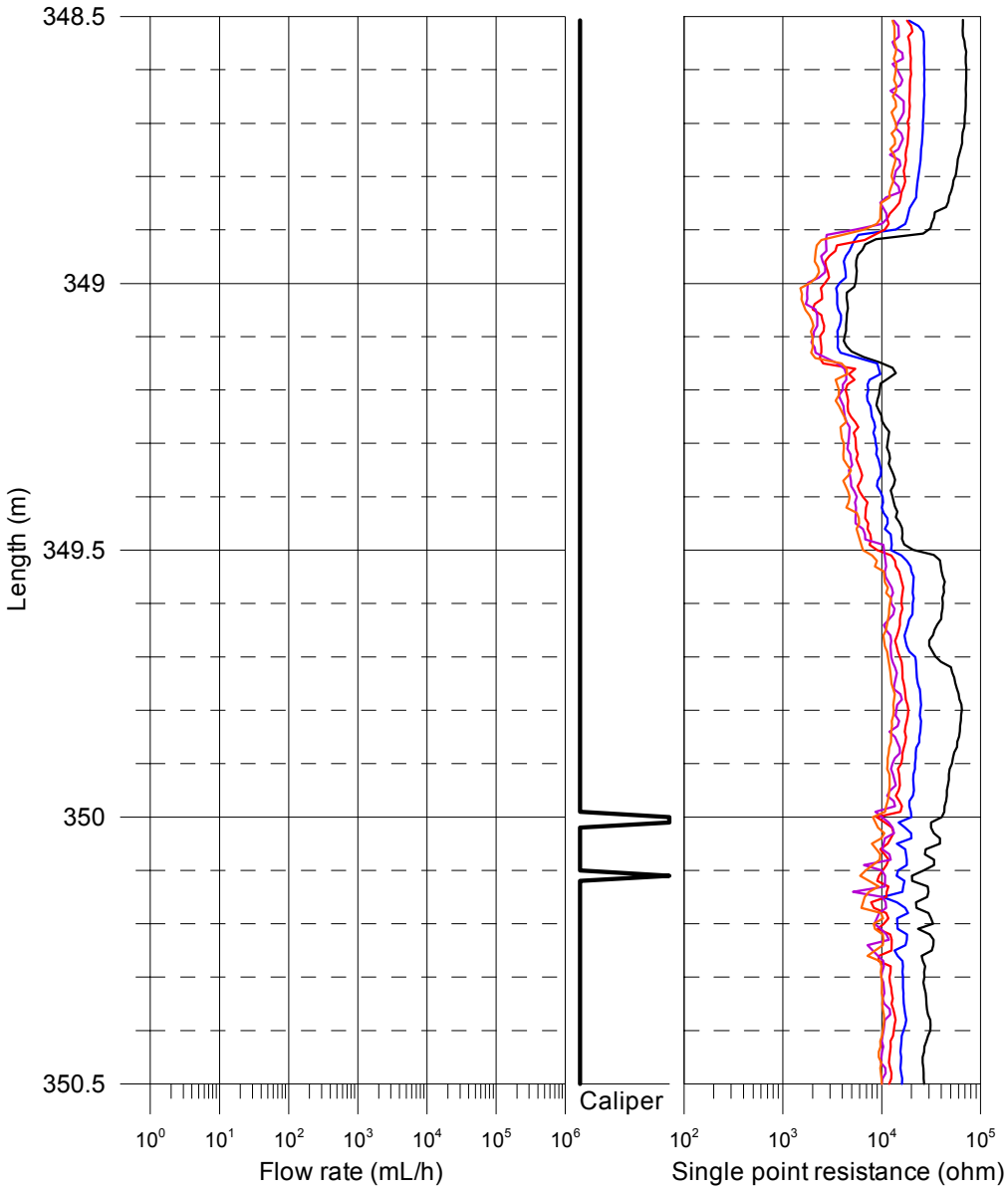

Appendix 1.15

Laxemar, borehole KLX13A
SPR and Caliper results after length correction

SPR+Caliper (downwards), 2006-09-23 - 2006-09-24
SPR without pumping (upwards) (L = 5 m), 2006-09-24 - 2006-09-25
SPR with pumping (upwards) (L = 5 m), 2006-09-26 - 2006-09-27
SPR with pumping (upwards) (L = 1 m), 2006-09-27 - 2006-09-29
SPR with pumping (upwards during fracture-EC) (L = 0.5 m), 2006-09-29 - 2006-09-30

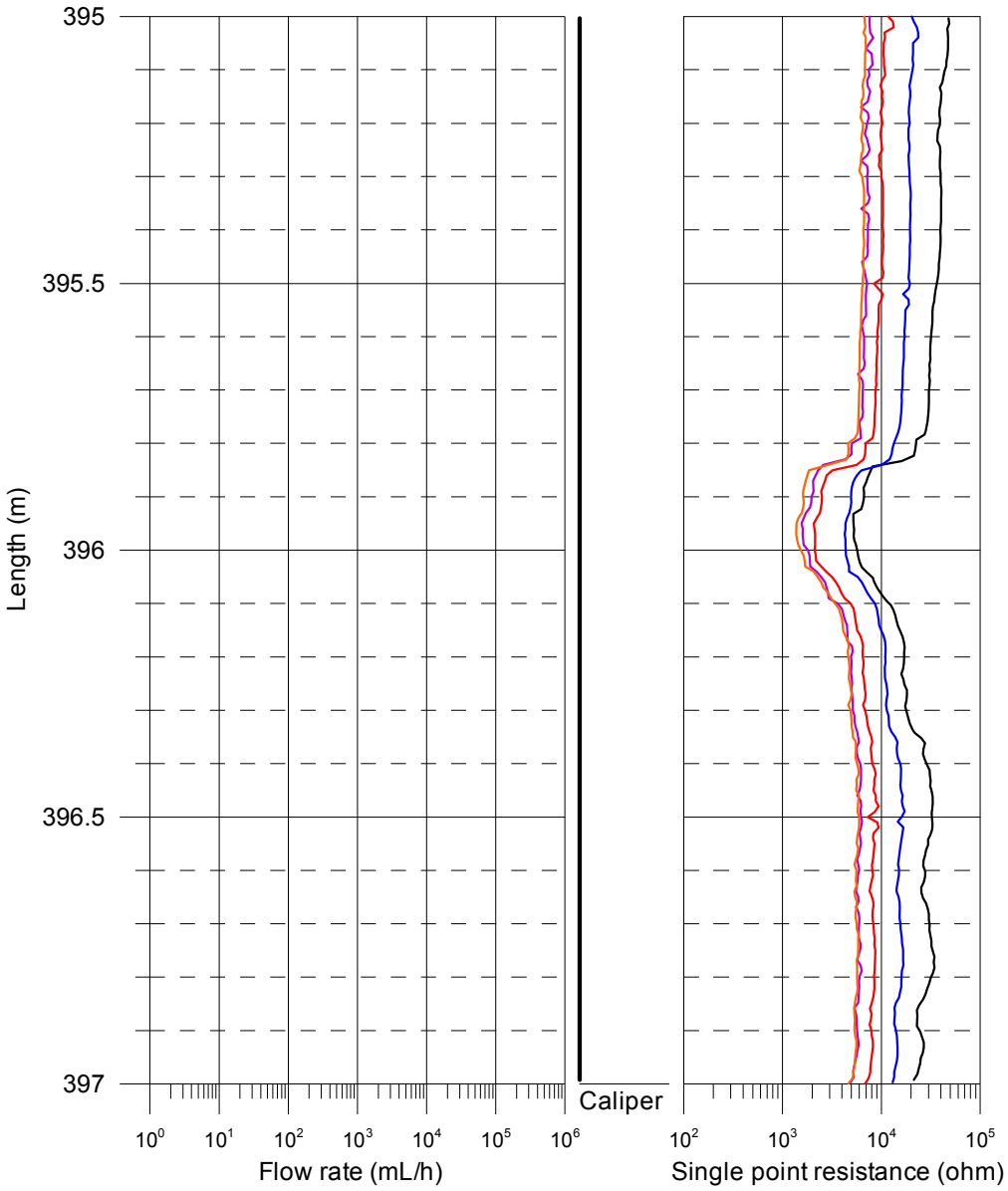

Appendix 1.16

Laxemar, borehole KLX13A
SPR and Caliper results after length correction

SPR+Caliper (downwards), 2006-09-23 - 2006-09-24
SPR without pumping (upwards) (L = 5 m), 2006-09-24 - 2006-09-25
SPR with pumping (upwards) (L = 5 m), 2006-09-26 - 2006-09-27
SPR with pumping (upwards) (L = 1 m), 2006-09-27 - 2006-09-29
SPR with pumping (upwards during fracture-EC) (L = 0.5 m), 2006-09-29 - 2006-09-30

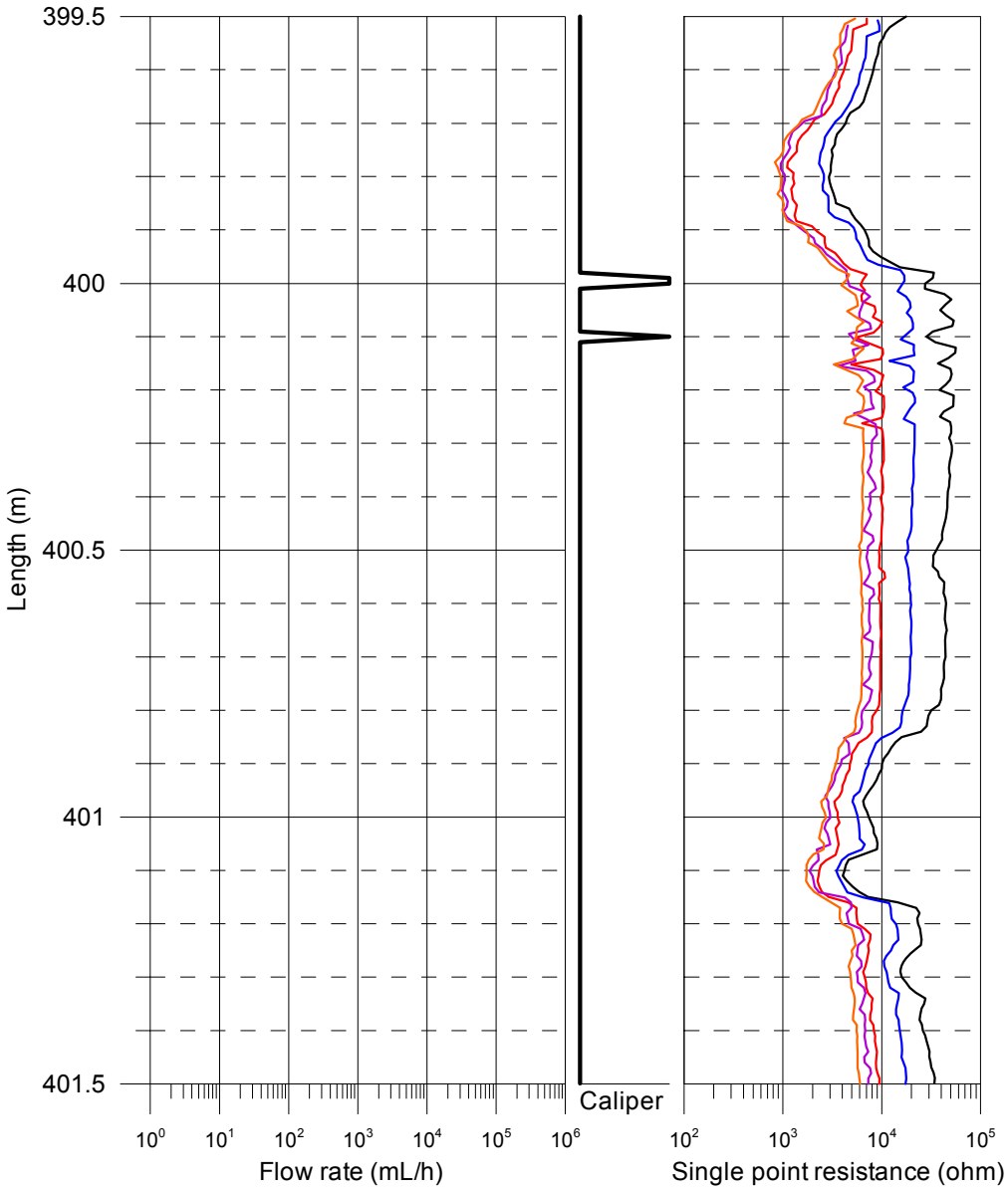

Appendix 1.17

Laxemar, borehole KLX13A
SPR and Caliper results after length correction

SPR+Caliper (downwards), 2006-09-23 - 2006-09-24
SPR without pumping (upwards) (L = 5 m), 2006-09-24 - 2006-09-25
SPR with pumping (upwards) (L = 5 m), 2006-09-26 - 2006-09-27
SPR with pumping (upwards) (L = 1 m), 2006-09-27 - 2006-09-29
SPR with pumping (upwards during fracture-EC) (L = 0.5 m), 2006-09-29 - 2006-09-30

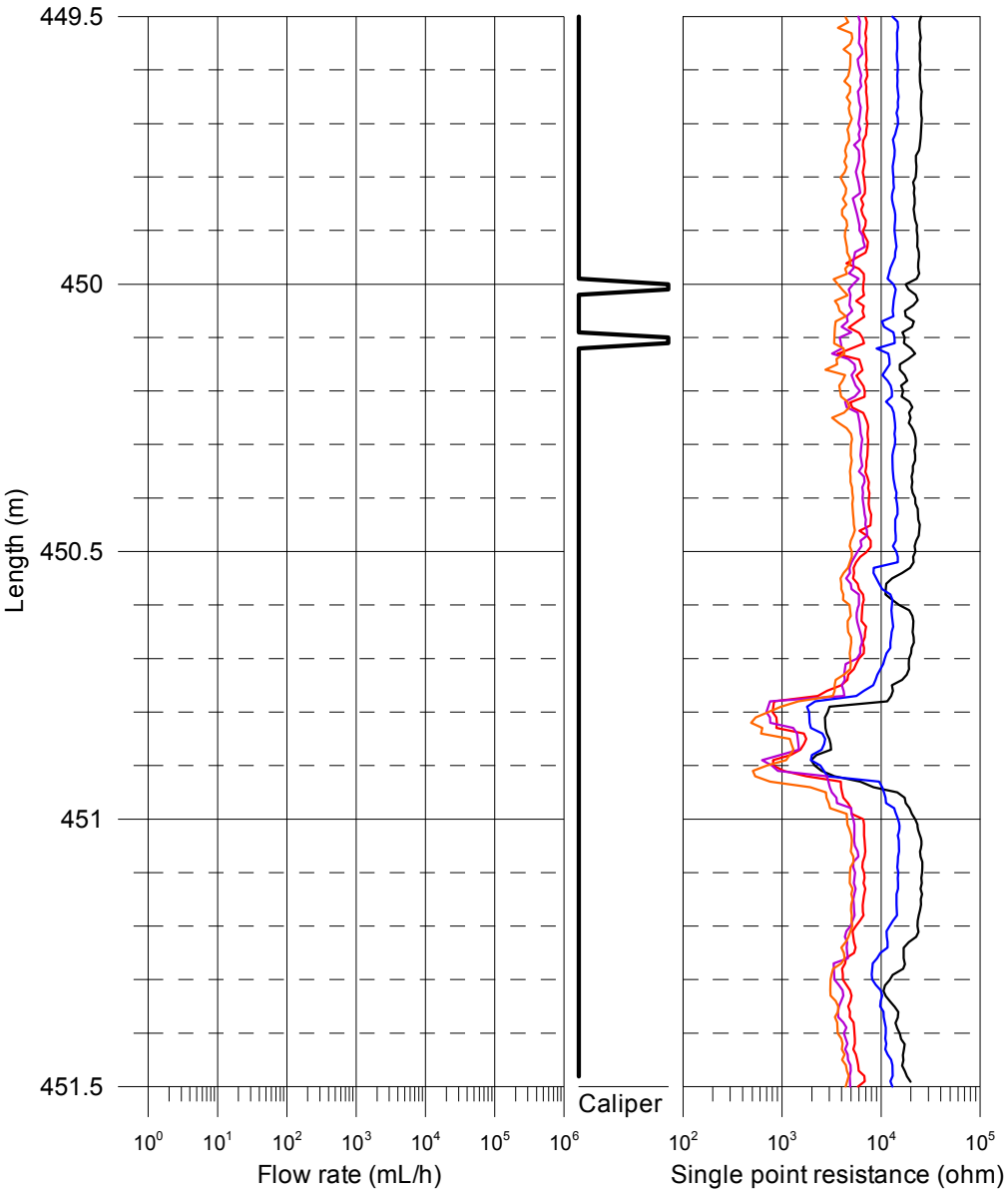

Appendix 1.18

Laxemar, borehole KLX13A
SPR and Caliper results after length correction

SPR+Caliper (downwards), 2006-09-23 - 2006-09-24
SPR without pumping (upwards) (L = 5 m), 2006-09-24 - 2006-09-25
SPR with pumping (upwards) (L = 5 m), 2006-09-26 - 2006-09-27
SPR with pumping (upwards) (L = 1 m), 2006-09-27 - 2006-09-29
SPR with pumping (upwards during fracture-EC) (L = 0.5 m), 2006-09-29 - 2006-09-30

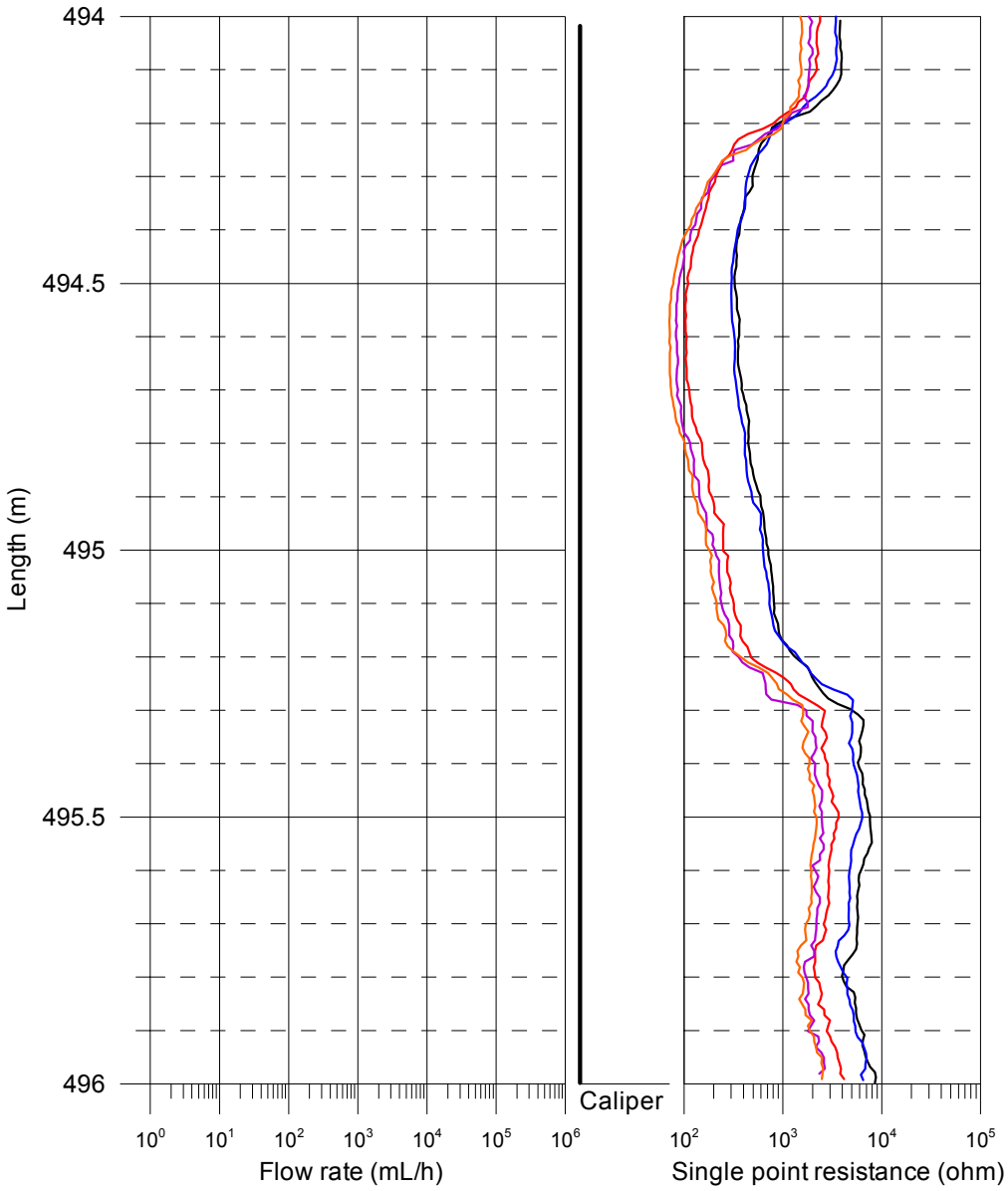

Appendix 1.19

Laxemar, borehole KLX13A
SPR and Caliper results after length correction

SPR+Caliper (downwards), 2006-09-23 - 2006-09-24
SPR without pumping (upwards) (L = 5 m), 2006-09-24 - 2006-09-25
SPR with pumping (upwards) (L = 5 m), 2006-09-26 - 2006-09-27
SPR with pumping (upwards) (L = 1 m), 2006-09-27 - 2006-09-29
SPR with pumping (upwards during fracture-EC) (L = 0.5 m), 2006-09-29 - 2006-09-30

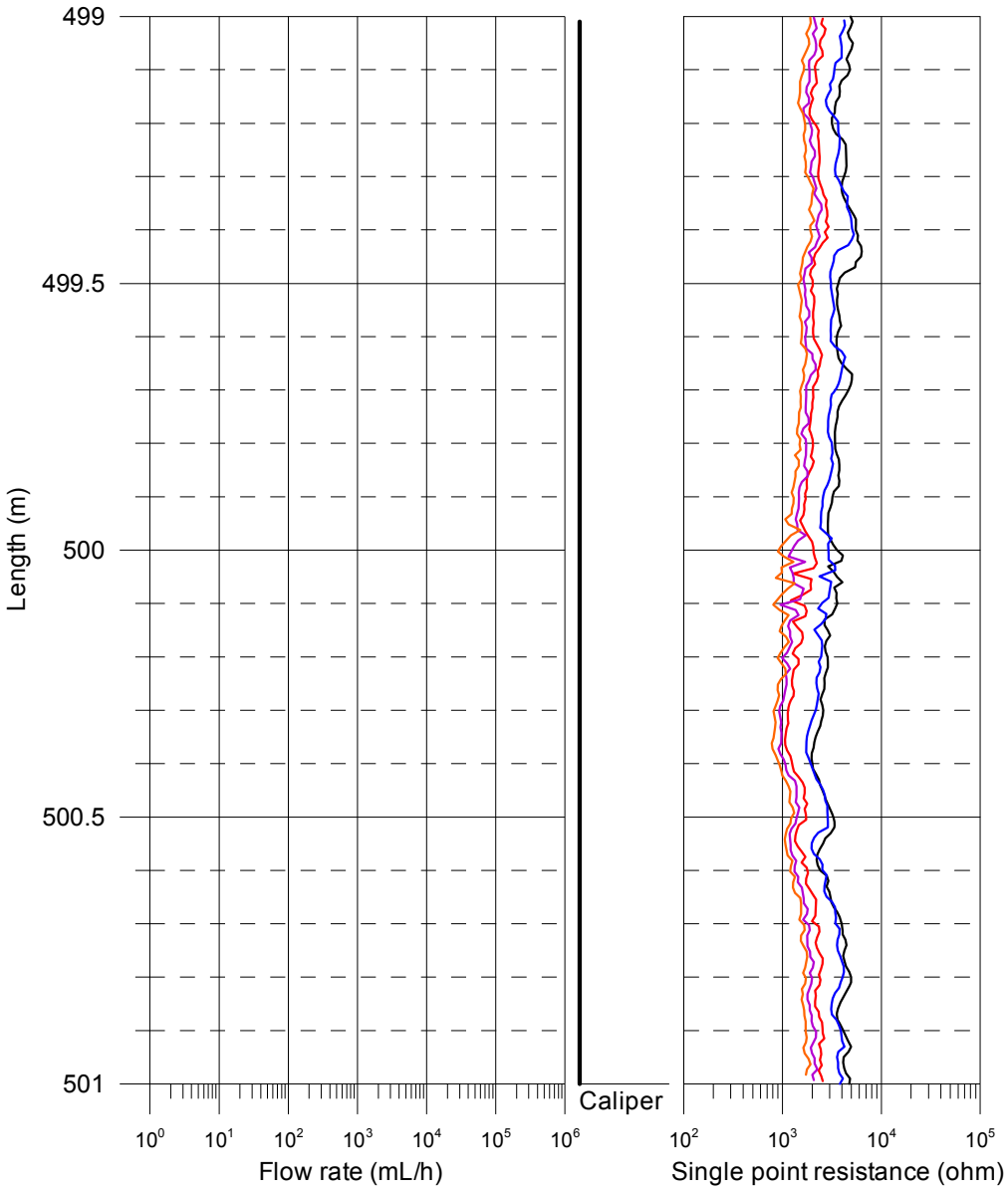

Appendix 1.20

Laxemar, borehole KLX13A
SPR and Caliper results after length correction

SPR+Caliper (downwards), 2006-09-23 - 2006-09-24
SPR without pumping (upwards) (L = 5 m), 2006-09-24 - 2006-09-25
SPR with pumping (upwards) (L = 5 m), 2006-09-26 - 2006-09-27
SPR with pumping (upwards) (L = 1 m), 2006-09-27 - 2006-09-29
SPR with pumping (upwards during fracture-EC) (L = 0.5 m), 2006-09-29 - 2006-09-30

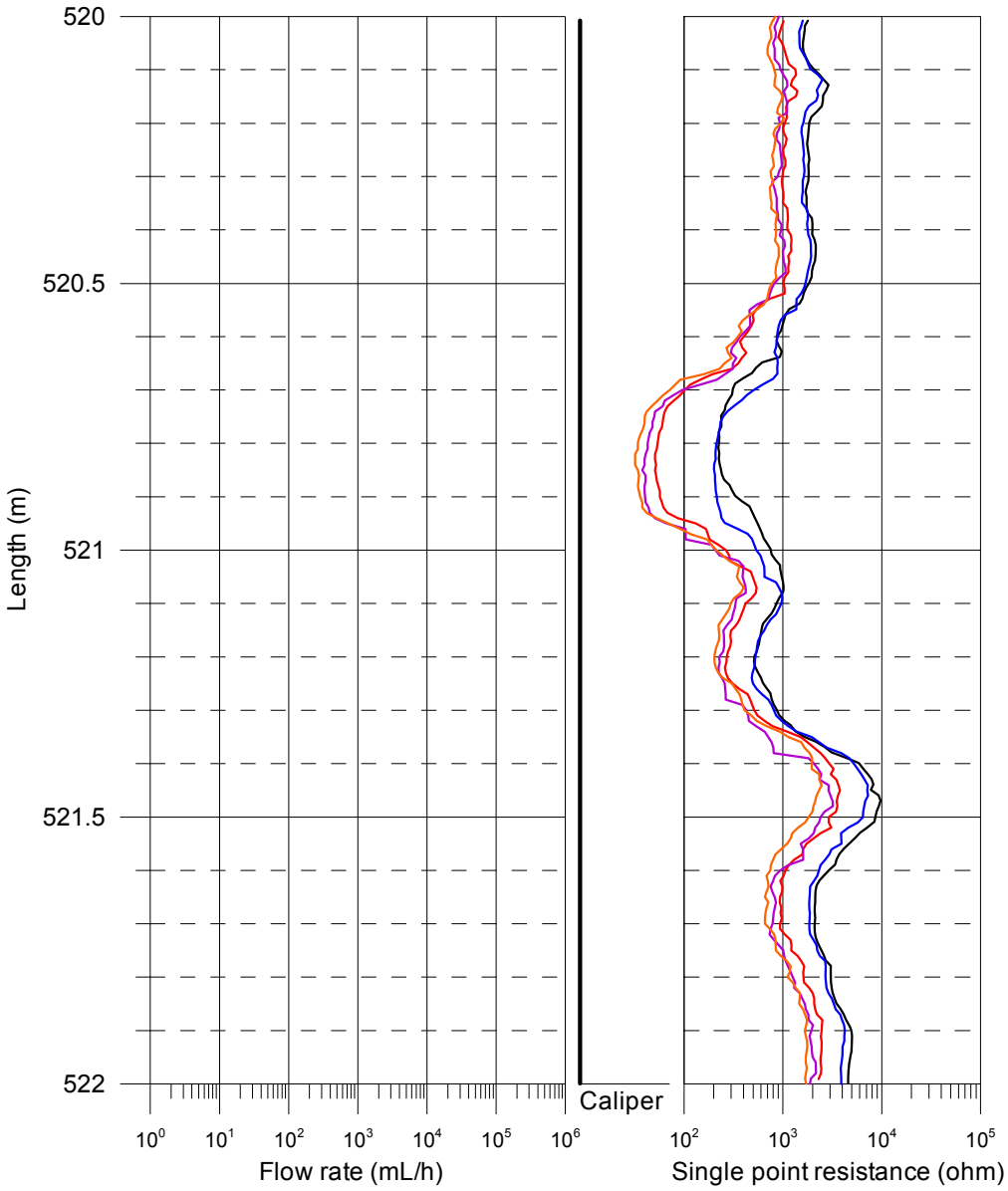

Appendix 1.21

Laxemar, borehole KLX13A
SPR and Caliper results after length correction

SPR+Caliper (downwards), 2006-09-23 - 2006-09-24
SPR without pumping (upwards) (L = 5 m), 2006-09-24 - 2006-09-25
SPR with pumping (upwards) (L = 5 m), 2006-09-26 - 2006-09-27
SPR with pumping (upwards) (L = 1 m), 2006-09-27 - 2006-09-29
SPR with pumping (upwards during fracture-EC) (L = 0.5 m), 2006-09-29 - 2006-09-30

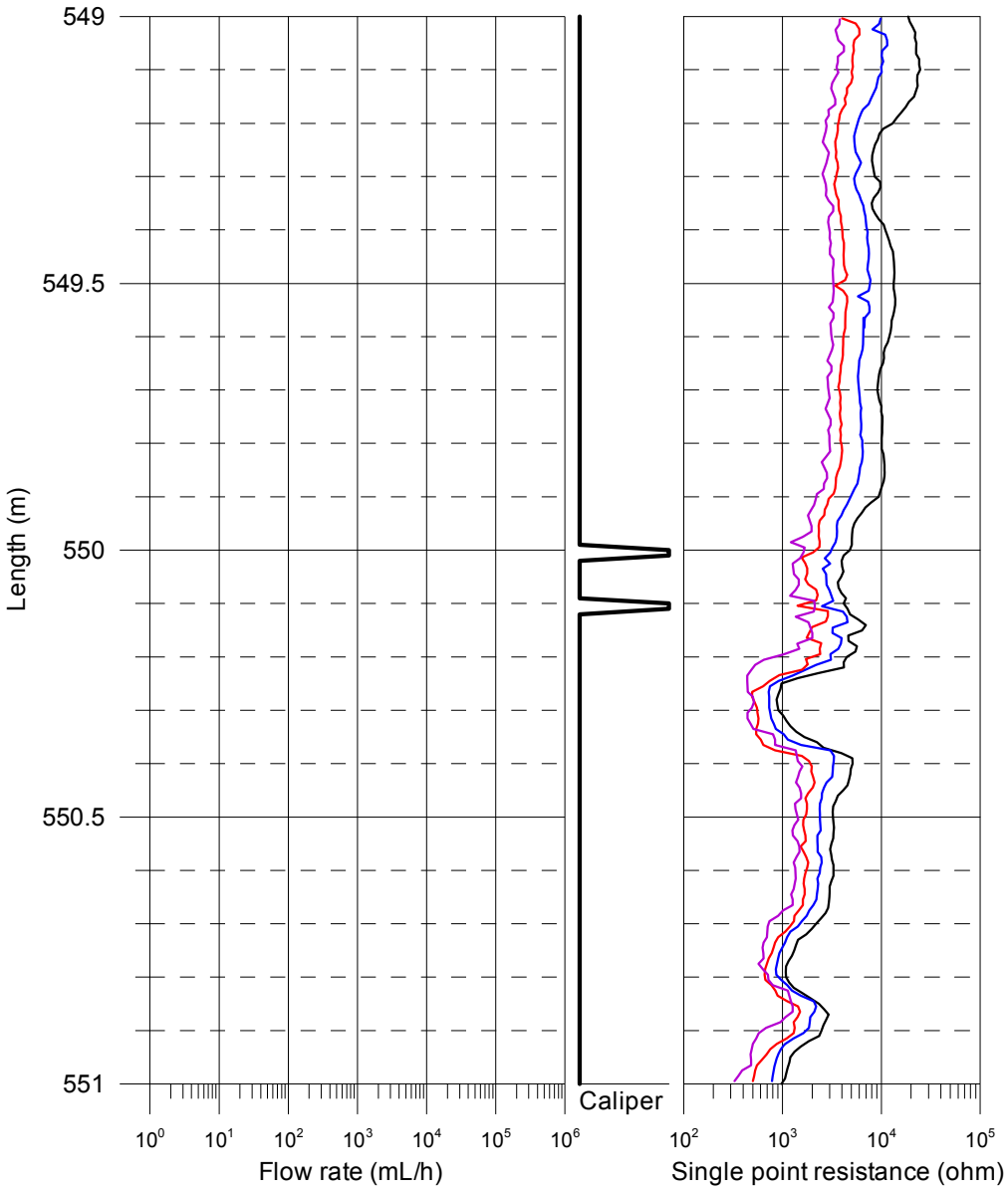

Appendix 1.22

Laxemar, borehole KLX13A
SPR and Caliper results after length correction

SPR+Caliper (downwards), 2006-09-23 - 2006-09-24
SPR without pumping (upwards) (L = 5 m), 2006-09-24 - 2006-09-25
SPR with pumping (upwards) (L = 5 m), 2006-09-26 - 2006-09-27
SPR with pumping (upwards) (L = 1 m), 2006-09-27 - 2006-09-29
SPR with pumping (upwards during fracture-EC) (L = 0.5 m), 2006-09-29 - 2006-09-30

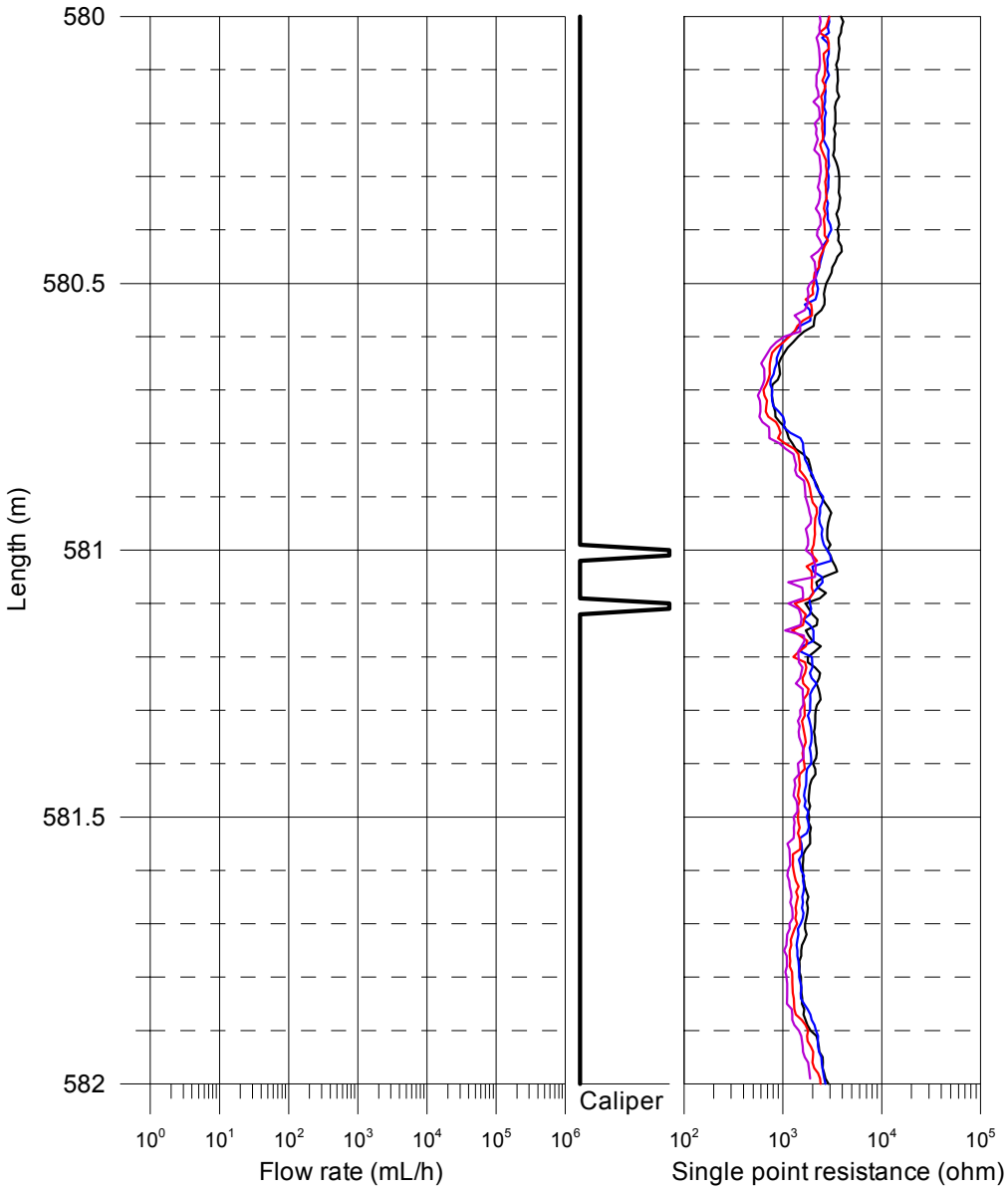

Appendix 1.23

Laxemar, borehole KLX13A
Length correction

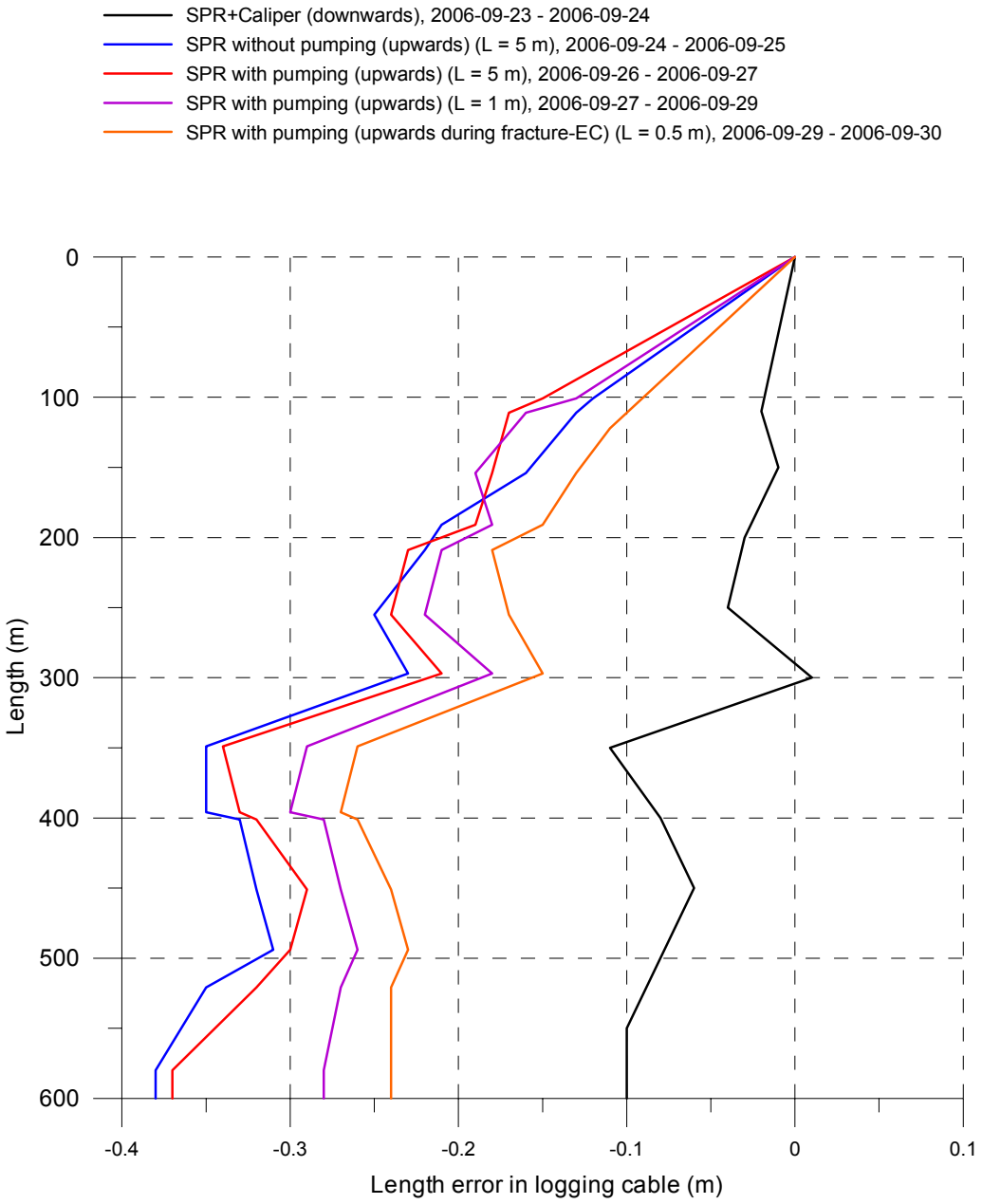

Appendix 2.1

Laxemar, borehole KLX13A
Electric conductivity of borehole water

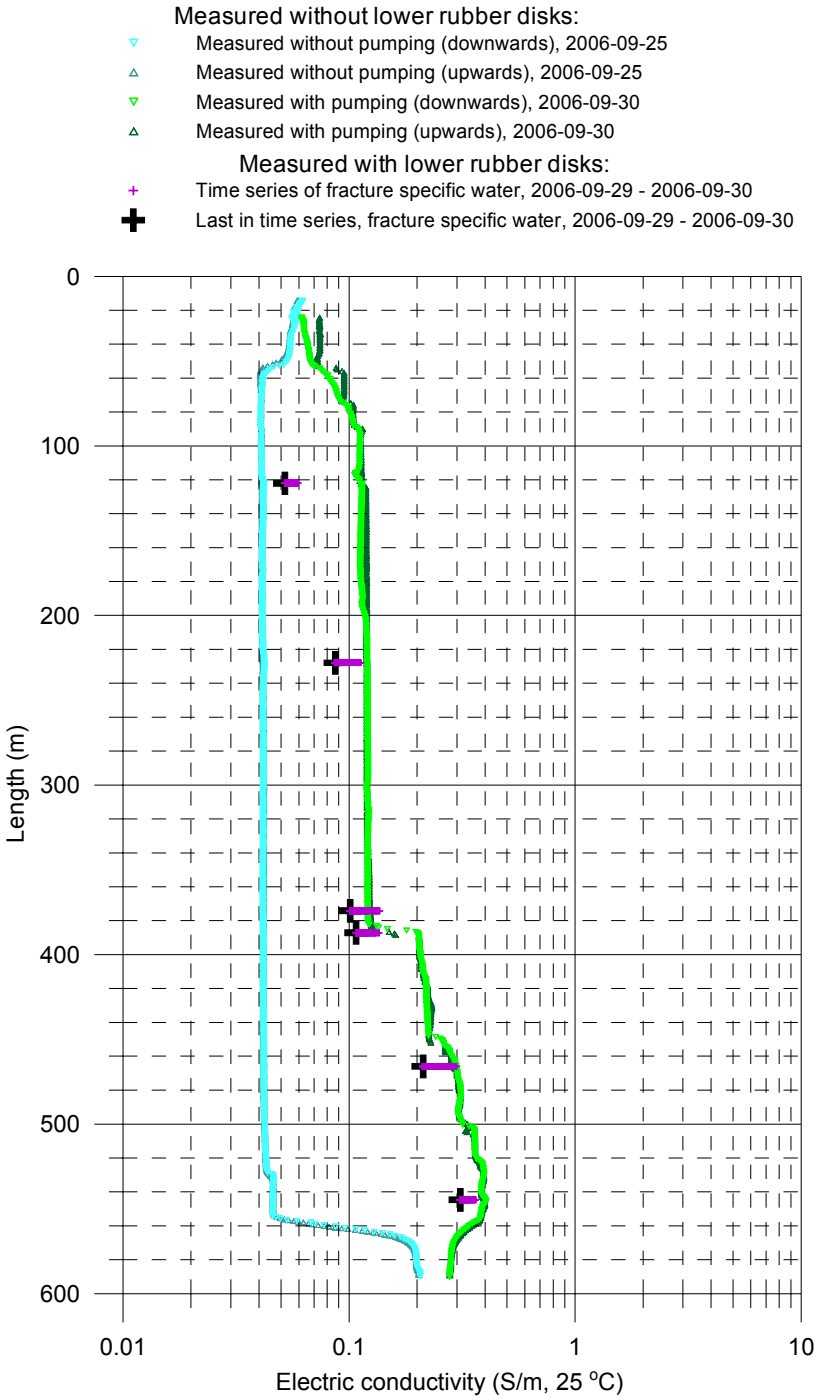

Appendix 2.2

Laxemar, borehole KLX13A
Temperature of borehole water

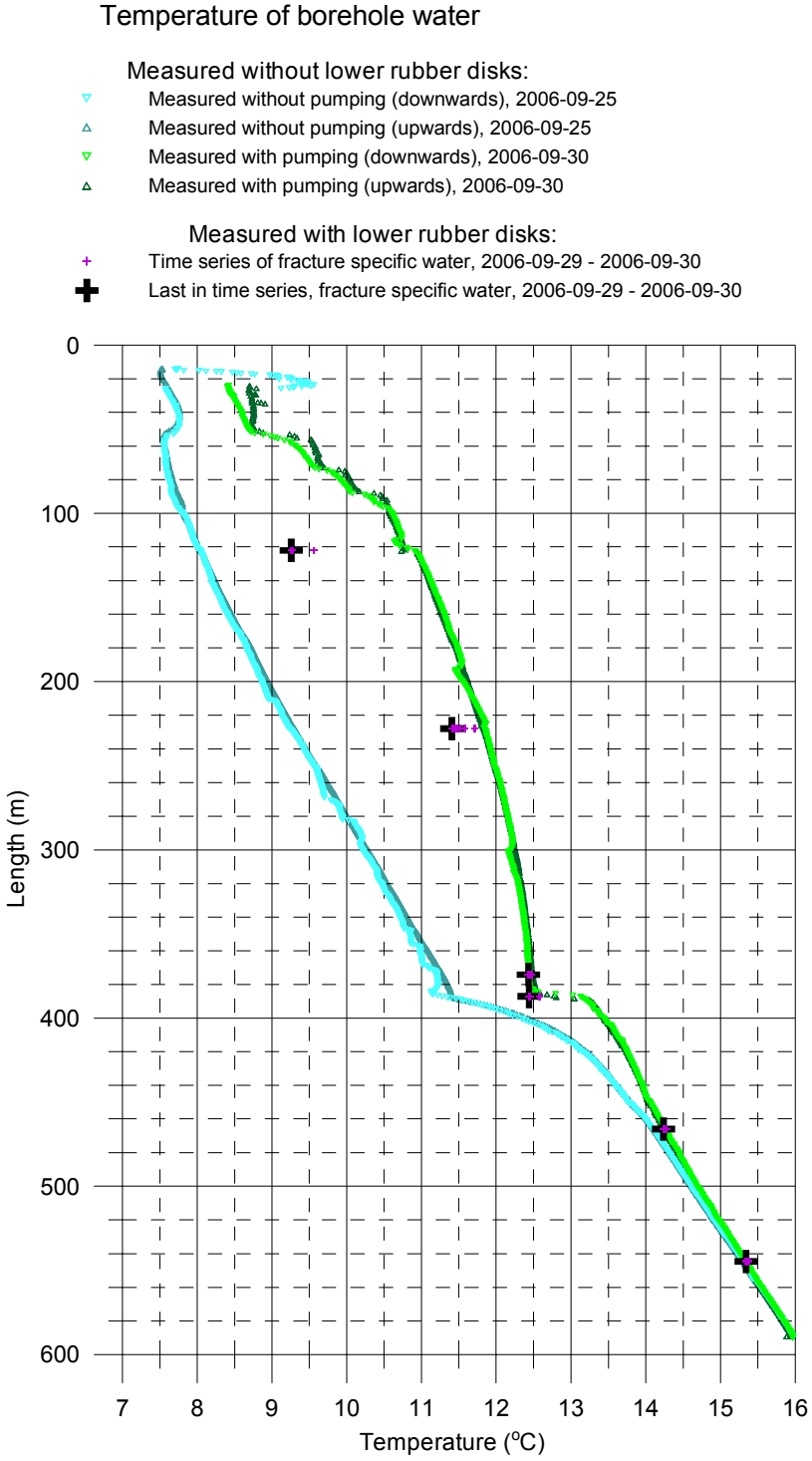

Appendix 3.1

Laxemar, borehole KLX13A
Flow rate, caliper and single point resistance

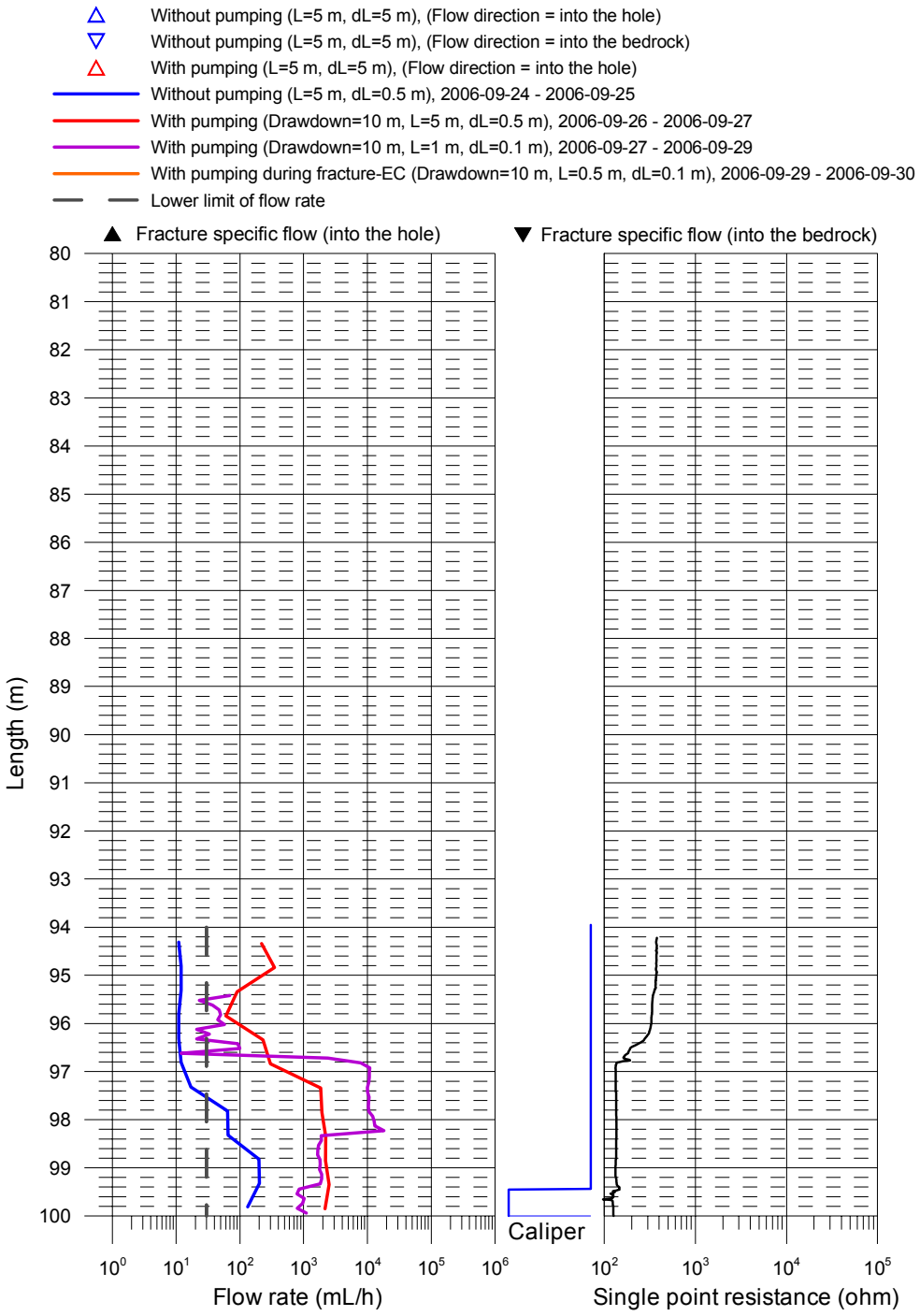

Appendix 3.2

Laxemar, borehole KLX13A
Flow rate, caliper and single point resistance

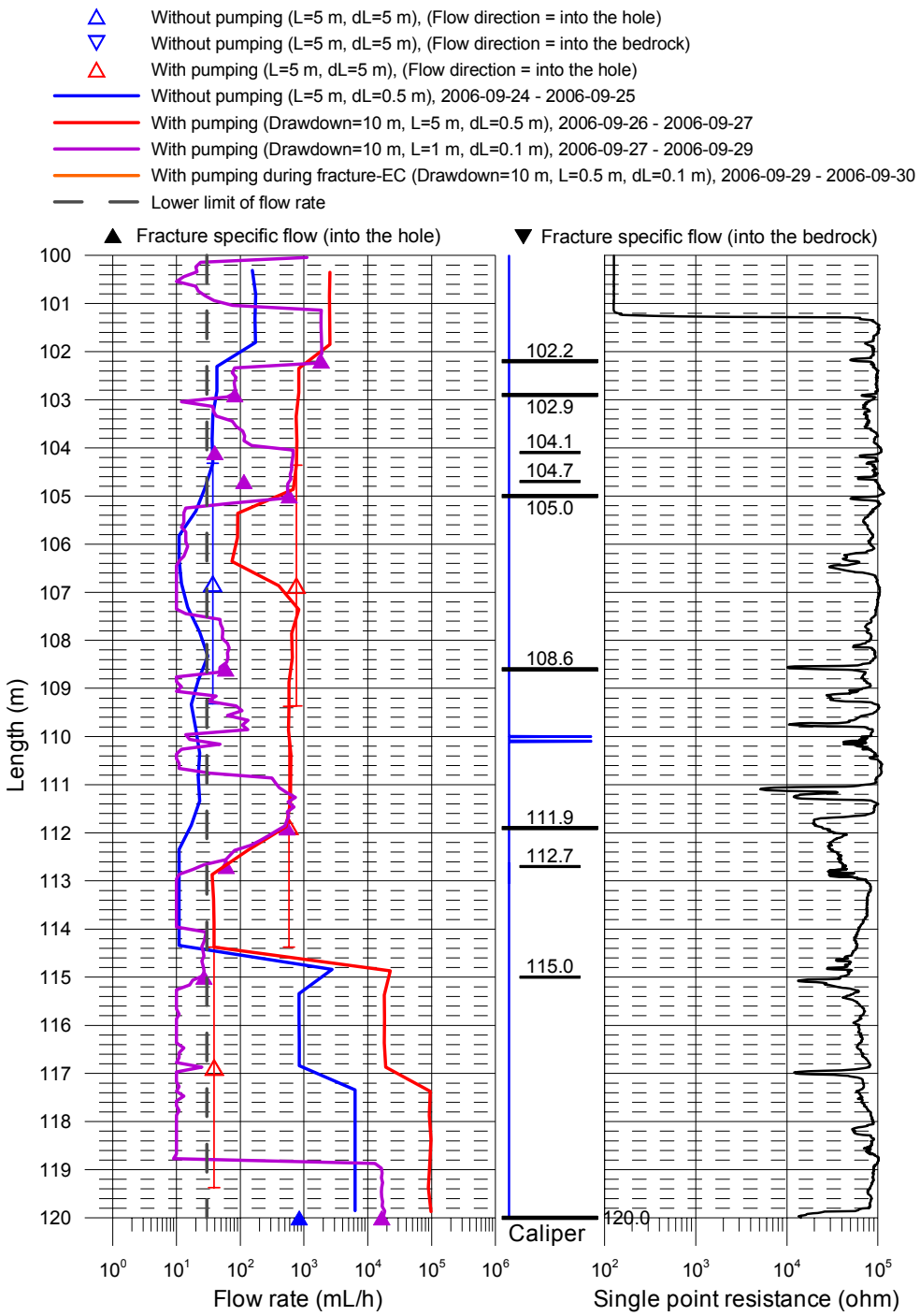

Appendix 3.3

Laxemar, borehole KLX13A
Flow rate, caliper and single point resistance

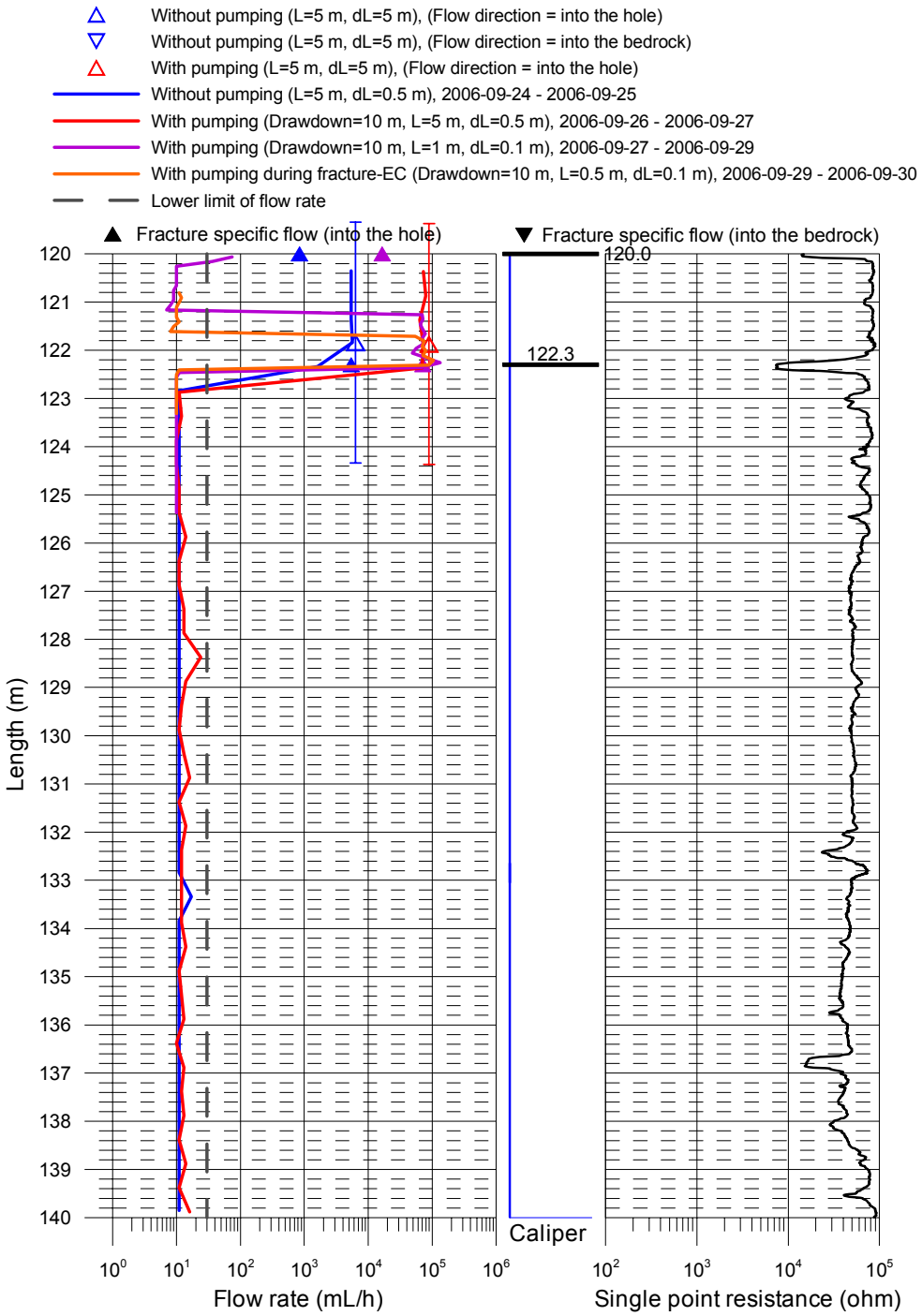

Appendix 3.4

Laxemar, borehole KLX13A
Flow rate, caliper and single point resistance

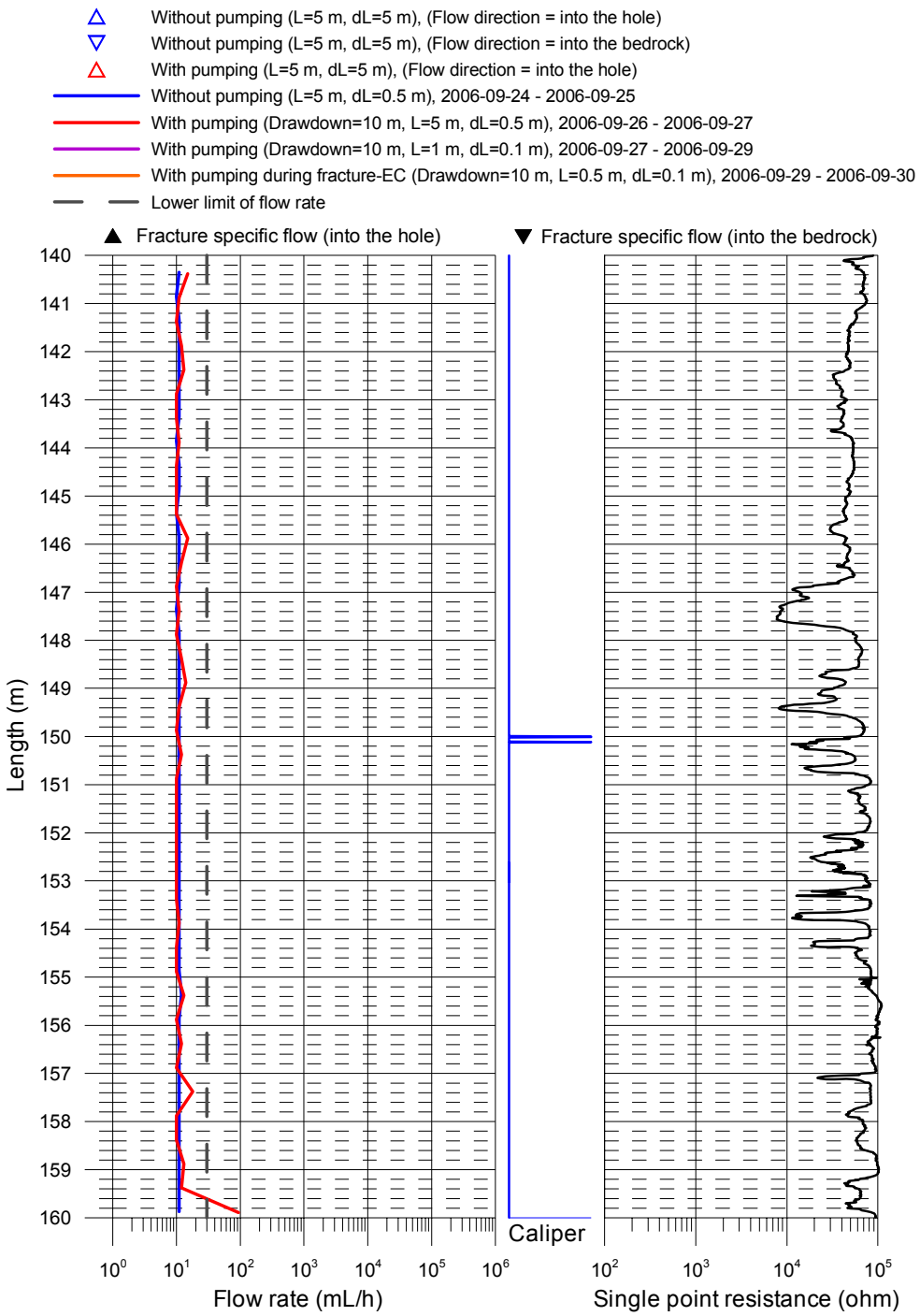

Appendix 3.5

Laxemar, borehole KLX13A
Flow rate, caliper and single point resistance

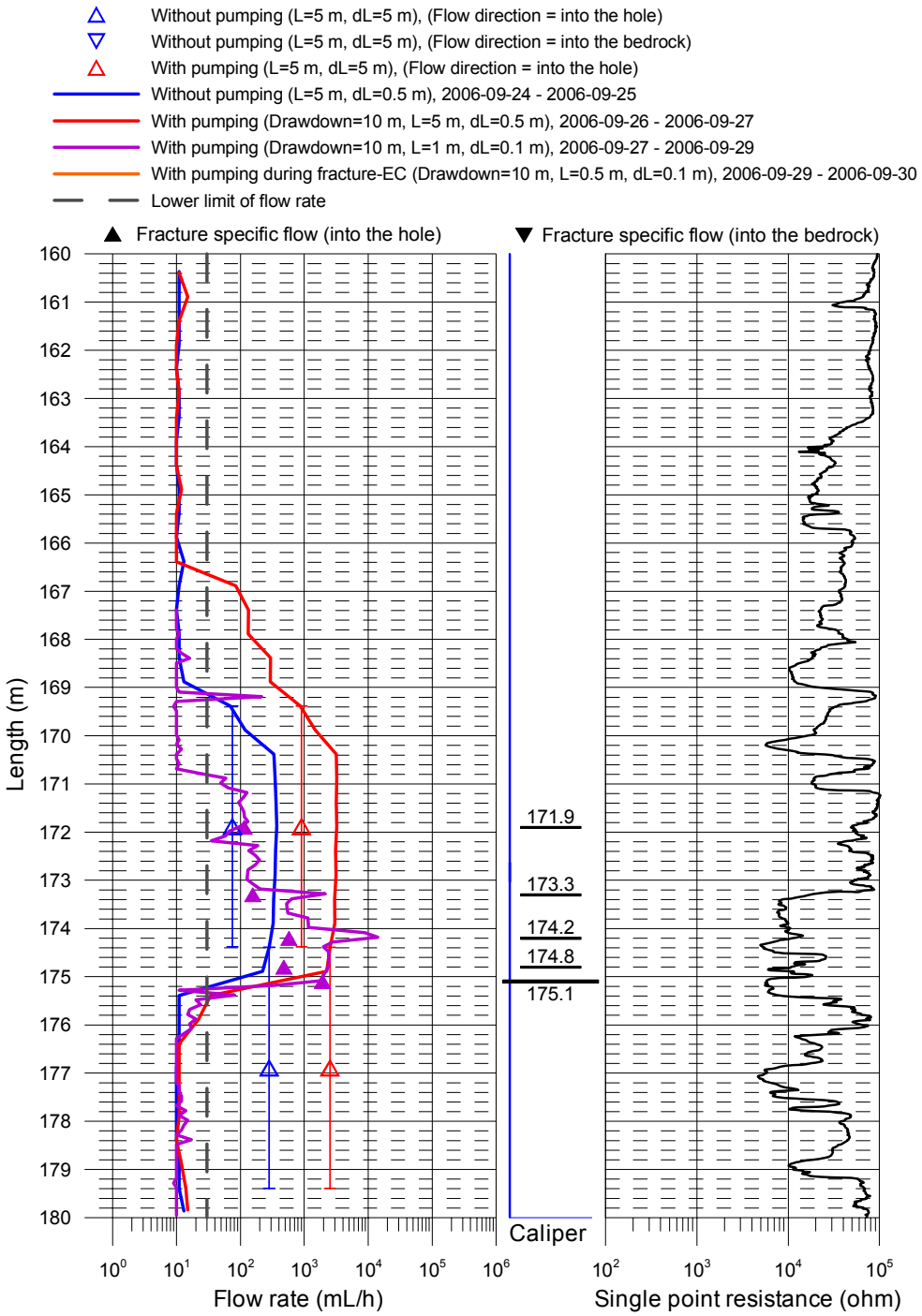

Appendix 3.6

Laxemar, borehole KLX13A
Flow rate, caliper and single point resistance

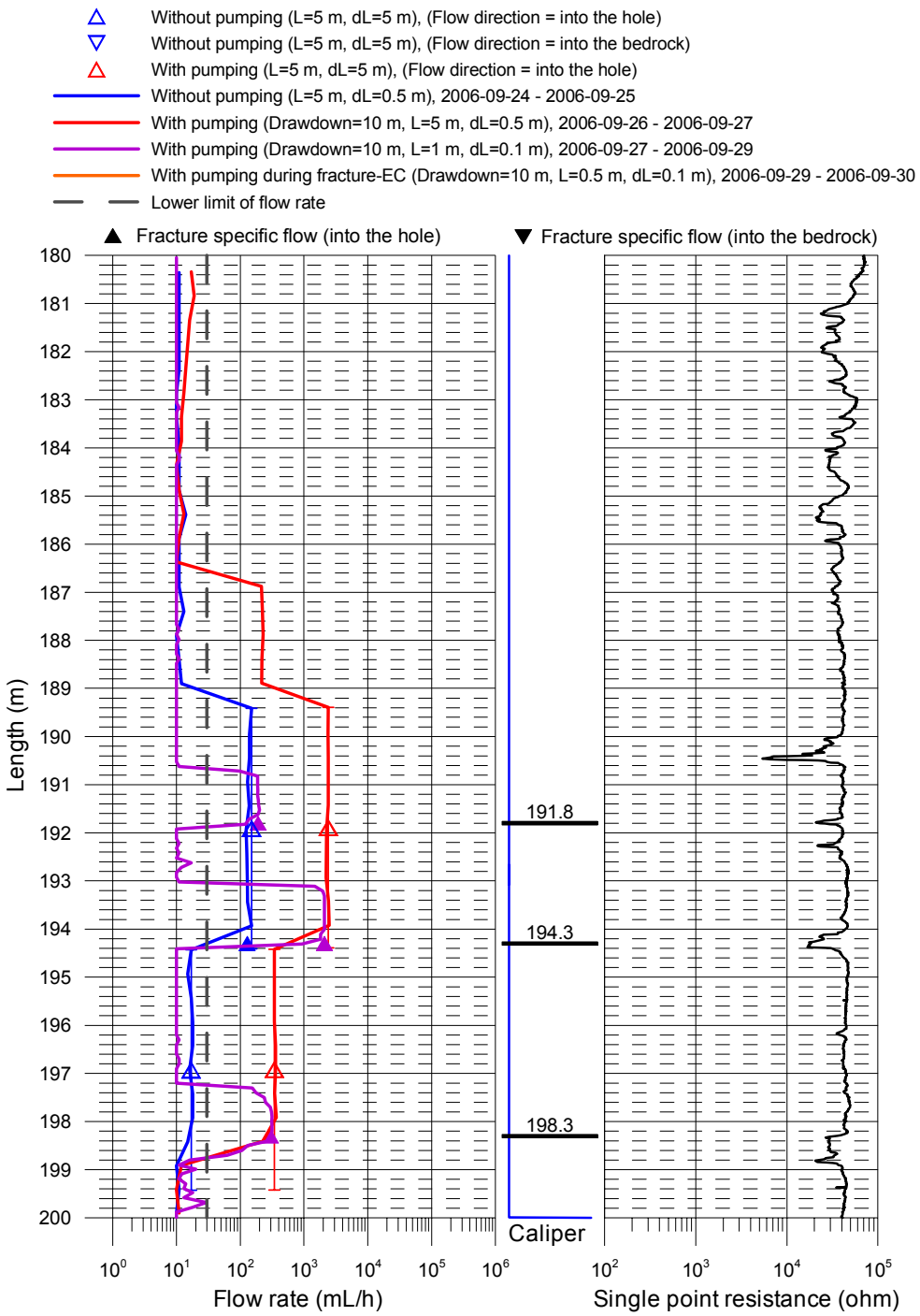

Appendix 3.7

Laxemar, borehole KLX13A
Flow rate, caliper and single point resistance

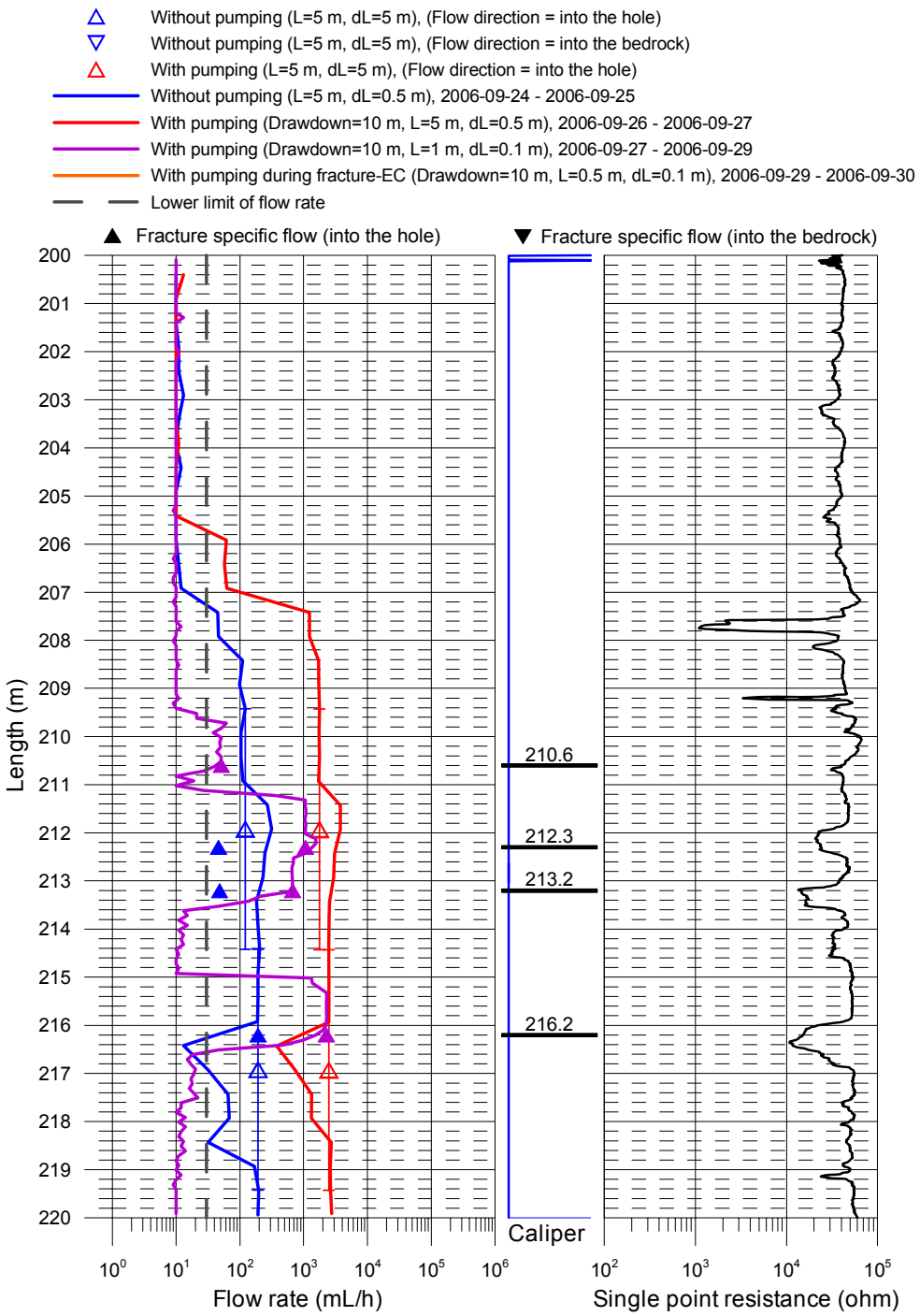

Appendix 3.8

Laxemar, borehole KLX13A
Flow rate, caliper and single point resistance

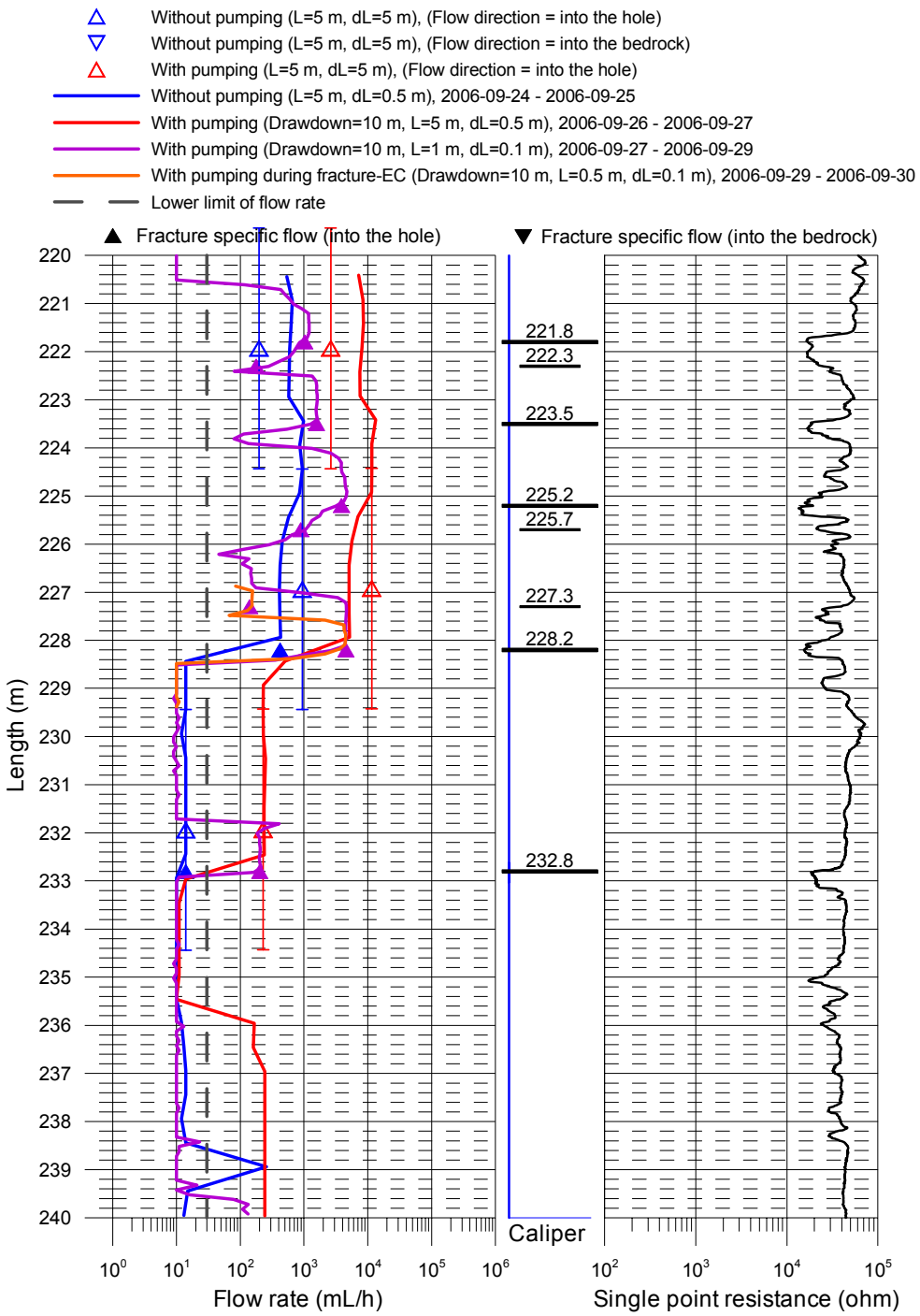

Appendix 3.9

Laxemar, borehole KLX13A
Flow rate, caliper and single point resistance

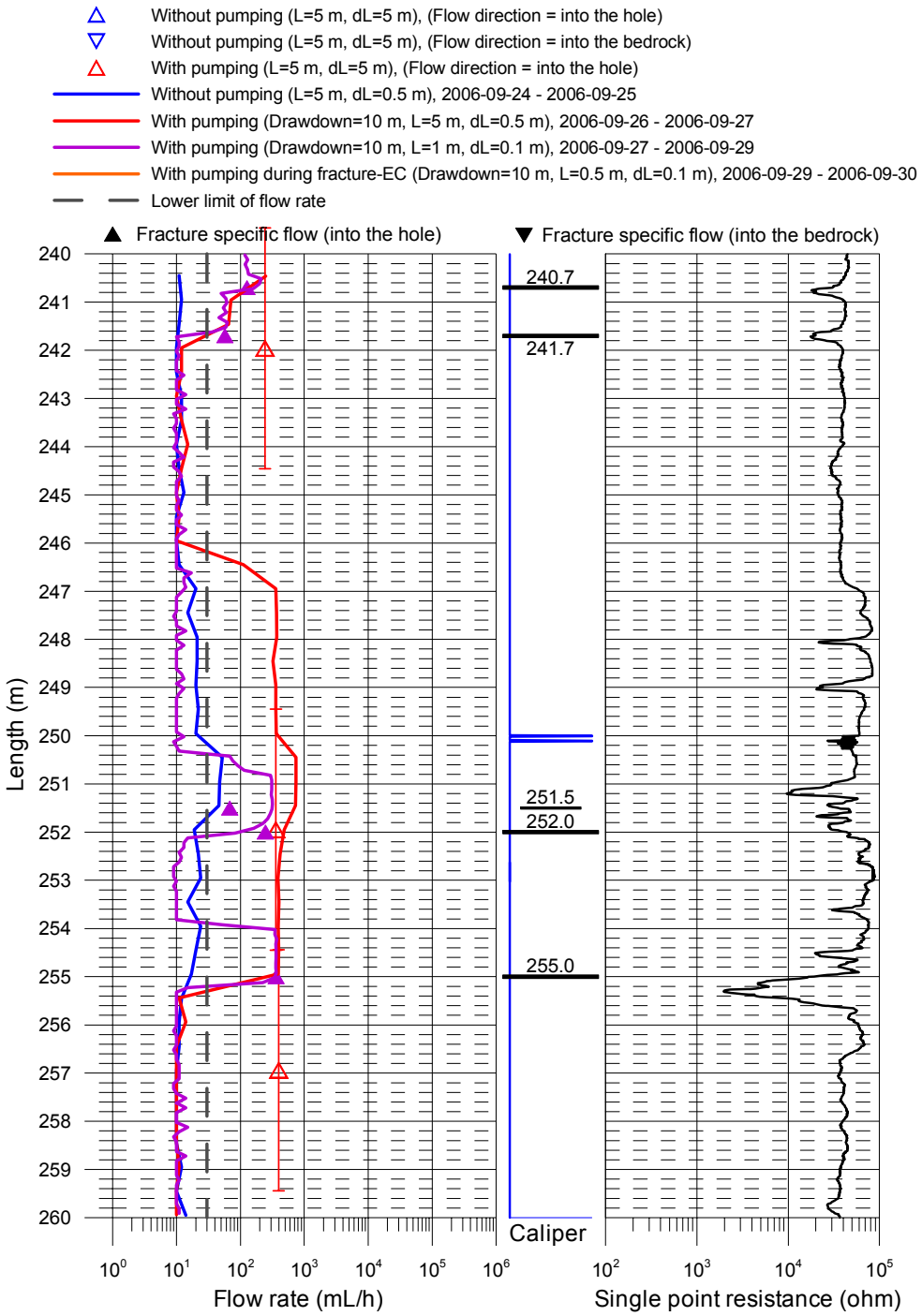

Appendix 3.10

Laxemar, borehole KLX13A
Flow rate, caliper and single point resistance

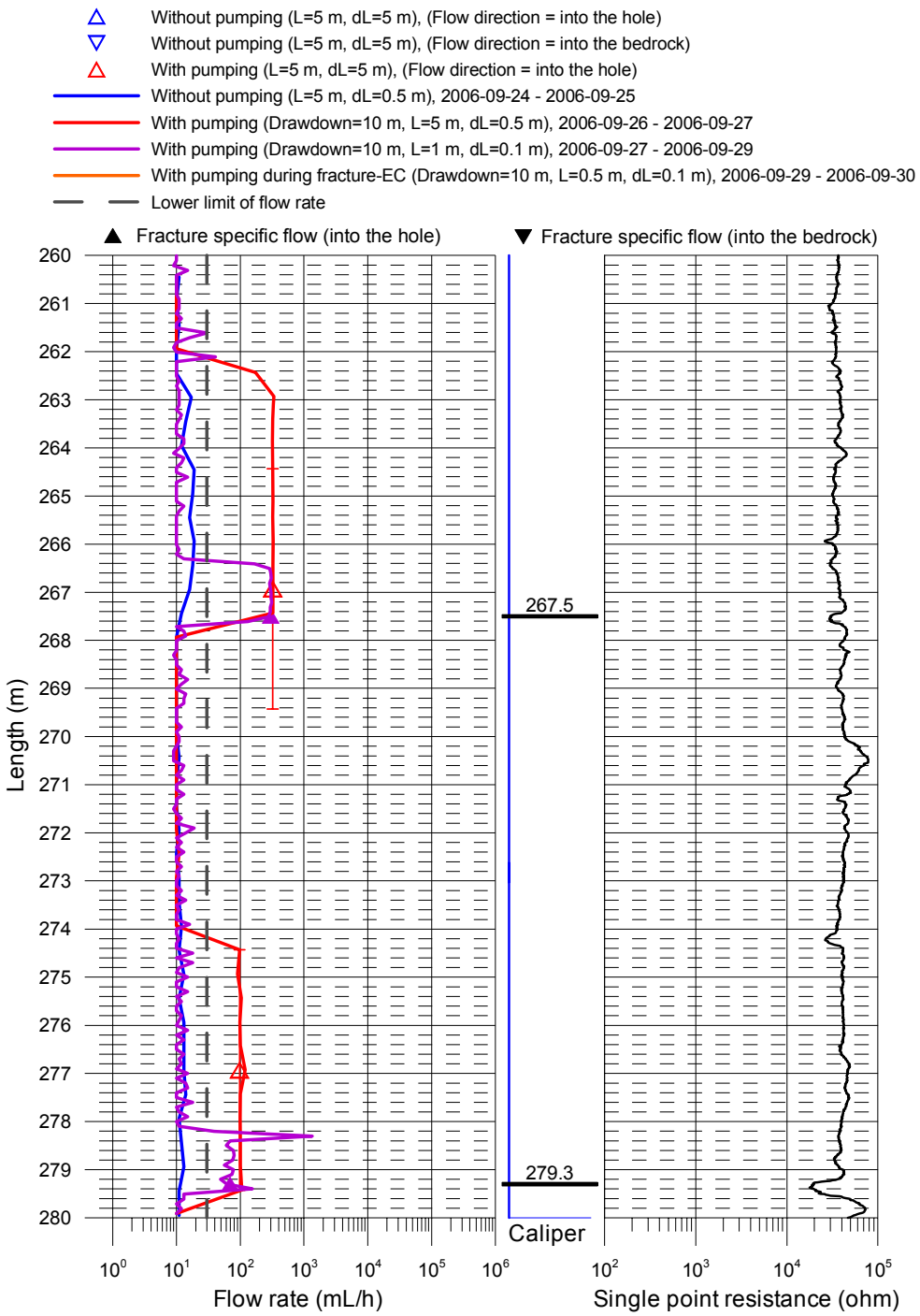

Appendix 3.11

Laxemar, borehole KLX13A
Flow rate, caliper and single point resistance

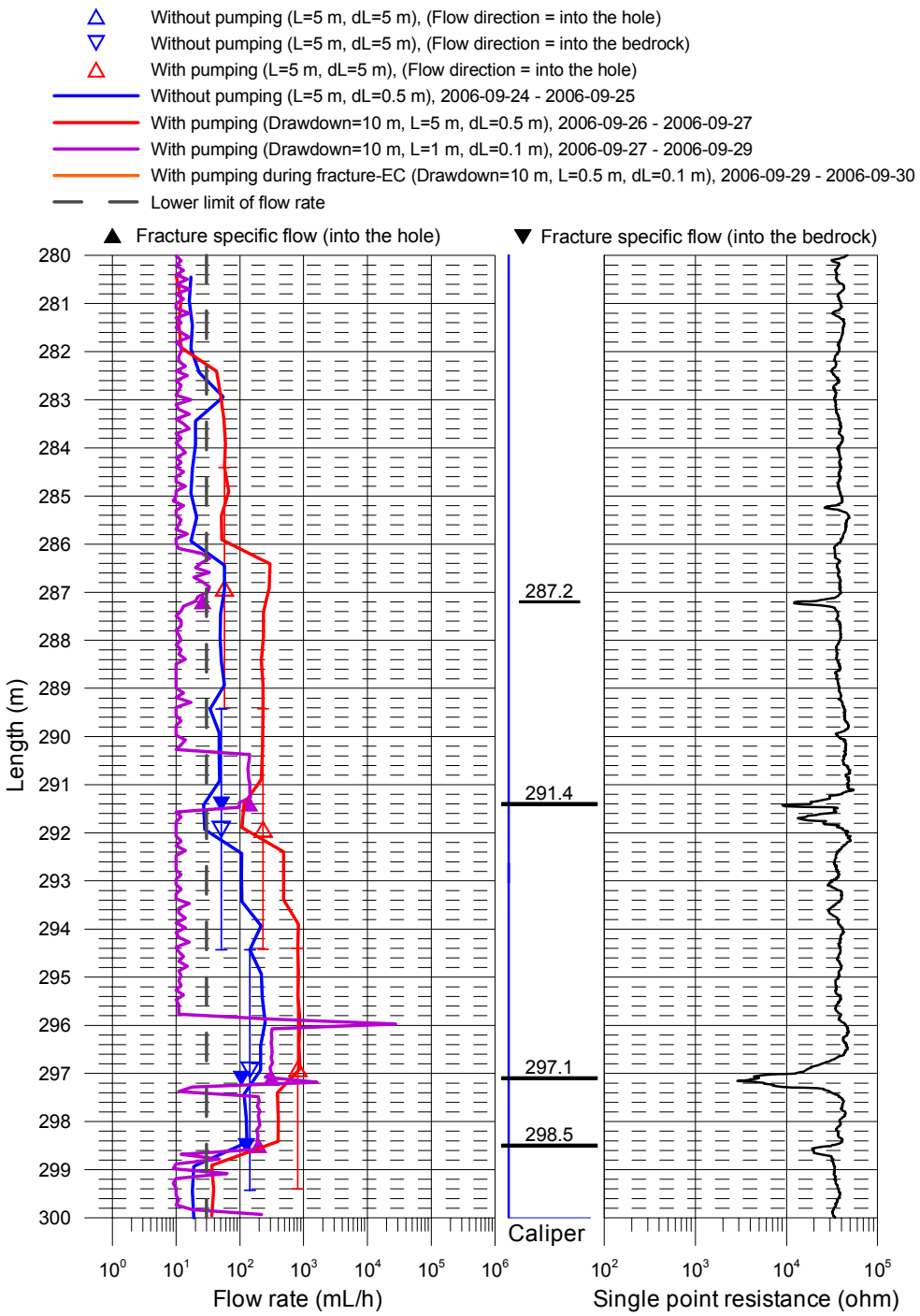

Appendix 3.12

Laxemar, borehole KLX13A
Flow rate, caliper and single point resistance

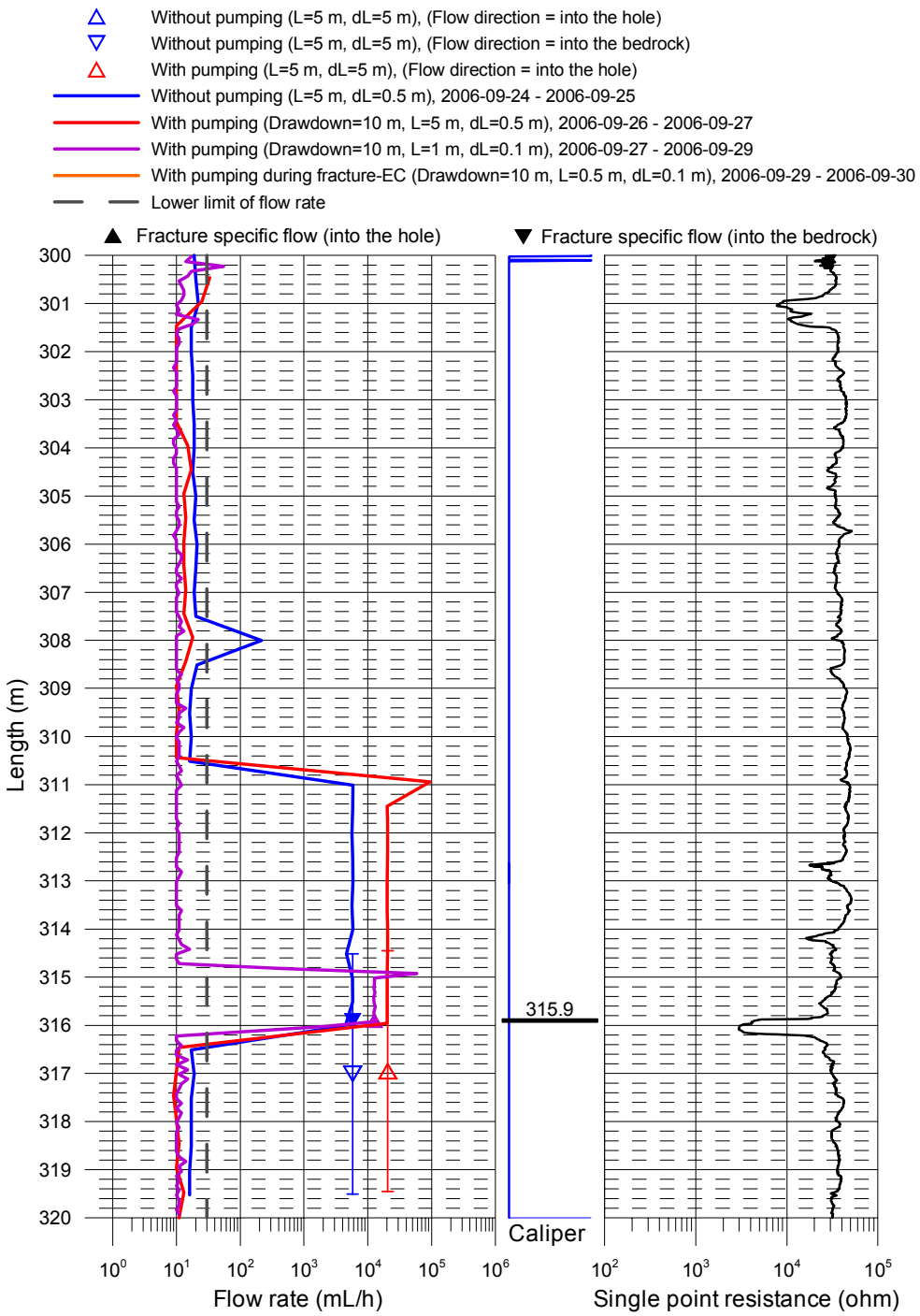

Appendix 3.13

Laxemar, borehole KLX13A
Flow rate, caliper and single point resistance

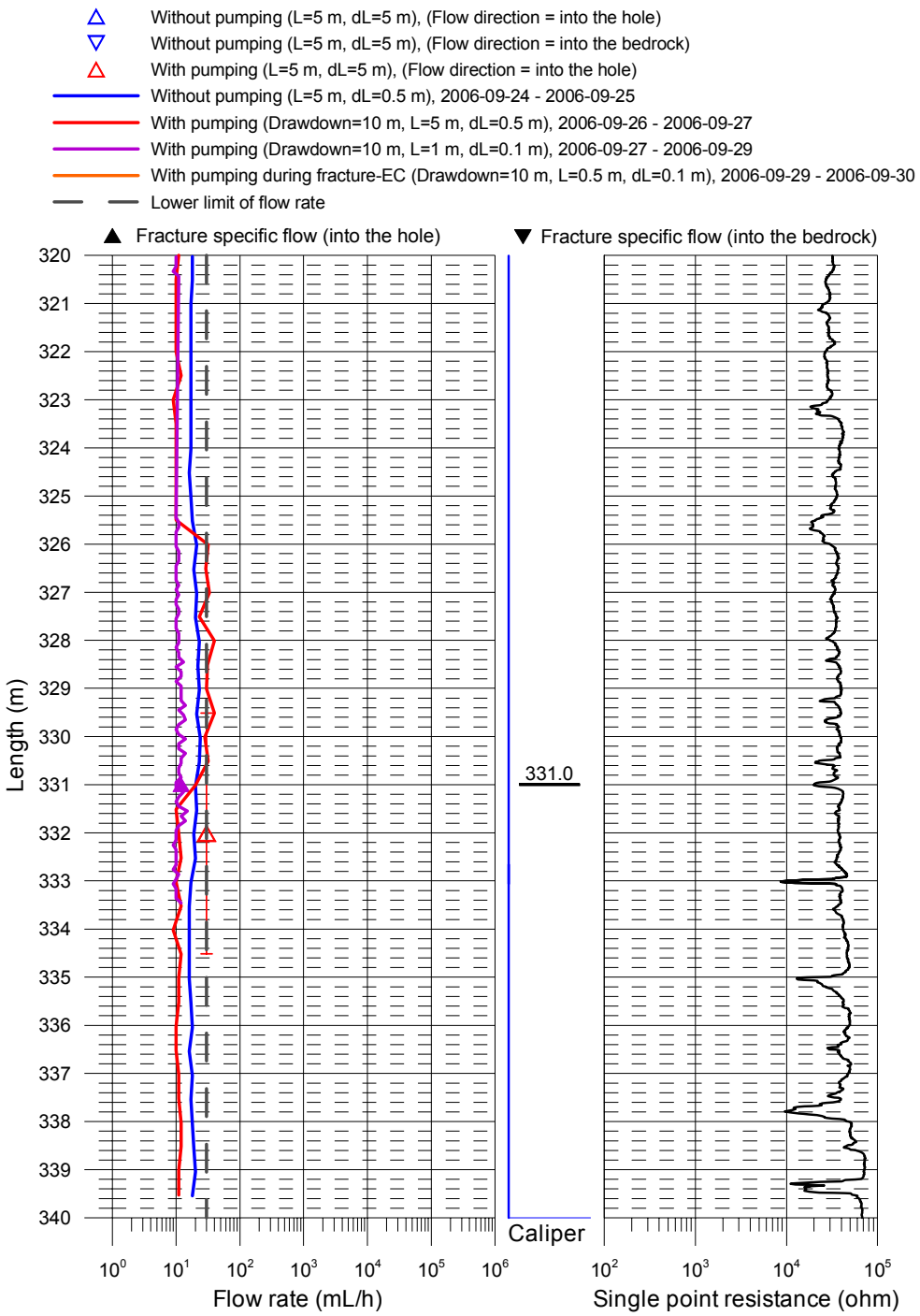

Appendix 3.14

Laxemar, borehole KLX13A
Flow rate, caliper and single point resistance

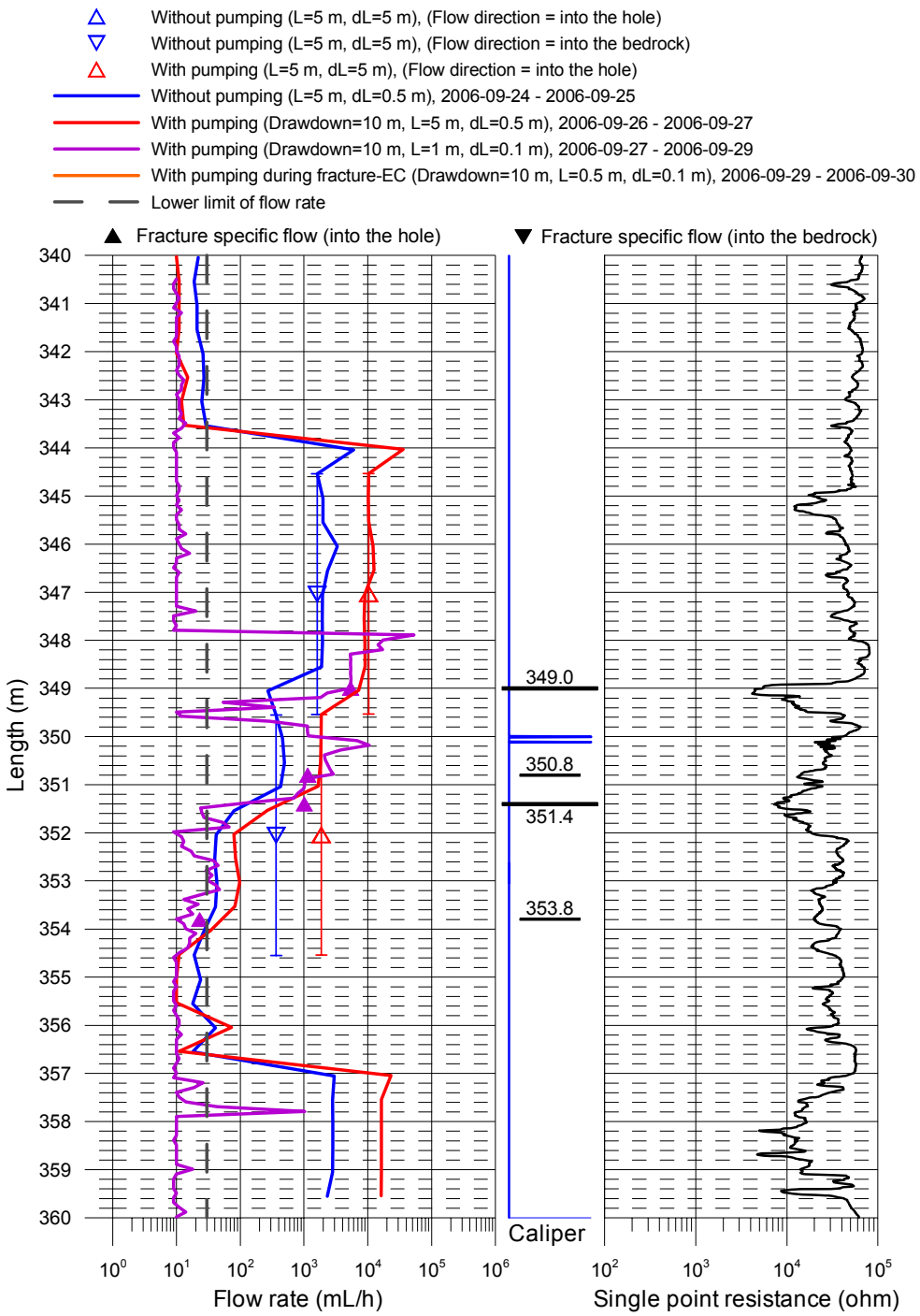

Appendix 3.15

Laxemar, borehole KLX13A
Flow rate, caliper and single point resistance

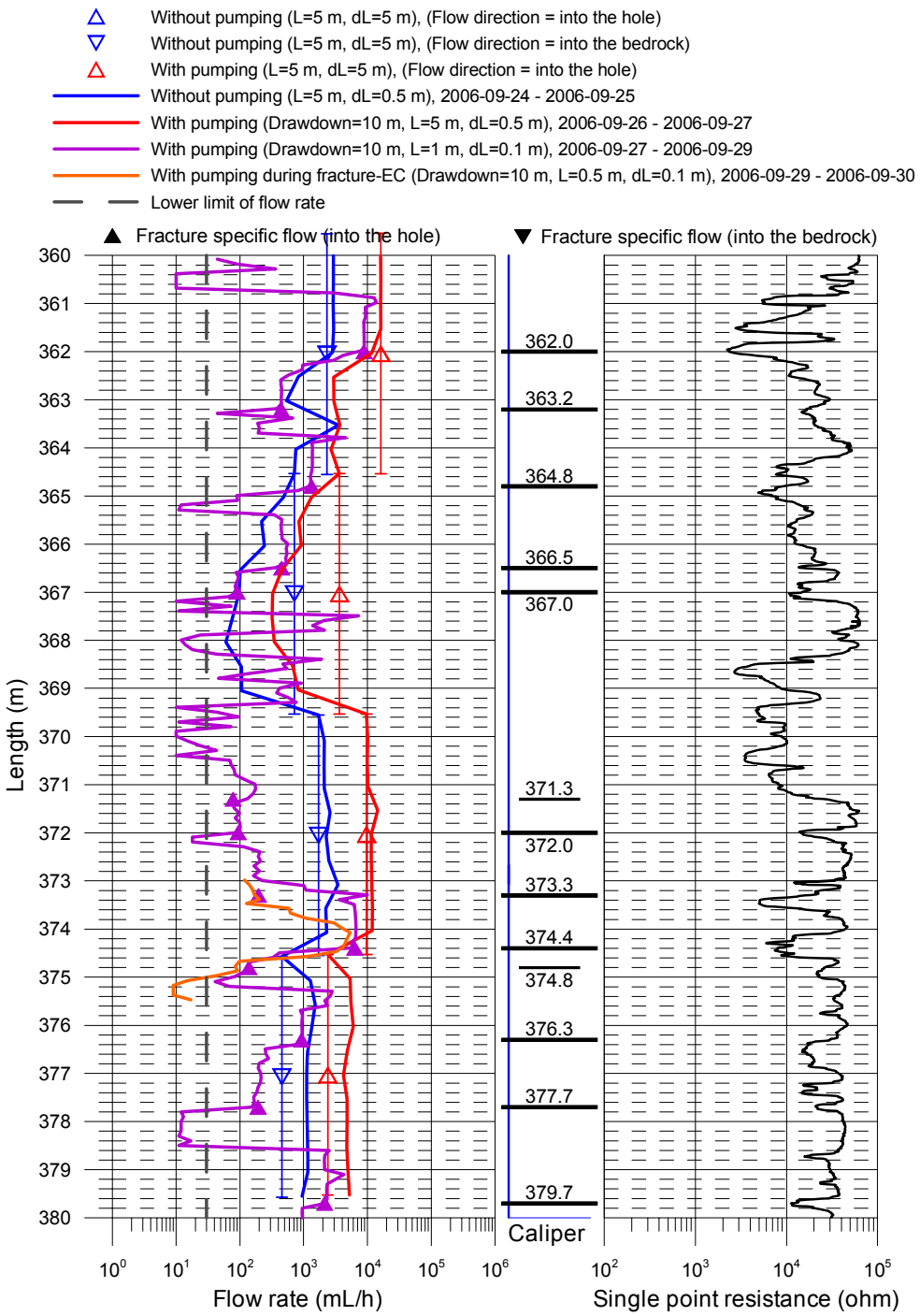

Appendix 3.16

Laxemar, borehole KLX13A
Flow rate, caliper and single point resistance

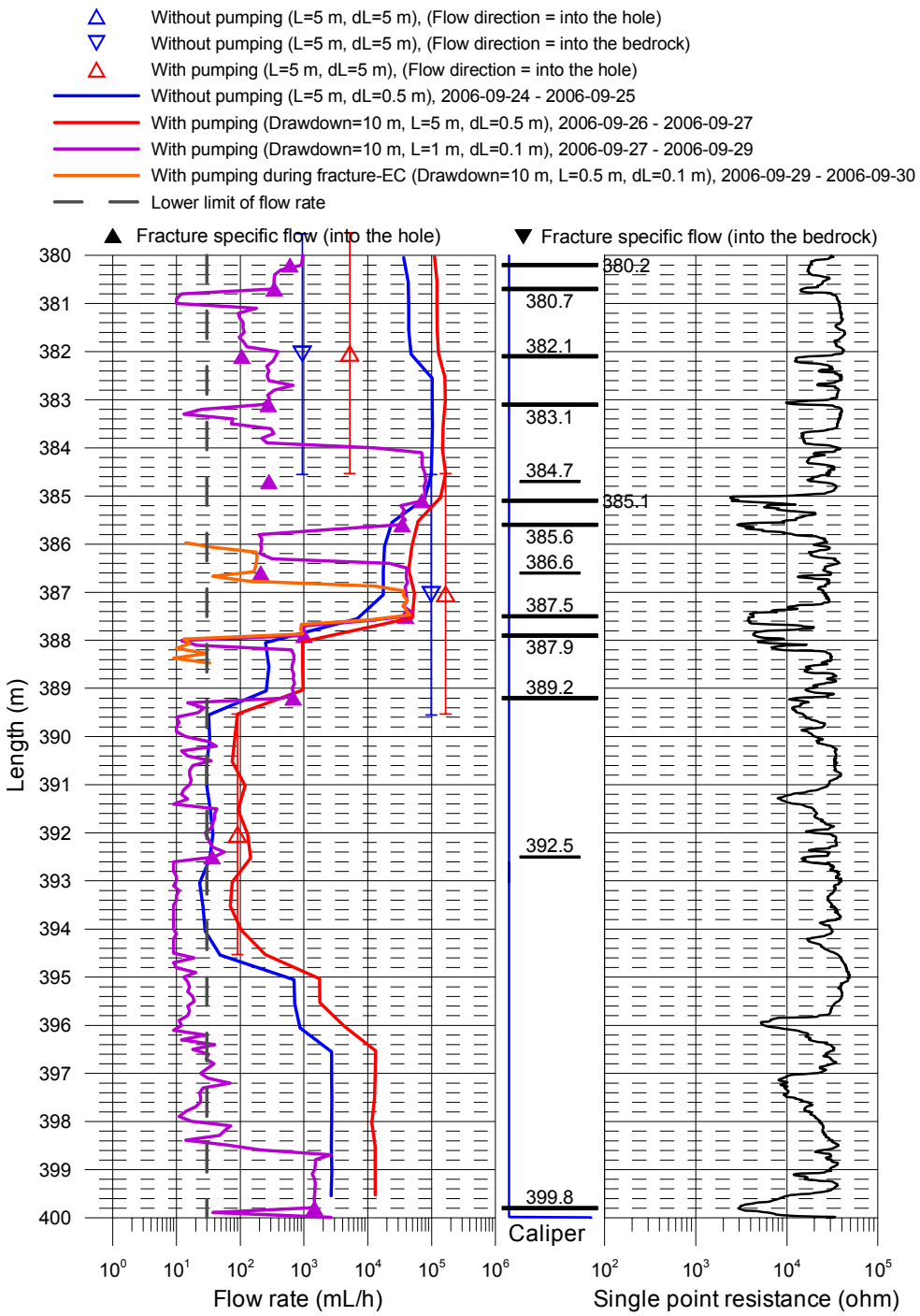

Appendix 3.17

Laxemar, borehole KLX13A
Flow rate, caliper and single point resistance

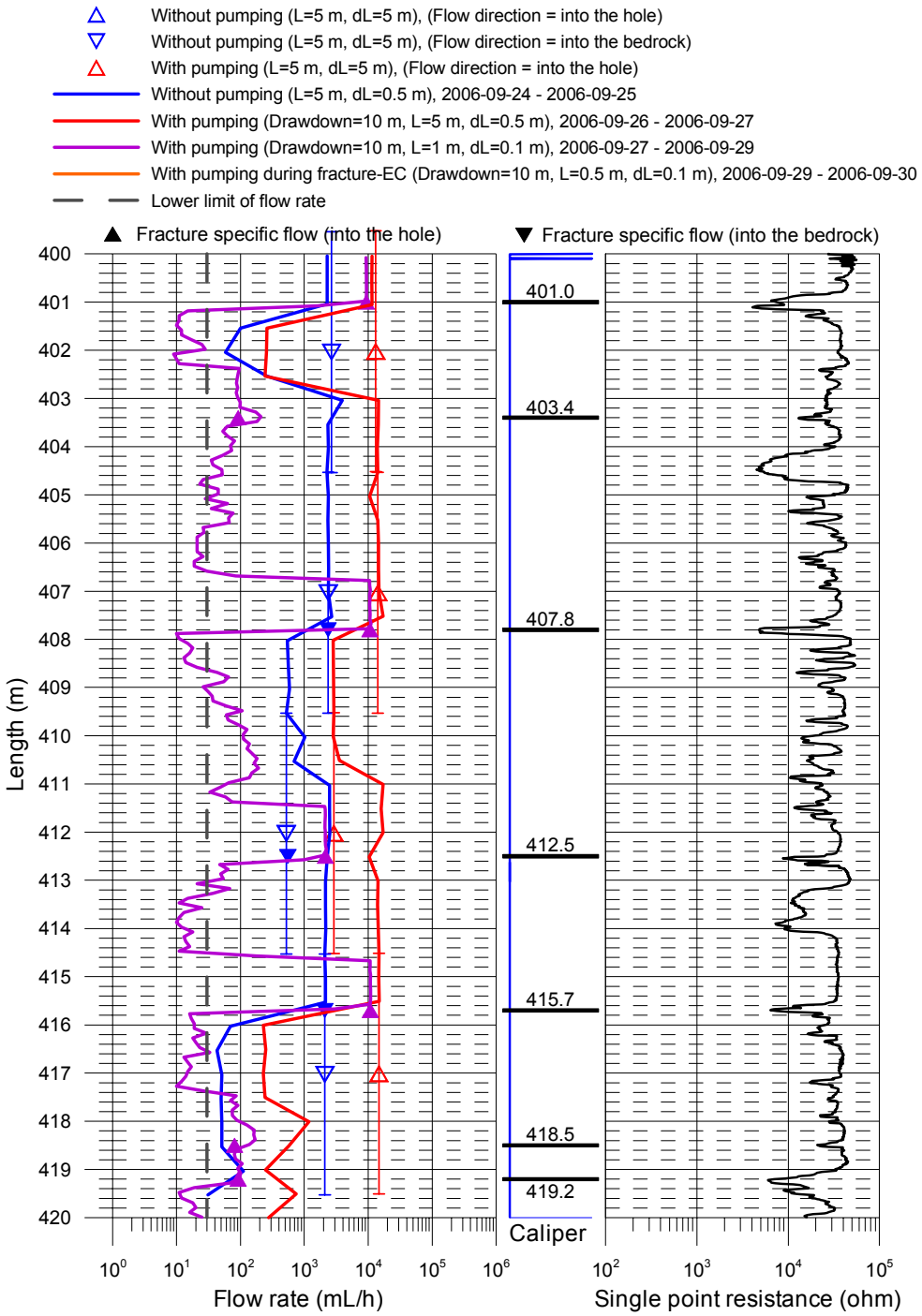

Appendix 3.18

Laxemar, borehole KLX13A
Flow rate, caliper and single point resistance

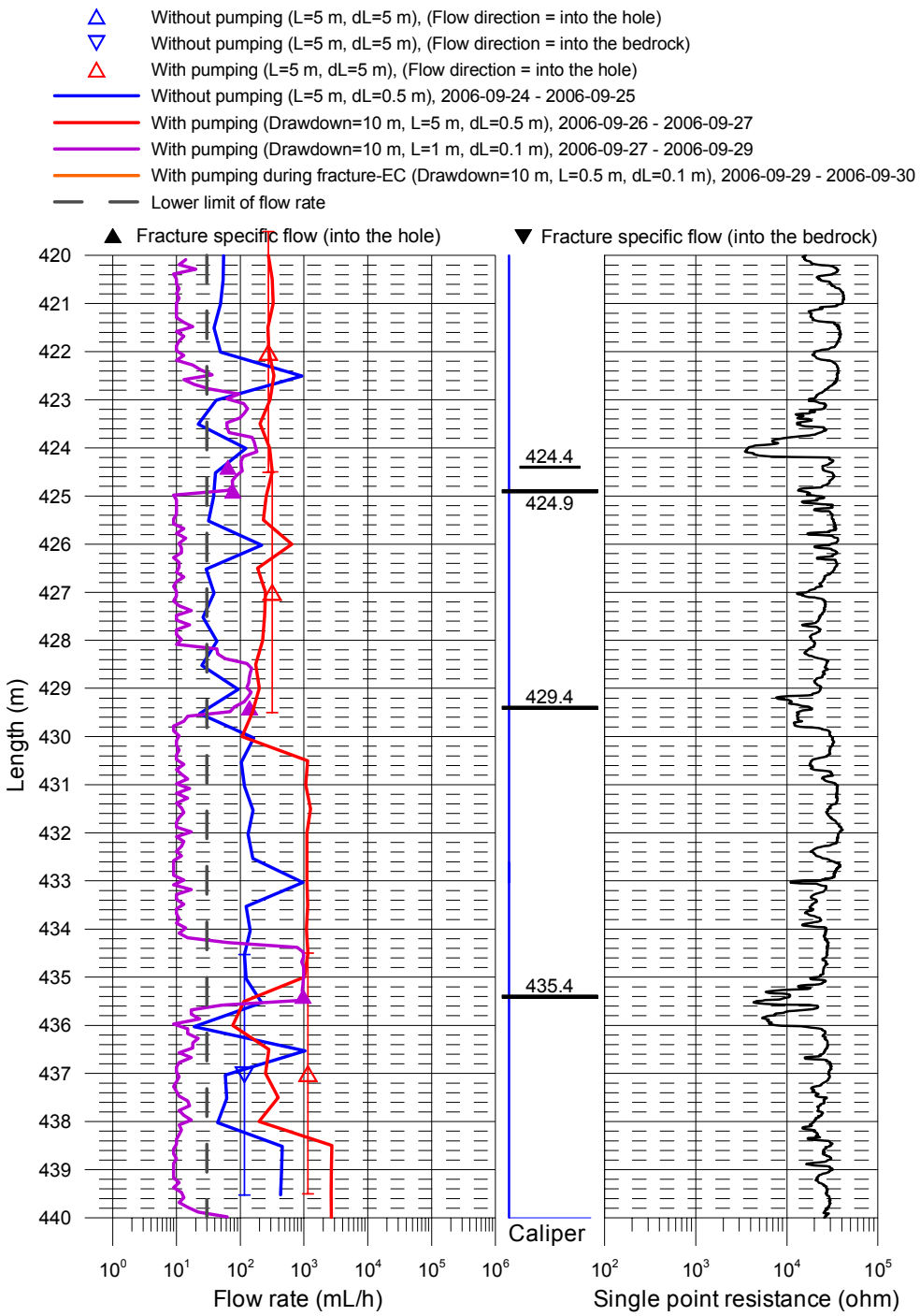

Appendix 3.19

Laxemar, borehole KLX13A
Flow rate, caliper and single point resistance

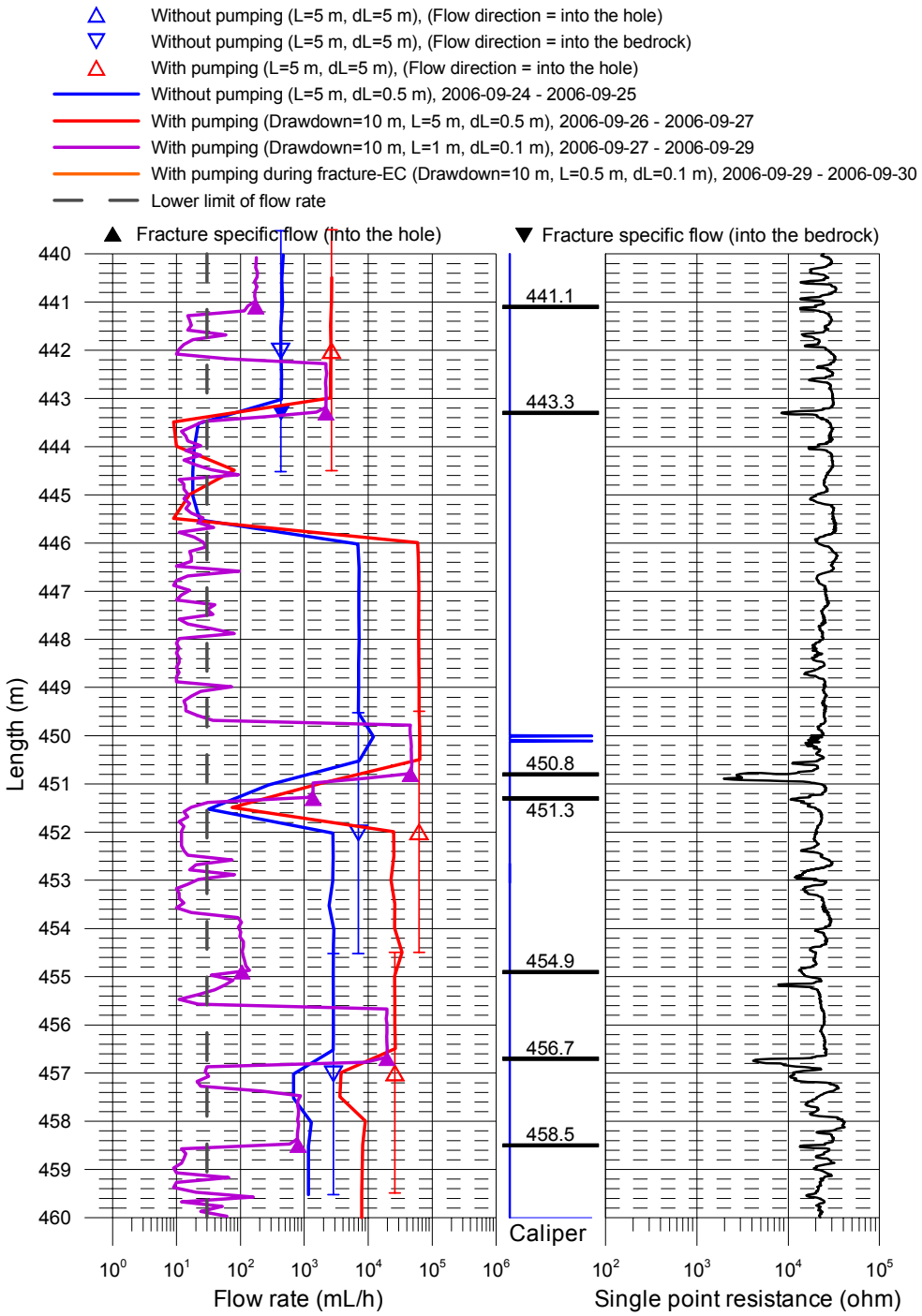

Appendix 3.20

Laxemar, borehole KLX13A
Flow rate, caliper and single point resistance

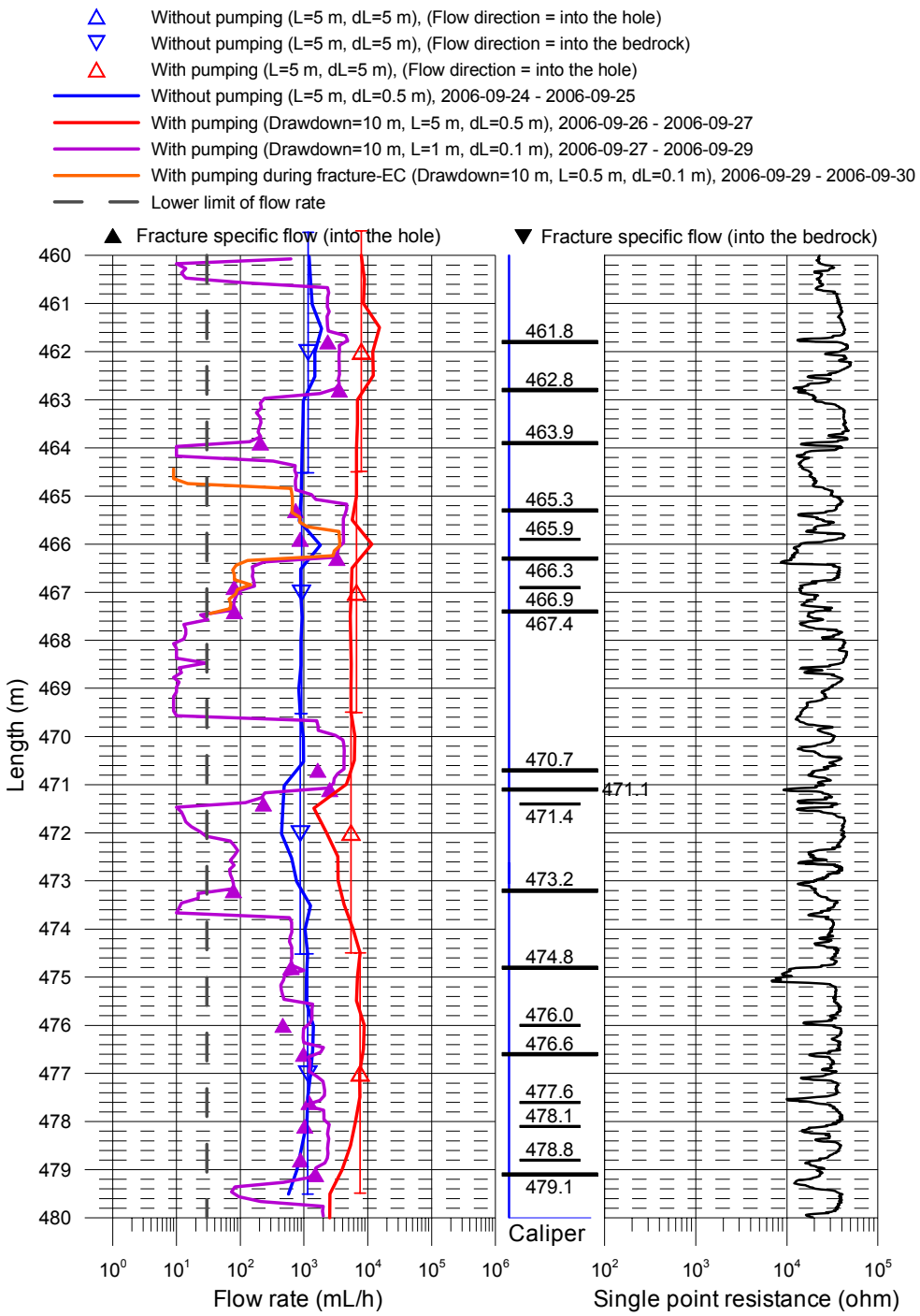

Appendix 3.21

Laxemar, borehole KLX13A
Flow rate, caliper and single point resistance

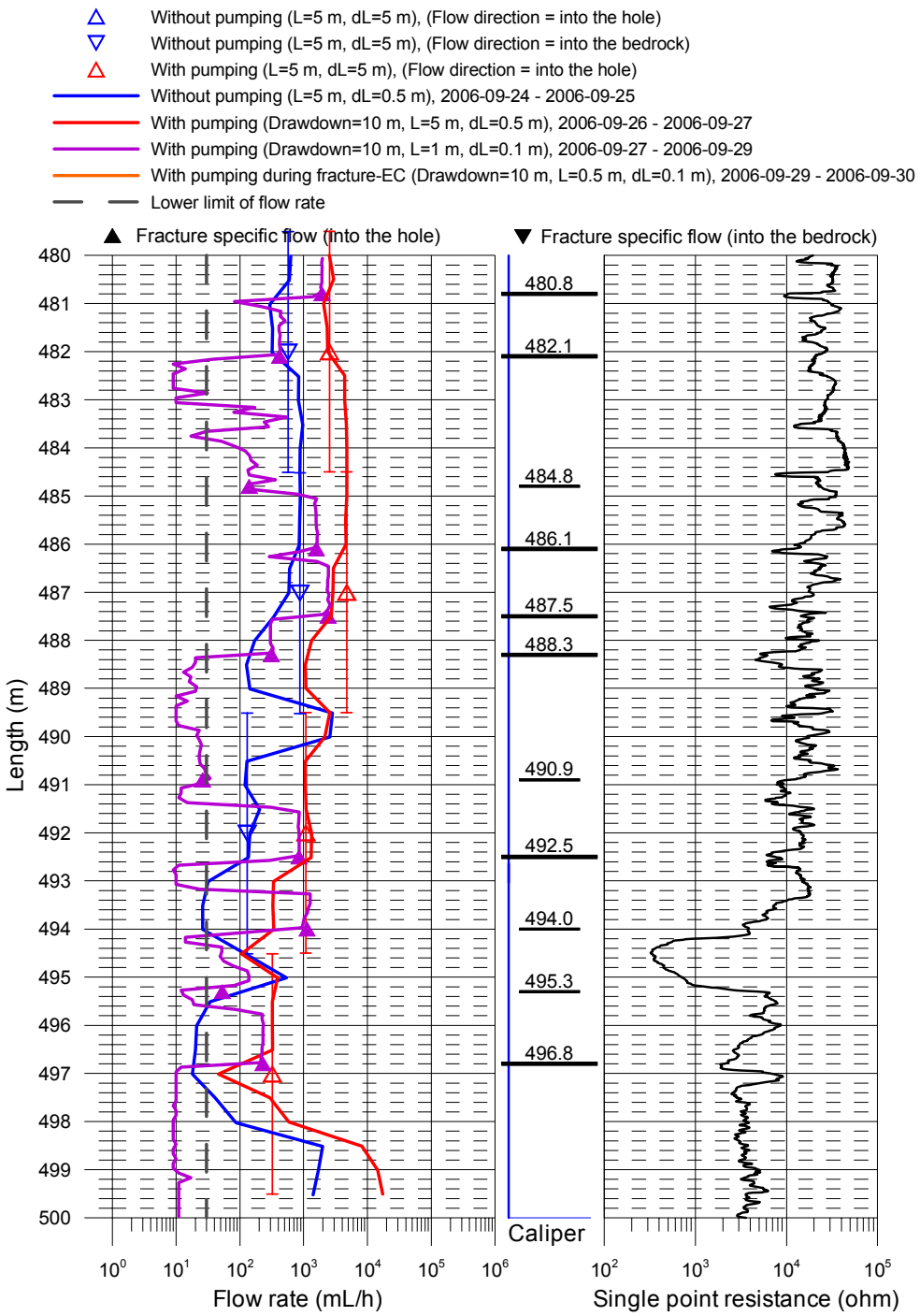

Appendix 3.22

Laxemar, borehole KLX13A
Flow rate, caliper and single point resistance

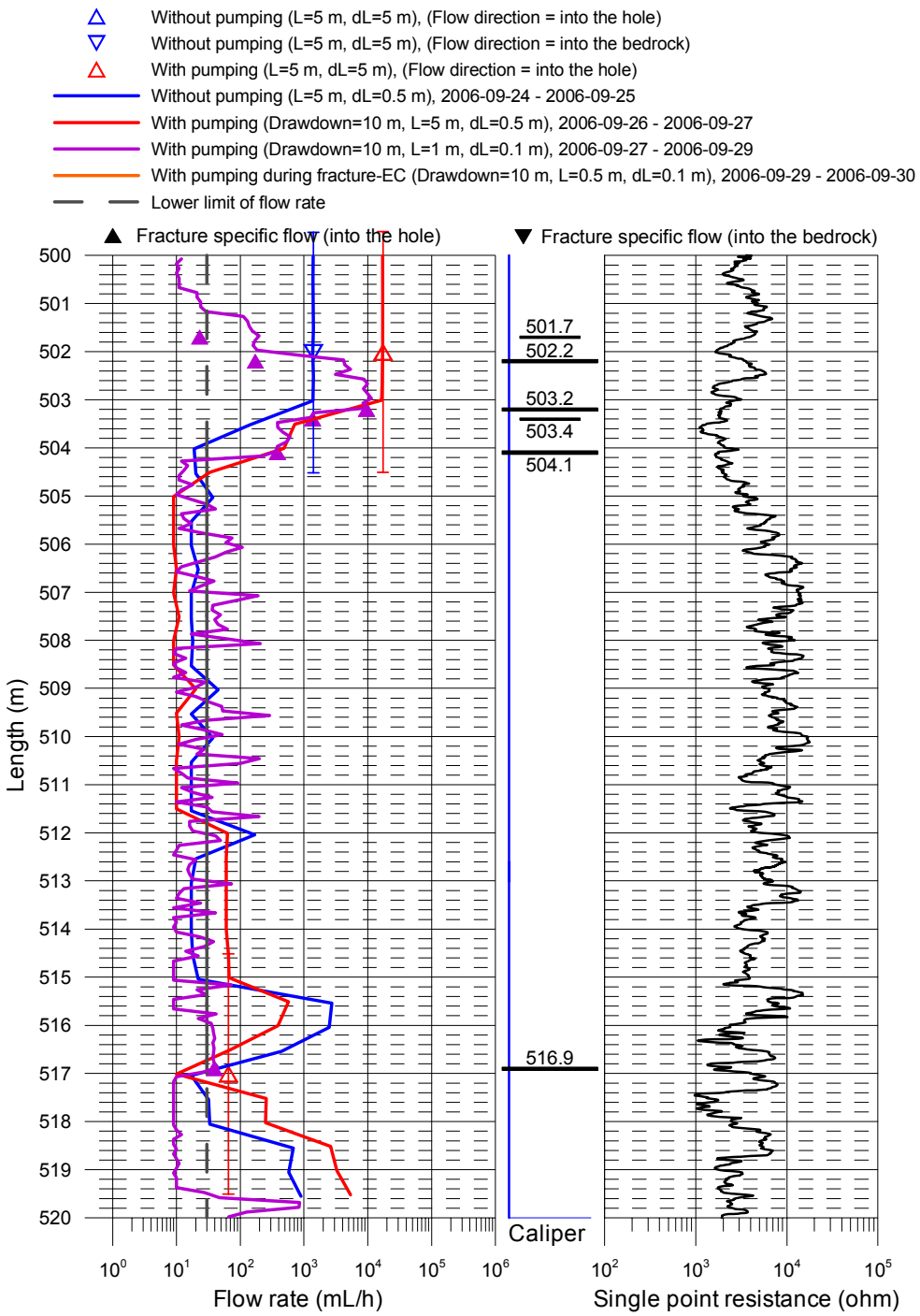

Appendix 3.23

Laxemar, borehole KLX13A
Flow rate, caliper and single point resistance

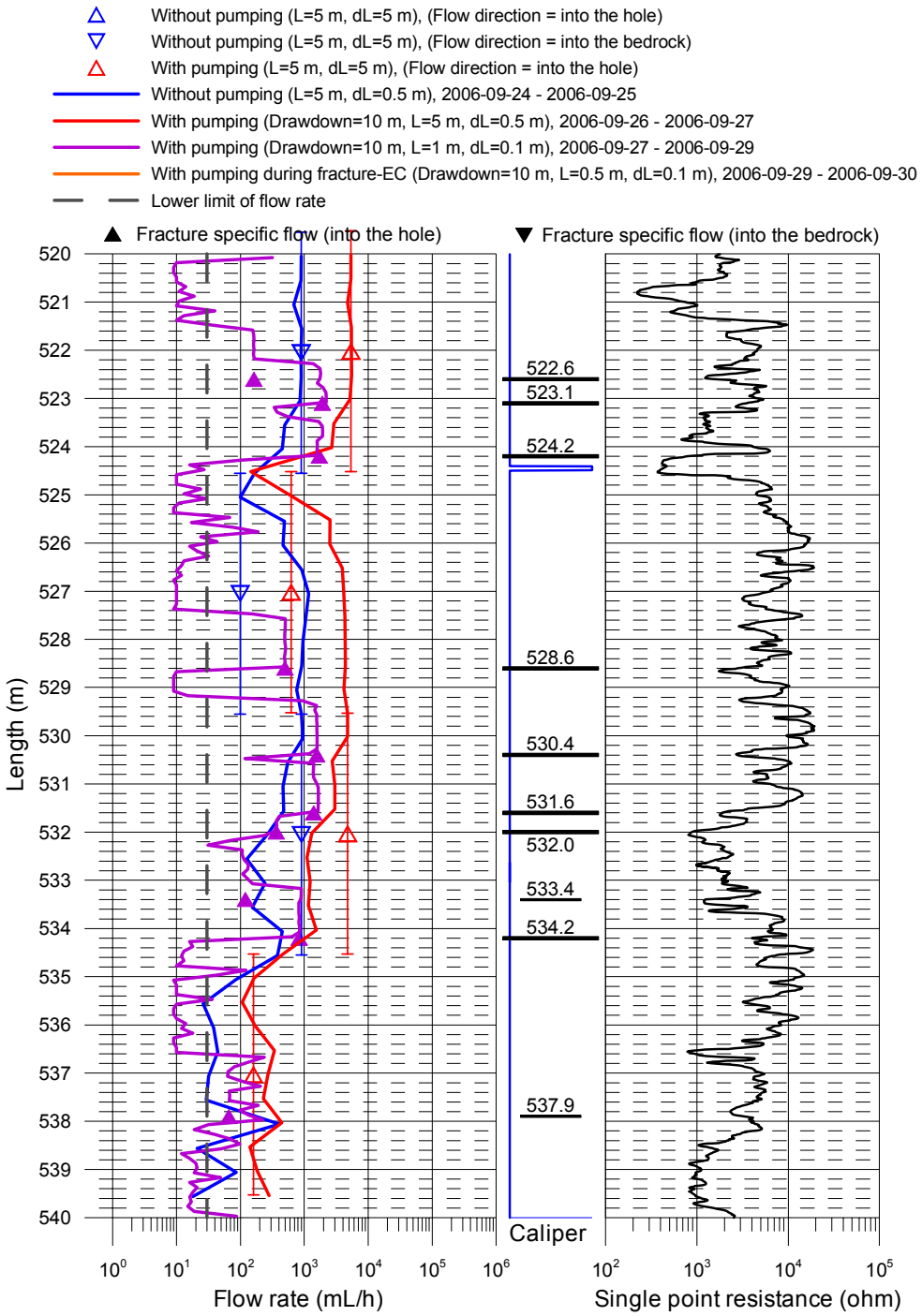

Appendix 3.24

Laxemar, borehole KLX13A
Flow rate, caliper and single point resistance

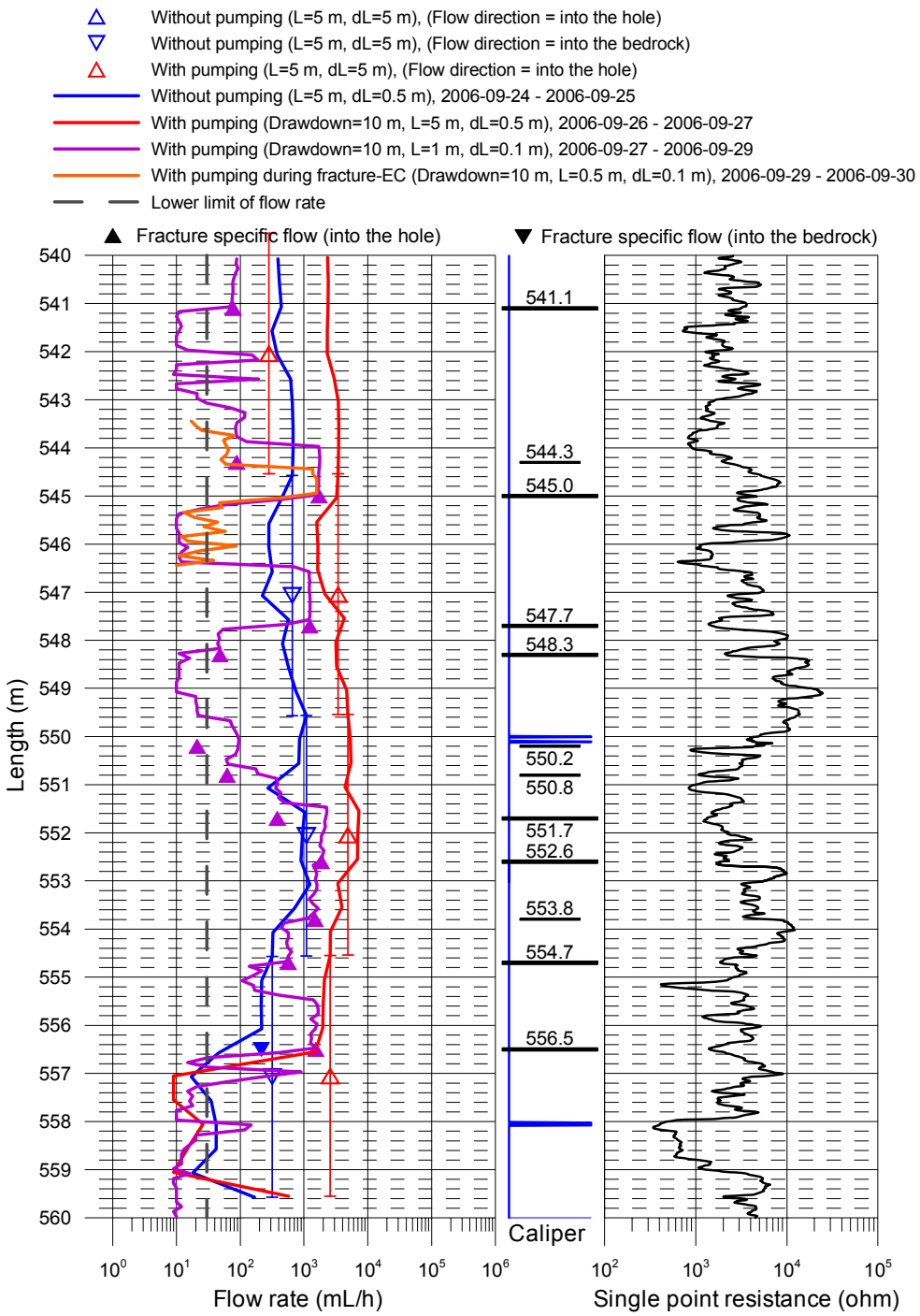

Appendix 3.25

Laxemar, borehole KLX13A
Flow rate, caliper and single point resistance

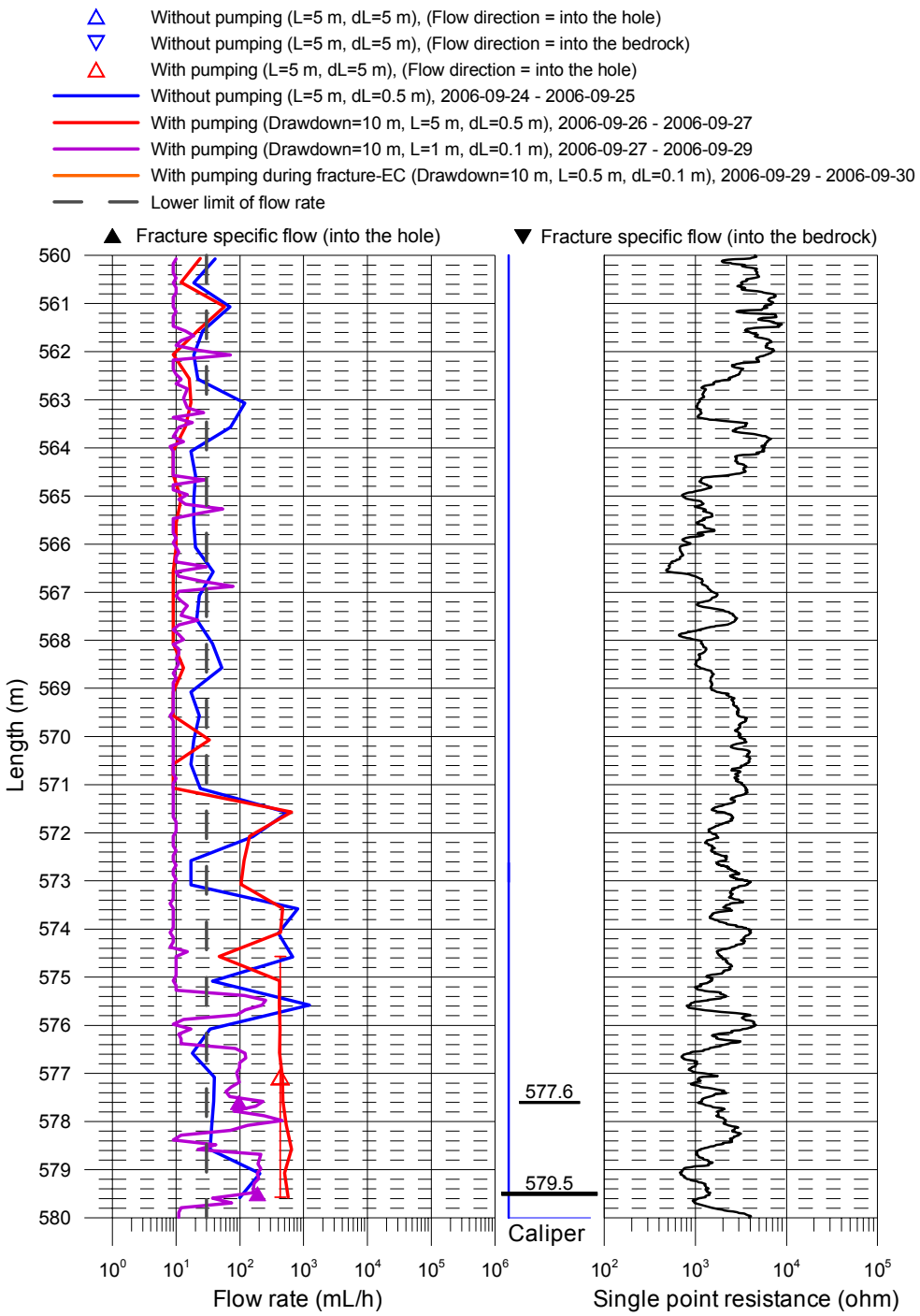

Appendix 3.26

Laxemar, borehole KLX13A
Flow rate, caliper and single point resistance

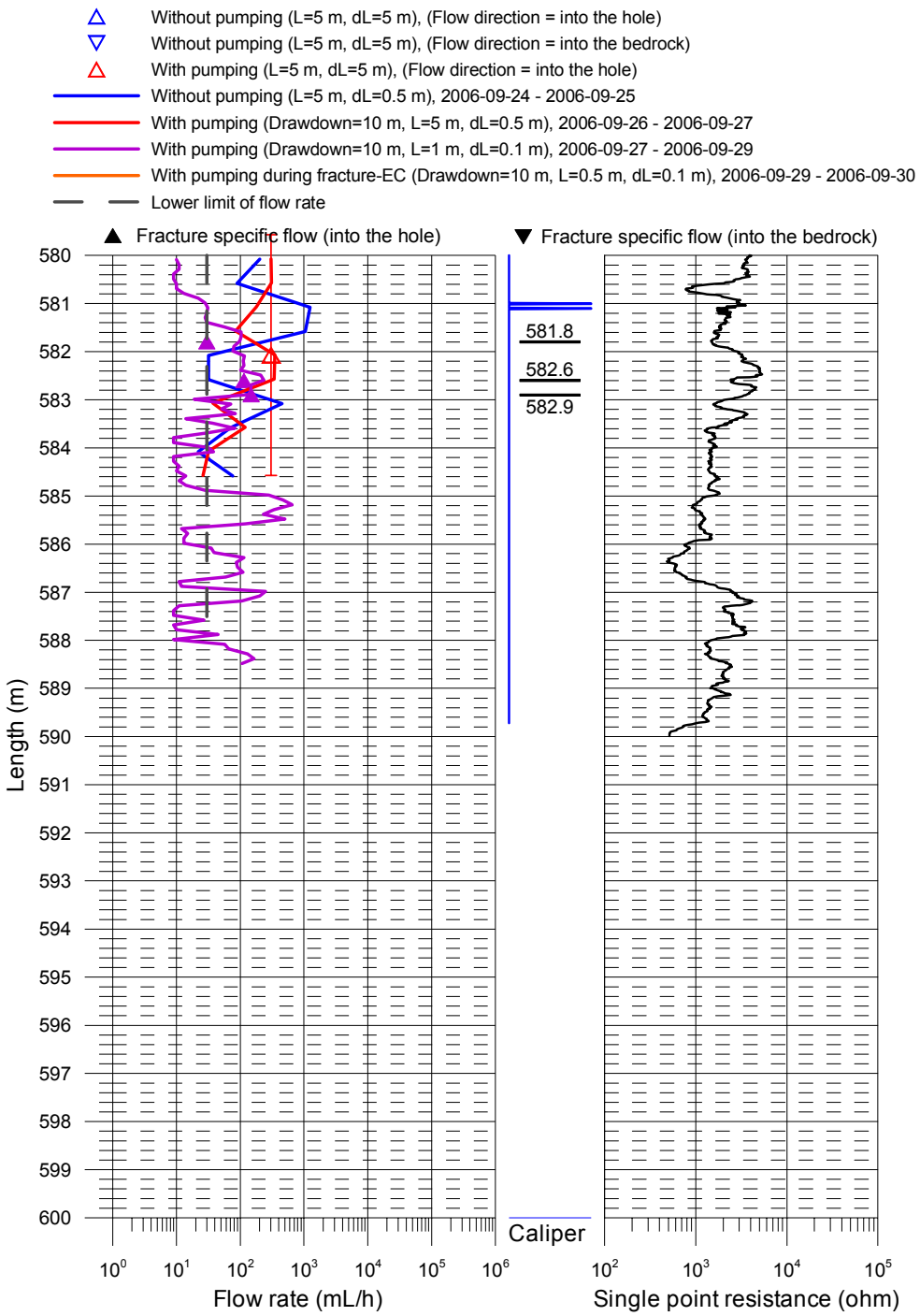

Appendix 4.1

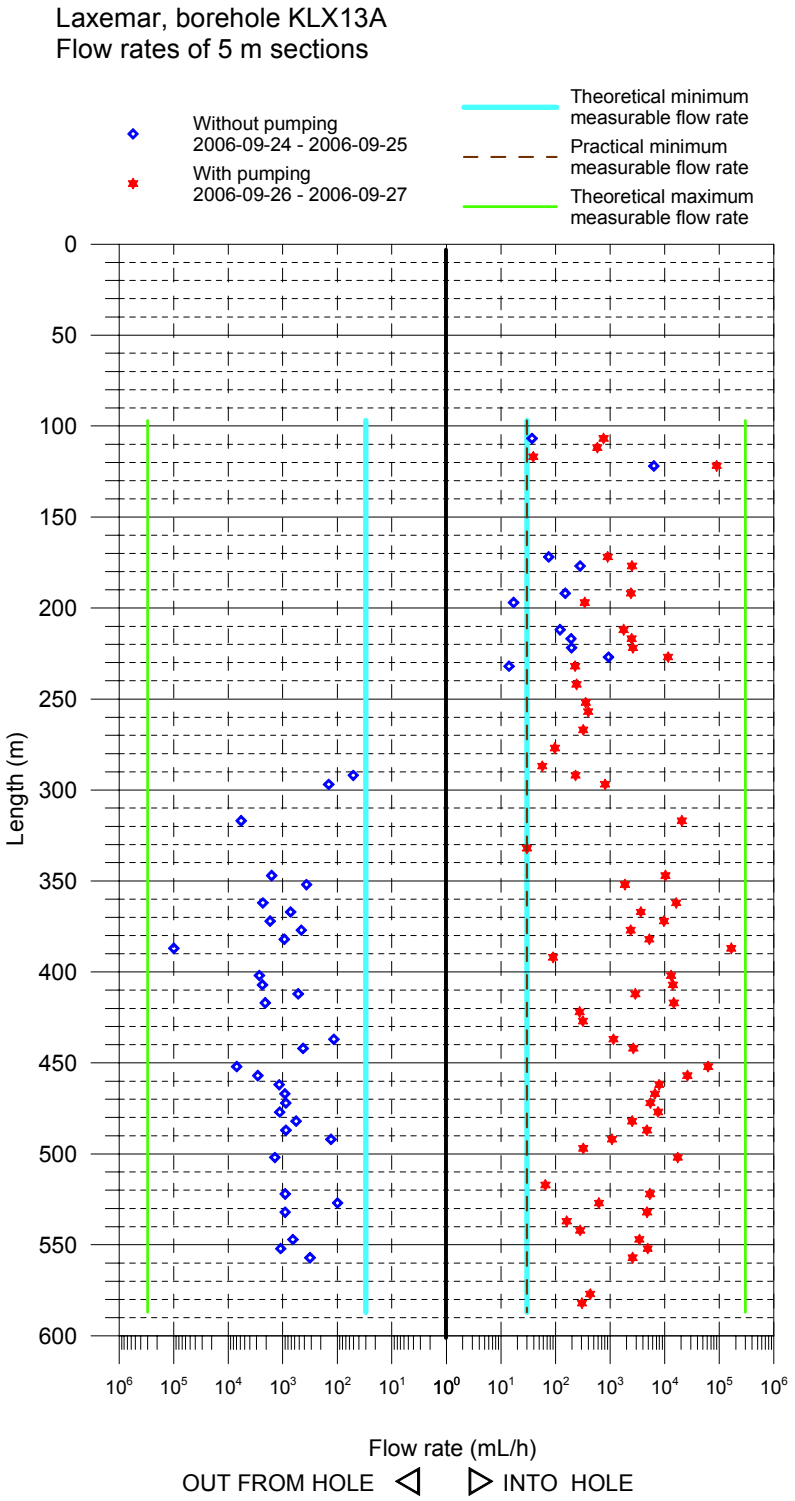
Laxemar, borehole KLX13A
Flow rates of 5 m sections
Without pumping
2006-09-24 - 2006-09-25
With pumping
2006-09-26 - 2006-09-27
Theoretical minimum measurable flow rate
Practical minimum measurable flow rate
Theoretical maximum measurable flow rate
Length (m)
0
50
100
150
200
250
300
350
400
450
500
550
600
10^6 10^5 10^4 10^3 10^2 10^1 10^0 10^1 10^2 10^3 10^4 10^5 10^6
Flow rate (mL/h)
OUT FROM HOLE
INTO HOLE

Appendix 4.2

Laxemar, borehole KLX13A
Transmissivity and head of 5 m sections

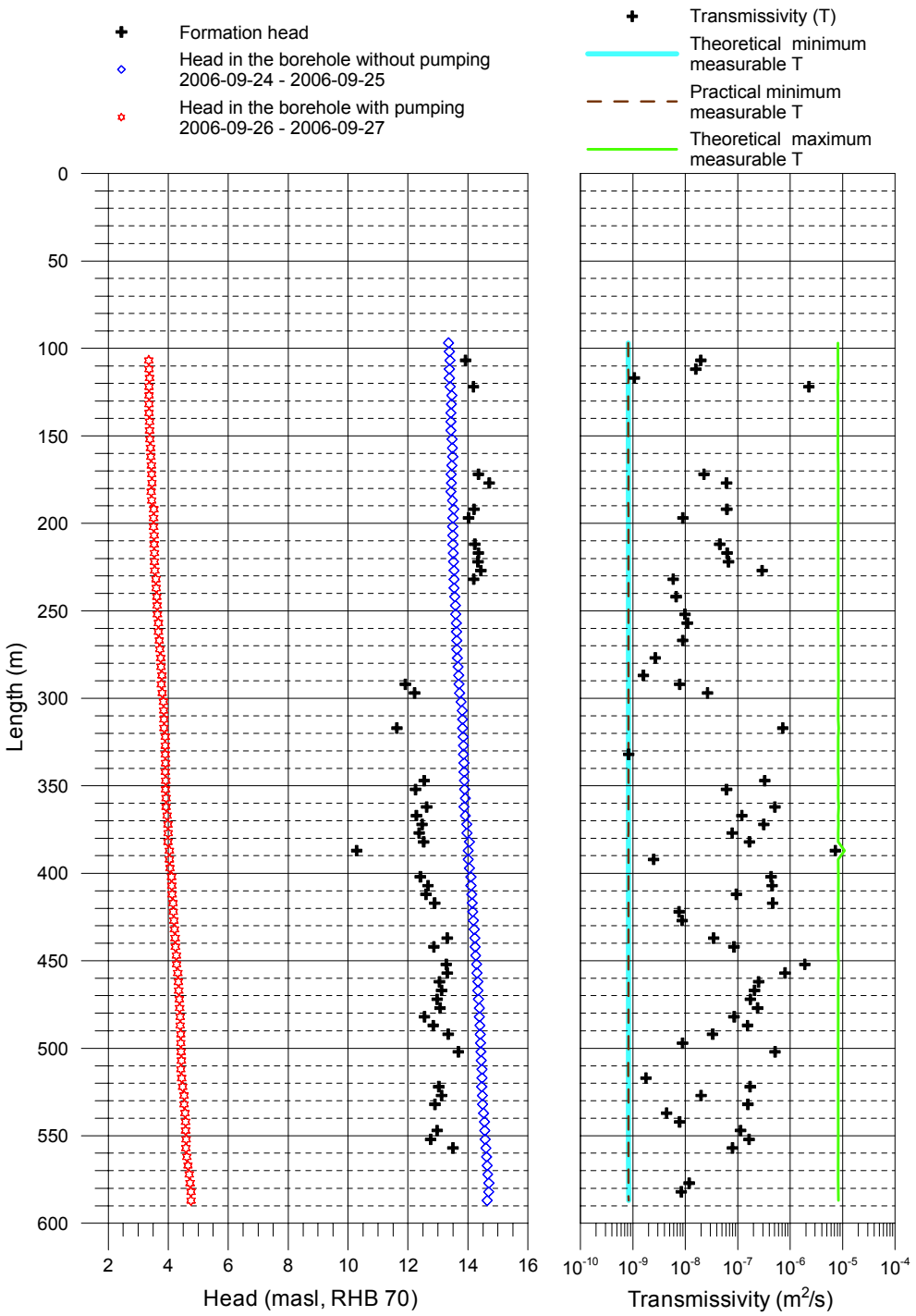

Appendix 5

Laxemar, borehole KLX13A
Transmissivity and head of detected fractures

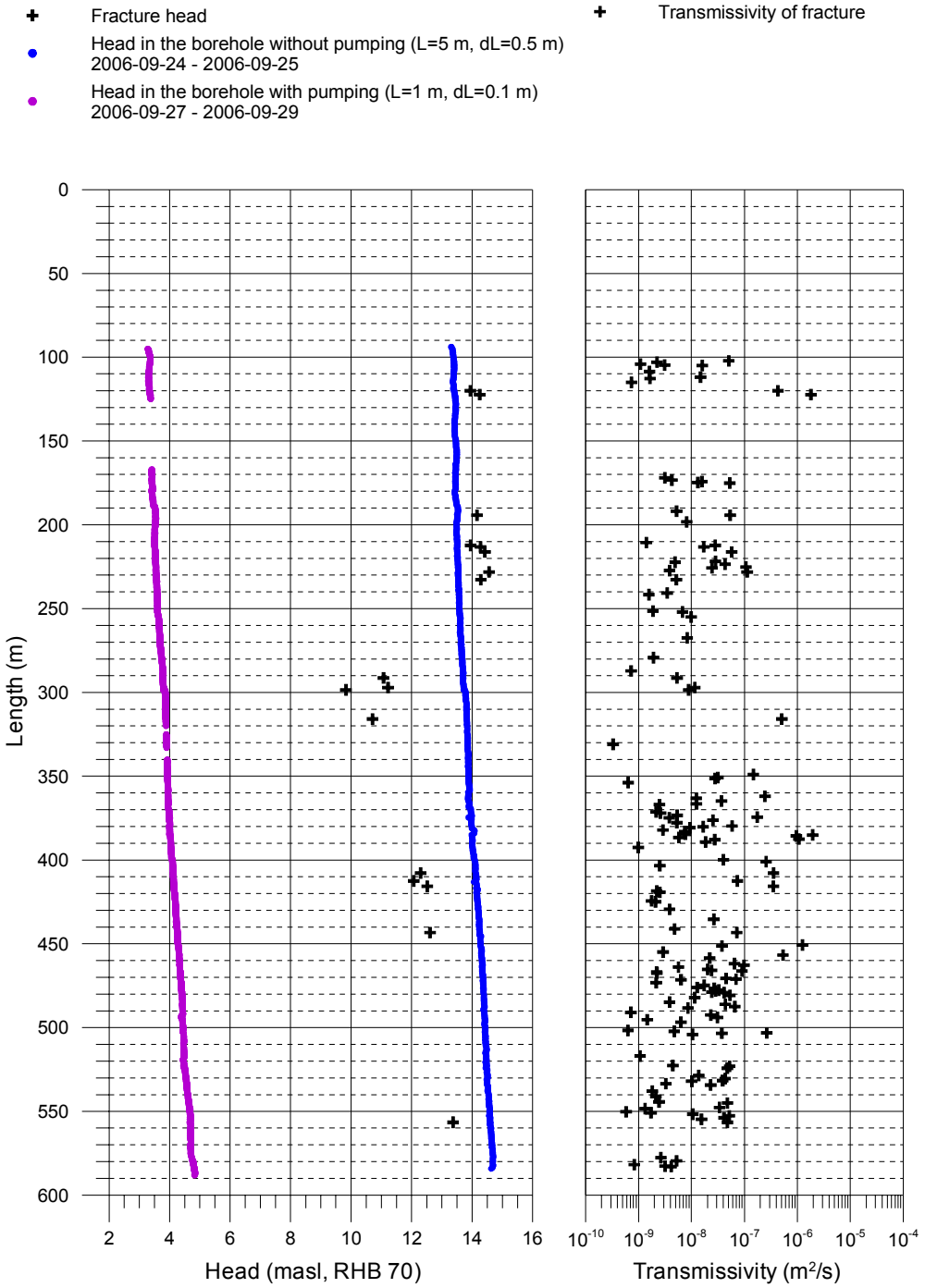

Appendix 6

5. PFL-Difference flow logging – Basic test data

Borehole ID	Logged interval Secup (m)	Seclow (m)	Test type (1–6)	Date of test, start YYYYMMDD	Time of test, start hh:mm	Date of flowl. start YYYYMMDD	Time of flowl. start hh:mm	Date of test, stop YYYYMMDD	Time of test, stop hh:mm	Lw (m)	dL (m)	Qp1 (m3/s)	Qp2 (m3/s)
KLX13A	11.75	595.85	5A	20060925	16:05	20060926	15:01	20060930	13:20	5	0.5	6.50E–04	–

5. PFL-Difference flow logging – Basic test data

t_{p1} (s)	t_{p2} (s)	t_{F1} (s)	t_{F2} (s)	h_0 (m.a.s.l.)	h_1 (m.a.s.l.)	h_2 (m.a.s.l.)	s_1 (m)	s_2 (m)	T Entire hole (m^2/s)	Reference (–)	Comments (–)
422,100	–	686,350	–	13.48	3.46	–	–10.02	–	6.42E–05	–	–

Appendix 7

Difference flow logging – Sequential flow logging

Borehole ID	Secup L(m)	Seclow L(m)	L_w (m)	Q_0 (m^3/s)	h_{0FW} (m.a.s.l.)	Q_1 (m^3/s)	h_{1FW} (m.a.s.l.)	T_D (m^2/s)	h_i (m.a.s.l.)	Q-lower limit P (mL/h)	T_D-measl$_{LT}$ (m^2/s)	T_D-measl$_{LP}$ (m^2/s)	T_D-measl$_U$ (m^2/s)	Comments
KLX13A	94.33	99.33	5	–	13.35	–	3.31	–	–	30	8.2E–10	8.2E–10	8.2E–06	
KLX13A	99.34	104.34	5	–	13.38	–	3.32	–	–	30	8.2E–10	8.2E–10	8.2E–06	
KLX13A	104.34	109.34	5	1.03E–08	13.40	2.10E–07	3.35	2.0E–08	13.9	30	8.2E–10	8.2E–10	8.2E–06	
KLX13A	109.35	114.35	5	–	13.38	1.61E–07	3.36	1.6E–08	–	30	8.2E–10	8.2E–10	8.2E–06	
KLX13A	114.36	119.36	5	–	13.38	1.08E–08	3.38	1.1E–09	–	30	8.2E–10	8.2E–10	8.2E–06	
KLX13A	119.36	124.36	5	1.76E–06	13.41	2.48E–05	3.36	2.3E–06	14.2	30	8.2E–10	8.2E–10	8.0E–06	
KLX13A	124.36	129.36	5	–	13.46	–	3.36	–	–	30	8.2E–10	8.2E–10	8.2E–06	
KLX13A	129.36	134.36	5	–	13.45	–	3.36	–	–	30	8.2E–10	8.2E–10	8.2E–06	
KLX13A	134.36	139.36	5	–	13.43	–	3.36	–	–	30	8.2E–10	8.2E–10	8.2E–06	
KLX13A	139.36	144.36	5	–	13.43	–	3.38	–	–	30	8.2E–10	8.2E–10	8.2E–06	
KLX13A	144.37	149.37	5	–	13.43	–	3.38	–	–	30	8.2E–10	8.2E–10	8.2E–06	
KLX13A	149.37	154.37	5	–	13.47	–	3.39	–	–	30	8.2E–10	8.2E–10	8.2E–06	
KLX13A	154.37	159.37	5	–	13.48	–	3.41	–	–	30	8.2E–10	8.2E–10	8.2E–06	
KLX13A	159.38	164.38	5	–	13.49	–	3.42	–	–	30	8.2E–10	8.2E–10	8.2E–06	
KLX13A	164.38	169.38	5	–	13.46	–	3.44	–	–	30	8.2E–10	8.2E–10	8.2E–06	
KLX13A	169.38	174.38	5	2.08E–08	13.44	2.50E–07	3.45	2.3E–08	14.4	30	8.3E–10	8.3E–10	8.2E–06	
KLX13A	174.39	179.39	5	7.83E–08	13.45	6.97E–07	3.46	6.1E–08	14.7	30	8.3E–10	8.3E–10	8.2E–06	
KLX13A	179.39	184.39	5	–	13.43	–	3.43	–	–	30	8.2E–10	8.2E–10	8.2E–06	
KLX13A	184.37	189.37	5	–	13.48	–	3.45	–	–	30	8.2E–10	8.2E–10	8.2E–06	
KLX13A	189.40	194.40	5	4.17E–08	13.53	6.67E–07	3.52	6.2E–08	14.2	30	8.2E–10	8.2E–10	8.2E–06	
KLX13A	194.43	199.43	5	4.72E–09	13.50	9.50E–08	3.51	8.9E–09	14.0	30	8.3E–10	8.3E–10	8.3E–06	
KLX13A	199.41	204.41	5	–	13.49	–	3.51	–	–	30	8.3E–10	8.3E–10	8.3E–06	
KLX13A	204.41	209.41	5	–	13.50	–	3.53	–	–	30	8.3E–10	8.3E–10	8.3E–06	
KLX13A	209.43	214.43	5	3.36E–08	13.50	4.92E–07	3.53	4.5E–08	14.2	30	8.3E–10	8.3E–10	8.3E–06	

Borehole ID	Secup L(m)	Seclow L(m)	L_w (m)	Q_0 (m^3/s)	h_{0FW} (m.a.s.l.)	Q_1 (m^3/s)	h_{1FW} (m.a.s.l.)	T_D (m^2/s)	h_i (m.a.s.l.)	Q-lower limit P (mL/h)	T_D-measl$_{LT}$ (m^2/s)	T_D-measl$_{LP}$ (m^2/s)	T_D-measl$_U$ (m^2/s)	Comments
KLX13A	214.43	219.43	5	5.33E–08	13.51	6.86E–07	3.54	6.3E–08	14.4	30	8.3E–10	8.3E–10	8.3E–06	
KLX13A	219.43	224.43	5	5.44E–08	13.52	7.25E–07	3.54	6.6E–08	14.3	30	8.3E–10	8.3E–10	8.3E–06	
KLX13A	224.43	229.43	5	2.60E–07	13.54	3.19E–06	3.55	2.9E–07	14.4	30	8.3E–10	8.3E–10	8.2E–06	
KLX13A	229.44	234.44	5	3.89E–09	13.54	6.33E–08	3.59	5.9E–09	14.2	30	8.3E–10	8.3E–10	8.3E–06	
KLX13A	234.45	239.45	5	–	13.54	–	3.60	–	–	30	8.3E–10	8.3E–10	8.3E–06	
KLX13A	239.45	244.45	5	–	13.56	6.72E–08	3.62	6.7E–09	–	30	8.3E–10	8.3E–10	8.3E–06	
KLX13A	244.45	249.45	5	–	13.58	–	3.63	–	–	30	8.3E–10	8.3E–10	8.3E–06	
KLX13A	249.45	254.45	5	–	13.59	9.94E–08	3.64	9.9E–09	–	30	8.3E–10	8.3E–10	8.3E–06	
KLX13A	254.45	259.45	5	–	13.61	1.10E–07	3.67	1.1E–08	–	30	8.3E–10	8.3E–10	8.3E–06	
KLX13A	259.45	264.45	5	–	13.62	–	3.67	–	–	30	8.3E–10	8.3E–10	8.3E–06	
KLX13A	264.44	269.44	5	–	13.63	8.94E–08	3.70	8.9E–09	–	30	8.3E–10	8.3E–10	8.3E–06	
KLX13A	269.44	274.44	5	–	13.63	–	3.72	–	–	30	8.3E–10	8.3E–10	8.3E–06	
KLX13A	274.44	279.44	5	–	13.65	2.69E–08	3.75	2.7E–09	–	30	8.3E–10	8.3E–10	8.3E–06	
KLX13A	279.43	284.43	5	–	13.67	–	3.76	–	–	30	8.3E–10	8.3E–10	8.3E–06	
KLX13A	284.43	289.43	5	–	13.69	1.58E–08	3.79	1.6E–09	–	30	8.3E–10	8.3E–10	8.3E–06	
KLX13A	289.43	294.43	5	–1.42E–08	13.70	6.44E–08	3.77	7.8E–09	11.9	30	8.3E–10	8.3E–10	8.3E–06	
KLX13A	294.42	299.42	5	–4.00E–08	13.72	2.25E–07	3.80	2.6E–08	12.2	30	8.3E–10	8.3E–10	8.3E–06	
KLX13A	299.43	304.43	5	–	13.77	–	3.84	–	–	30	8.3E–10	8.3E–10	8.3E–06	
KLX13A	304.48	309.48	5	–	13.81	–	3.85	–	–	30	8.3E–10	8.3E–10	8.3E–06	
KLX13A	309.48	314.48	5	–	13.82	–	3.86	–	–	30	8.3E–10	8.3E–10	8.3E–06	
KLX13A	314.48	319.48	5	–1.61E–06	13.82	5.69E–06	3.86	7.3E–07	11.6	30	8.3E–10	8.3E–10	8.4E–06	
KLX13A	319.50	324.50	5	–	13.84	–	3.90	–	–	30	8.3E–10	8.3E–10	8.3E–06	
KLX13A	324.51	329.51	5	–	13.85	–	3.90	–	–	30	8.3E–10	8.3E–10	8.3E–06	
KLX13A	329.52	334.52	5	–	13.85	8.33E–09	3.90	8.3E–10	–	30	8.3E–10	8.3E–10	8.3E–06	
KLX13A	334.53	339.53	5	–	13.87	–	3.91	–	–	30	8.3E–10	8.3E–10	8.3E–06	
KLX13A	339.54	344.54	5	–	13.87	–	3.90	–	–	30	8.3E–10	8.3E–10	8.3E–06	
KLX13A	344.54	349.54	5	–4.44E–07	13.88	2.86E–06	3.92	3.3E–07	12.5	30	8.3E–10	8.3E–10	8.3E–06	
KLX13A	349.55	354.55	5	–1.02E–07	13.89	5.17E–07	3.91	6.1E–08	12.3	30	8.3E–10	8.3E–10	8.3E–06	

Borehole ID	Secup L(m)	Seclow L(m)	L_w (m)	Q_0 (m^3/s)	h_{0FW} (m.a.s.l.)	Q_1 (m^3/s)	h_{1FW} (m.a.s.l.)	T_D (m^2/s)	h_i (m.a.s.l.)	Q-lower limit P (mL/h)	T_D-measl$_{LT}$ (m^2/s)	T_D-measl$_{LP}$ (m^2/s)	T_D-measl$_U$ (m^2/s)	Comments
KLX13A	354.54	359.54	5	–	13.91	–	3.93	–	–	30	8.3E–10	8.3E–10	8.3E–06	
KLX13A	359.55	364.55	5	–6.44E–07	13.87	4.50E–06	3.93	5.1E–07	12.6	30	8.3E–10	8.3E–10	8.4E–06	
KLX13A	364.53	369.53	5	–1.98E–07	13.91	1.01E–06	3.96	1.2E–07	12.3	30	8.3E–10	8.3E–10	8.3E–06	
KLX13A	369.54	374.54	5	–4.75E–07	13.96	2.70E–06	3.99	3.1E–07	12.5	30	8.3E–10	8.3E–10	8.3E–06	
KLX13A	374.55	379.55	5	–1.27E–07	13.97	6.64E–07	4.00	7.8E–08	12.4	30	8.3E–10	8.3E–10	8.3E–06	
KLX13A	379.54	384.54	5	–2.60E–07	14.05	1.44E–06	3.99	1.7E–07	12.5	30	8.2E–10	8.2E–10	8.2E–06	
KLX13A	384.54	389.54	5	–2.75E–05	14.01	4.61E–05	4.04	7.3E–06	10.3	30	8.3E–10	8.3E–10	1.1E–05	
KLX13A	389.54	394.54	5	–	14.01	2.50E–08	4.04	2.5E–09	–	30	8.3E–10	8.3E–10	8.3E–06	
KLX13A	394.54	399.54	5	–	14.05	–	4.06	–	–	30	8.3E–10	8.3E–10	8.3E–06	
KLX13A	399.53	404.53	5	–7.42E–07	14.10	3.64E–06	4.11	4.3E–07	12.4	30	8.3E–10	8.3E–10	8.3E–06	
KLX13A	404.53	409.53	5	–6.56E–07	14.10	3.92E–06	4.12	4.5E–07	12.7	30	8.3E–10	8.3E–10	8.3E–06	
KLX13A	409.53	414.53	5	–1.45E–07	14.13	8.06E–07	4.13	9.4E–08	12.6	30	8.2E–10	8.2E–10	8.3E–06	
KLX13A	414.52	419.52	5	–5.83E–07	14.14	4.08E–06	4.16	4.6E–07	12.9	30	8.3E–10	8.3E–10	8.3E–06	
KLX13A	419.52	424.52	5	–	14.16	7.67E–08	4.17	7.6E–09	–	30	8.3E–10	8.3E–10	8.3E–06	
KLX13A	424.51	429.51	5	–	14.18	8.78E–08	4.19	8.7E–09	–	30	8.3E–10	8.3E–10	8.3E–06	
KLX13A	429.51	434.51	5	–	14.21	–	4.21	–	–	30	8.2E–10	8.2E–10	8.2E–06	
KLX13A	434.52	439.52	5	–3.22E–08	14.23	3.19E–07	4.23	3.5E–08	13.3	30	8.2E–10	8.2E–10	8.2E–06	
KLX13A	439.51	444.51	5	–1.18E–07	14.24	7.39E–07	4.24	8.5E–08	12.9	30	8.2E–10	8.2E–10	8.3E–06	
KLX13A	444.51	449.51	5	–	14.26	–	4.27	–	–	30	8.3E–10	8.3E–10	8.3E–06	
KLX13A	449.51	454.51	5	–1.94E–06	14.29	1.73E–05	4.28	1.9E–06	13.3	30	8.2E–10	8.2E–10	8.4E–06	
KLX13A	454.51	459.51	5	–7.94E–07	14.30	7.25E–06	4.32	8.0E–07	13.3	30	8.3E–10	8.3E–10	8.3E–06	
KLX13A	459.51	464.51	5	–3.22E–07	14.33	2.20E–06	4.34	2.5E–07	13.1	30	8.3E–10	8.3E–10	8.3E–06	
KLX13A	464.51	469.51	5	–2.54E–07	14.33	1.84E–06	4.35	2.1E–07	13.1	30	8.3E–10	8.3E–10	8.3E–06	
KLX13A	469.51	474.51	5	–2.43E–07	14.35	1.51E–06	4.37	1.7E–07	13.0	30	8.3E–10	8.3E–10	8.3E–06	
KLX13A	474.50	479.50	5	–3.17E–07	14.38	2.10E–06	4.38	2.4E–07	13.1	30	8.2E–10	8.2E–10	8.3E–06	
KLX13A	479.51	484.51	5	–1.58E–07	14.38	7.03E–07	4.40	8.5E–08	12.6	30	8.3E–10	8.3E–10	8.3E–06	
KLX13A	484.51	489.51	5	–2.42E–07	14.40	1.31E–06	4.40	1.5E–07	12.8	30	8.2E–10	8.2E–10	8.3E–06	
KLX13A	489.51	494.51	5	–3.61E–08	14.41	3.00E–07	4.42	3.3E–08	13.3	30	8.3E–10	8.3E–10	8.3E–06	

Borehole ID	Secup L(m)	Seclow L(m)	L_w (m)	Q_0 (m^3/s)	h_{0FW} (m.a.s.l.)	Q_1 (m^3/s)	h_{1FW} (m.a.s.l.)	T_D (m^2/s)	h_i (m.a.s.l.)	Q-lower limit P (mL/h)	T_D-measl$_{LT}$ (m^2/s)	T_D-measl$_{LP}$ (m^2/s)	T_D-measl$_U$ (m^2/s)	Comments
KLX13A	494.51	499.51	5	–	14.42	8.94E–08	4.42	8.8E–09	–	30	8.2E–10	8.2E–10	8.2E–06	
KLX13A	499.52	504.52	5	–3.89E–07	14.43	4.81E–06	4.43	5.1E–07	13.7	30	8.2E–10	8.2E–10	8.3E–06	
KLX13A	504.52	509.52	5	–	14.44	–	4.44	–	–	30	8.2E–10	8.2E–10	8.2E–06	
KLX13A	509.52	514.52	5	–	14.47	–	4.42	–	–	30	8.2E–10	8.2E–10	8.2E–06	
KLX13A	514.53	519.53	5	–	14.47	1.81E–08	4.45	1.8E–09	–	30	8.2E–10	8.2E–10	8.2E–06	
KLX13A	519.54	524.54	5	–2.49E–07	14.46	1.49E–06	4.48	1.7E–07	13.0	30	8.3E–10	8.3E–10	8.3E–06	
KLX13A	524.54	529.54	5	–2.75E–08	14.48	1.73E–07	4.53	2.0E–08	13.1	30	8.3E–10	8.3E–10	8.3E–06	
KLX13A	529.54	534.54	5	–2.51E–07	14.49	1.32E–06	4.53	1.6E–07	12.9	30	8.3E–10	8.3E–10	8.3E–06	
KLX13A	534.55	539.55	5	–	14.52	4.44E–08	4.56	4.4E–09	–	30	8.3E–10	8.3E–10	8.3E–06	
KLX13A	539.55	544.55	5	–	14.55	7.83E–08	4.58	7.8E–09	–	30	8.3E–10	8.3E–10	8.3E–06	
KLX13A	544.56	549.56	5	–1.81E–07	14.56	9.53E–07	4.58	1.1E–07	13.0	30	8.3E–10	8.3E–10	8.3E–06	
KLX13A	549.55	554.55	5	–3.03E–07	14.57	1.36E–06	4.60	1.6E–07	12.8	30	8.3E–10	8.3E–10	8.3E–06	
KLX13A	554.56	559.56	5	–8.78E–08	14.60	7.14E–07	4.59	7.9E–08	13.5	30	8.2E–10	8.2E–10	8.2E–06	
KLX13A	559.56	564.56	5	–	14.62	–	4.62	–	–	30	8.2E–10	8.2E–10	8.2E–06	
KLX13A	564.57	569.57	5	–	14.64	–	4.66	–	–	30	8.3E–10	8.3E–10	8.3E–06	
KLX13A	569.57	574.57	5	–	14.66	–	4.70	–	–	30	8.3E–10	8.3E–10	8.3E–06	
KLX13A	574.58	579.58	5	–	14.70	1.19E–07	4.73	1.2E–08	–	30	8.3E–10	8.3E–10	8.3E–06	
KLX13A	579.58	584.58	5	–	14.69	8.44E–08	4.76	8.4E–09	–	30	8.3E–10	8.3E–10	8.3E–06	
KLX13A	584.58	589.58	5	–	14.64	–	4.76	–	–	30	8.3E–10	8.3E–10	8.3E–06	

Appendix 8

PFL-Difference flow logging – Inferred flow anomalies from overlapping flow logging

Borehole ID	Length to flow anom. L (m)	L_w (m)	d_L (m)	Q_0 (m^3/s)	h_{0FW} (m.a.s.l.)	Q_1 (m^3/s)	h_{1FW} (m.a.s.l.)	T_D (m^2/s)	h_i (m.a.s.l.)	Comments
KLX13A	102.2	1	0.1	–	13.40	5.14E–07	3.37	5.1E–08	–	
KLX13A	102.9	1	0.1	–	13.40	2.28E–08	3.35	2.2E–09	–	
KLX13A	104.1	1	0.1	–	13.40	1.11E–08	3.35	1.1E–09	–	*
KLX13A	104.7	1	0.1	–	13.41	3.17E–08	3.35	3.1E–09	–	*
KLX13A	105.0	1	0.1	–	13.41	1.63E–07	3.34	1.6E–08	–	
KLX13A	108.6	1	0.1	–	13.40	1.64E–08	3.31	1.6E–09	–	
KLX13A	111.9	1	0.1	–	13.38	1.51E–07	3.31	1.5E–08	–	
KLX13A	112.7	1	0.1	–	13.39	1.67E–08	3.31	1.6E–09	–	*
KLX13A	115.0	1	0.1	–	13.36	7.50E–09	3.31	7.4E–10	–	*
KLX13A	120.0	1	0.1	2.33E–07	13.40	4.61E–06	3.34	4.3E–07	13.9	
KLX13A	122.3	1	0.1	1.50E–06	13.43	1.98E–05	3.35	1.8E–06	14.3	
KLX13A	171.9	1	0.1	–	13.45	3.17E–08	3.43	3.1E–09	–	*
KLX13A	173.3	1	0.1	–	13.45	4.33E–08	3.42	4.3E–09	–	*
KLX13A	174.2	1	0.1	–	13.45	1.59E–07	3.43	1.6E–08	–	*
KLX13A	174.8	1	0.1	–	13.44	1.33E–07	3.42	1.3E–08	–	*
KLX13A	175.1	1	0.1	–	13.45	5.33E–07	3.43	5.3E–08	–	
KLX13A	191.8	1	0.1	–	13.53	5.28E–08	3.54	5.2E–09	–	
KLX13A	194.3	1	0.1	3.56E–08	13.51	5.78E–07	3.55	5.4E–08	14.2	
KLX13A	198.3	1	0.1	–	13.49	8.19E–08	3.54	8.2E–09	–	
KLX13A	210.6	1	0.1	–	13.50	1.42E–08	3.52	1.4E–09	–	
KLX13A	212.3	1	0.1	1.28E–08	13.50	2.97E–07	3.51	2.8E–08	14.0	
KLX13A	213.2	1	0.1	1.33E–08	13.51	1.86E–07	3.51	1.7E–08	14.3	
KLX13A	216.2	1	0.1	5.33E–08	13.50	6.33E–07	3.54	5.8E–08	14.4	
KLX13A	221.8	1	0.1	–	13.52	2.86E–07	3.54	2.8E–08	–	
KLX13A	222.3	1	0.1	–	13.53	4.94E–08	3.54	4.9E–09	–	*
KLX13A	223.5	1	0.1	–	13.52	4.36E–07	3.54	4.3E–08	–	
KLX13A	225.2	1	0.1	–	13.53	1.08E–06	3.55	1.1E–07	–	
KLX13A	225.7	1	0.1	–	13.53	2.46E–07	3.55	2.4E–08	–	*
KLX13A	227.3	1	0.1	–	13.54	3.89E–08	3.55	3.9E–09	–	*
KLX13A	228.2	1	0.1	1.17E–07	13.54	1.26E–06	3.55	1.1E–07	14.6	
KLX13A	232.8	1	0.1	3.89E–09	13.55	5.61E–08	3.57	5.2E–09	14.3	
KLX13A	240.7	1	0.1	–	13.57	3.50E–08	3.60	3.5E–09	–	
KLX13A	241.7	1	0.1	–	13.56	1.58E–08	3.59	1.6E–09	–	
KLX13A	251.5	1	0.1	–	13.59	1.89E–08	3.61	1.9E–09	–	*
KLX13A	252.0	1	0.1	–	13.59	6.83E–08	3.59	6.8E–09	–	
KLX13A	255.0	1	0.1	–	13.61	9.97E–08	3.63	9.9E–09	–	
KLX13A	267.5	1	0.1	–	13.63	8.33E–08	3.69	8.3E–09	–	
KLX13A	279.3	1	0.1	–	13.66	1.92E–08	3.74	1.9E–09	–	
KLX13A	287.2	1	0.1	–	13.69	7.22E–09	3.79	7.2E–10	–	*
KLX13A	291.4	1	0.1	–1.42E–08	13.71	3.92E–08	3.77	5.3E–09	11.1	
KLX13A	297.1	1	0.1	–2.94E–08	13.72	8.72E–08	3.80	1.2E–08	11.2	
KLX13A	298.5	1	0.1	–3.50E–08	13.72	5.42E–08	3.81	8.9E–09	9.8	
KLX13A	315.9	1	0.1	–1.61E–06	13.83	3.53E–06	3.86	5.1E–07	10.7	

Borehole ID	Length to flow anom. L (m)	L_w (m)	d_L (m)	Q_0 (m^3/s)	h_{0FW} (m.a.s.l.)	Q_1 (m^3/s)	h_{1FW} (m.a.s.l.)	T_D (m^2/s)	h_i (m.a.s.l.)	Comments
KLX13A	331.0	1	0.1	–	13.85	3.33E–09	3.89	3.3E–10	–	
KLX13A	349.0	1	0.1	–	13.88	1.49E–06	3.93	1.5E–07	–	
KLX13A	350.8	1	0.1	–	13.88	3.17E–07	3.93	3.2E–08	–	*
KLX13A	351.4	1	0.1	–	13.89	2.81E–07	3.93	2.8E–08	–	
KLX13A	353.8	1	0.1	–	13.89	6.39E–09	3.94	6.4E–10	–	*
KLX13A	362.0	1	0.1	–	13.88	2.46E–06	3.95	2.5E–07	–	
KLX13A	363.2	1	0.1	–	13.86	1.24E–07	3.95	1.2E–08	–	
KLX13A	364.8	1	0.1	–	13.88	3.69E–07	3.96	3.7E–08	–	
KLX13A	366.5	1	0.1	–	13.91	1.25E–07	3.96	1.2E–08	–	
KLX13A	367.0	1	0.1	–	13.91	2.50E–08	3.95	2.5E–09	–	
KLX13A	371.3	1	0.1	–	13.96	2.17E–08	3.98	2.2E–09	–	*
KLX13A	372.0	1	0.1	–	13.97	2.61E–08	3.98	2.6E–09	–	
KLX13A	373.3	1	0.1	–	13.98	5.42E–08	3.99	5.4E–09	–	
KLX13A	374.4	1	0.1	–	13.91	1.76E–06	3.99	1.8E–07	–	
KLX13A	374.8	1	0.1	–	13.91	3.83E–08	3.99	3.8E–09	–	*
KLX13A	376.3	1	0.1	–	13.98	2.57E–07	3.99	2.5E–08	–	
KLX13A	377.7	1	0.1	–	13.97	5.33E–08	4.00	5.3E–09	–	
KLX13A	379.7	1	0.1	–	13.99	5.92E–07	4.00	5.9E–08	–	
KLX13A	380.2	1	0.1	–	13.99	1.67E–07	4.00	1.7E–08	–	
KLX13A	380.7	1	0.1	–	13.99	9.44E–08	4.00	9.4E–09	–	
KLX13A	382.1	1	0.1	–	14.06	2.94E–08	4.00	2.9E–09	–	
KLX13A	383.1	1	0.1	–	14.07	7.61E–08	4.00	7.5E–09	–	
KLX13A	384.7	1	0.1	–	14.01	7.78E–08	3.99	7.7E–09	–	*
KLX13A	385.1	1	0.1	–	13.98	1.96E–05	4.01	2.0E–06	–	
KLX13A	385.6	1	0.1	–	14.01	9.61E–06	4.03	9.5E–07	–	
KLX13A	386.6	1	0.1	–	14.01	5.81E–08	4.03	5.8E–09	–	*
KLX13A	387.5	1	0.1	–	14.01	1.08E–05	4.04	1.1E–06	–	
KLX13A	387.9	1	0.1	–	14.02	2.78E–07	4.03	2.8E–08	–	
KLX13A	389.2	1	0.1	–	14.01	1.87E–07	4.04	1.9E–08	–	
KLX13A	392.5	1	0.1	–	14.02	1.00E–08	4.04	9.9E–10	–	*
KLX13A	399.8	1	0.1	–	14.07	4.06E–07	4.08	4.0E–08	–	
KLX13A	401.0	1	0.1	–	14.10	2.59E–06	4.10	2.6E–07	–	
KLX13A	403.4	1	0.1	–	14.11	2.56E–08	4.10	2.5E–09	–	
KLX13A	407.8	1	0.1	–6.56E–07	14.12	2.94E–06	4.12	3.6E–07	12.3	
KLX13A	412.5	1	0.1	–1.53E–07	14.13	5.92E–07	4.13	7.4E–08	12.1	
KLX13A	415.7	1	0.1	–5.83E–07	14.15	3.00E–06	4.15	3.5E–07	12.5	
KLX13A	418.5	1	0.1	–	14.17	2.25E–08	4.15	2.2E–09	–	
KLX13A	419.2	1	0.1	–	14.16	2.56E–08	4.16	2.5E–09	–	
KLX13A	424.4	1	0.1	–	14.17	1.78E–08	4.19	1.8E–09	–	*
KLX13A	424.9	1	0.1	–	14.18	2.11E–08	4.19	2.1E–09	–	
KLX13A	429.4	1	0.1	–	14.20	3.89E–08	4.21	3.9E–09	–	
KLX13A	435.4	1	0.1	–	14.24	2.68E–07	4.23	2.7E–08	–	
KLX13A	441.1	1	0.1	–	14.24	4.86E–08	4.24	4.8E–09	–	
KLX13A	443.3	1	0.1	–1.20E–07	14.26	6.08E–07	4.26	7.2E–08	12.6	
KLX13A	450.8	1	0.1	–	14.28	1.26E–05	4.28	1.3E–06	–	
KLX13A	451.3	1	0.1	–	14.28	3.81E–07	4.29	3.8E–08	–	
KLX13A	454.9	1	0.1	–	14.31	2.94E–08	4.31	2.9E–09	–	
KLX13A	456.7	1	0.1	–	14.31	5.42E–06	4.32	5.4E–07	–	

Borehole ID	Length to flow anom. L (m)	L_w (m)	d_L (m)	Q_0 (m^3/s)	h_{0FW} (m.a.s.l.)	Q_1 (m^3/s)	h_{1FW} (m.a.s.l.)	T_D (m^2/s)	h_i (m.a.s.l.)	Comments
KLX13A	458.5	1	0.1	–	14.32	2.23E–07	4.31	2.2E–08	–	
KLX13A	461.8	1	0.1	–	14.33	6.56E–07	4.35	6.5E–08	–	
KLX13A	462.8	1	0.1	–	14.34	9.92E–07	4.34	9.8E–08	–	
KLX13A	463.9	1	0.1	–	14.33	5.72E–08	4.34	5.7E–09	–	
KLX13A	465.3	1	0.1	–	14.34	2.04E–07	4.35	2.0E–08	–	
KLX13A	465.9	1	0.1	–	14.34	2.42E–07	4.34	2.4E–08	–	*
KLX13A	466.3	1	0.1	–	14.34	9.08E–07	4.35	9.0E–08	–	
KLX13A	466.9	1	0.1	–	14.34	2.22E–08	4.36	2.2E–09	–	*
KLX13A	467.4	1	0.1	–	14.34	2.25E–08	4.36	2.2E–09	–	
KLX13A	470.7	1	0.1	–	14.36	4.56E–07	4.36	4.5E–08	–	
KLX13A	471.1	1	0.1	–	14.36	7.00E–07	4.38	6.9E–08	–	
KLX13A	471.4	1	0.1	–	14.36	6.39E–08	4.37	6.3E–09	–	*
KLX13A	473.2	1	0.1	–	14.36	2.17E–08	4.39	2.2E–09	–	
KLX13A	474.8	1	0.1	–	14.37	1.74E–07	4.39	1.7E–08	–	
KLX13A	476.0	1	0.1	–	14.37	1.29E–07	4.40	1.3E–08	–	*
KLX13A	476.6	1	0.1	–	14.36	2.72E–07	4.39	2.7E–08	–	
KLX13A	477.6	1	0.1	–	14.38	3.33E–07	4.39	3.3E–08	–	*
KLX13A	478.1	1	0.1	–	14.37	2.86E–07	4.40	2.8E–08	–	*
KLX13A	478.8	1	0.1	–	14.38	2.44E–07	4.41	2.4E–08	–	*
KLX13A	479.1	1	0.1	–	14.37	4.17E–07	4.40	4.1E–08	–	
KLX13A	480.8	1	0.1	–	14.39	5.36E–07	4.41	5.3E–08	–	
KLX13A	482.1	1	0.1	–	14.38	1.16E–07	4.41	1.2E–08	–	
KLX13A	484.8	1	0.1	–	14.40	3.89E–08	4.42	3.9E–09	–	*
KLX13A	486.1	1	0.1	–	14.39	4.39E–07	4.42	4.4E–08	–	
KLX13A	487.5	1	0.1	–	14.42	6.67E–07	4.42	6.6E–08	–	
KLX13A	488.3	1	0.1	–	14.40	8.64E–08	4.42	8.6E–09	–	
KLX13A	490.9	1	0.1	–	14.40	7.22E–09	4.43	7.2E–10	–	*
KLX13A	492.5	1	0.1	–	14.41	2.35E–07	4.41	2.3E–08	–	
KLX13A	494.0	1	0.1	–	14.40	3.14E–07	4.39	3.1E–08	–	*
KLX13A	495.3	1	0.1	–	14.43	1.47E–08	4.43	1.5E–09	–	*
KLX13A	496.8	1	0.1	–	14.43	6.36E–08	4.43	6.3E–09	–	
KLX13A	501.7	1	0.1	–	14.43	6.39E–09	4.44	6.3E–10	–	*
KLX13A	502.2	1	0.1	–	14.44	4.78E–08	4.45	4.7E–09	–	
KLX13A	503.2	1	0.1	–	14.43	2.66E–06	4.45	2.6E–07	–	
KLX13A	503.4	1	0.1	–	14.43	3.78E–07	4.46	3.8E–08	–	*
KLX13A	504.1	1	0.1	–	14.44	1.06E–07	4.46	1.1E–08	–	
KLX13A	516.9	1	0.1	–	14.47	1.08E–08	4.48	1.1E–09	–	
KLX13A	522.6	1	0.1	–	14.49	4.50E–08	4.47	4.4E–09	–	
KLX13A	523.1	1	0.1	–	14.48	5.31E–07	4.47	5.2E–08	–	
KLX13A	524.2	1	0.1	–	14.46	4.78E–07	4.50	4.7E–08	–	
KLX13A	528.6	1	0.1	–	14.50	1.39E–07	4.52	1.4E–08	–	
KLX13A	530.4	1	0.1	–	14.50	4.36E–07	4.53	4.3E–08	–	
KLX13A	531.6	1	0.1	–	14.49	3.89E–07	4.54	3.9E–08	–	
KLX13A	532.0	1	0.1	–	14.50	1.02E–07	4.55	1.0E–08	–	
KLX13A	533.4	1	0.1	–	14.49	3.31E–08	4.56	3.3E–09	–	*
KLX13A	534.2	1	0.1	–	14.50	2.31E–07	4.57	2.3E–08	–	
KLX13A	537.9	1	0.1	–	14.51	1.83E–08	4.58	1.8E–09	–	*

Borehole ID	Length to flow anom. L (m)	L_w (m)	d_L (m)	Q_0 (m^3/s)	h_{0FW} (m.a.s.l.)	Q_1 (m^3/s)	h_{1FW} (m.a.s.l.)	T_D (m^2/s)	h_i (m.a.s.l.)	Comments
KLX13A	541.1	1	0.1	–	14.55	2.14E–08	4.62	2.1E–09	–	
KLX13A	544.3	1	0.1	–	14.56	2.44E–08	4.64	2.4E–09	–	*
KLX13A	545.0	1	0.1	–	14.56	4.81E–07	4.64	4.8E–08	–	
KLX13A	547.7	1	0.1	–	14.58	3.39E–07	4.66	3.4E–08	–	
KLX13A	548.3	1	0.1	–	14.58	1.33E–08	4.67	1.3E–09	–	
KLX13A	550.2	1	0.1	–	14.58	5.83E–09	4.68	5.8E–10	–	*
KLX13A	550.8	1	0.1	–	14.58	1.72E–08	4.68	1.7E–09	–	*
KLX13A	551.7	1	0.1	–	14.59	1.06E–07	4.69	1.1E–08	–	
KLX13A	552.6	1	0.1	–	14.56	5.17E–07	4.69	5.2E–08	–	
KLX13A	553.8	1	0.1	–	14.60	4.11E–07	4.69	4.1E–08	–	*
KLX13A	554.7	1	0.1	–	14.59	1.56E–07	4.67	1.6E–08	–	
KLX13A	556.5	1	0.1	–5.94E–08	14.60	4.22E–07	4.66	4.8E–08	13.4	
KLX13A	577.6	1	0.1	–	14.69	2.67E–08	4.73	2.7E–09	–	*
KLX13A	579.5	1	0.1	–	14.69	5.22E–08	4.77	5.2E–09	–	
KLX13A	581.8	1	0.1	–	14.69	8.33E–09	4.79	8.3E–10	–	*
KLX13A	582.6	1	0.1	–	14.69	3.17E–08	4.80	3.2E–09	–	*
KLX13A	582.9	1	0.1	–	14.68	4.11E–08	4.80	4.1E–09	–	*

* Uncertain = The flow rate is less than 30 mL/h or the flow anomalies are overlapping or they are unclear because of noise.

Appendix 9

Explanations

Header	Unit	Explanations
Borehole		ID for borehole.
Secup	m	Length along the borehole for the upper limit of the test section (based on corrected length L).
Seclow	m	Length along the borehole for the lower limit of the test section (based on corrected length L).
L	m	Corrected length along borehole based on SKB procedures for length correction.
Length to flow anom.	m	Length along the borehole to inferred flow anomaly during overlapping flow logging.
Test type (1–6)	(–)	1A: Pumping test – wire-line eq., 1B: Pumping test-submersible pump, 1C: Pumping test-airlift pumping, 2: Interference test, 3: Injection test, 4: Slug test, 5A: Difference flow logging – PFL-DIFF-Sequential, 5B: Difference flow logging – PFL-DIFF-Overlapping, 6: Flow logging-Impeller.
Date of test, start	YY-MM-DD	Date for start of pumping.
Time of test, start	hh:mm	Time for start of pumping.
Date of flowl., start	YY-MM-DD	Date for start of the flow logging.
Time of flowl., start	hh:mm	Time for start of the flow logging.
Date of test, stop	YY-MM-DD	Date for stop of the test.
Time of test, stop	hh:mm	Time for stop of the test.
L_w	m	Section length used in the difference flow logging.
d_L	m	Step length (increment) used in the difference flow logging.
Q_{p1}	m^3/s	Flow rate at surface by the end of the first pumping period of the flow logging.
Q_{p2}	m^3/s	Flow rate at surface by the end of the second pumping period of the flow logging.
t_p1	s	Duration of the first pumping period.
t_{p2}	s	Duration of the second pumping period.
t_{F1}	s	Duration of the first recovery period.
t_{F2}	s	Duration of the second recovery period.
h_0	m.a.s.l.	Initial hydraulic head before pumping. Elevation of water level in open borehole in the local co-ordinates system with z=0 m.
h_1	m.a.s.l.	Stabilized hydraulic head during the first pumping period. Elevation of water level in open borehole in the local co-ordinates system with z=0 m.
h_2	m.a.s.l.	Stabilized hydraulic head during the second pumping period. Elevation of water level in open borehole in the local co-ordinates system with z=0 m.

Header	Unit	Explanations
s_1	m	Drawdown of the water level in the borehole during first pumping period. Difference between the actual hydraulic head and the initial head ($s_1 = h_1 - h_0$)
s_2	m	Drawdown of the water level in the borehole during second pumping period. Difference between the actual hydraulic head and the initial head ($s_2 = h_2 - h_0$)
T	m^2/s	Transmissivity of the entire borehole
Q_0	m^3/s	Measured flow rate through the test section or flow anomaly under natural conditions (no pumping) with $h=h_0$ in the open borehole
Q_1	m^3/s	Measured flow rate through the test section or flow anomaly during the first pumping period
Q_2	m^3/s	Measured flow rate through the test section or flow anomaly during the second pumping period
h_{0FW}	m.a.s.l.	Corrected initial hydraulic head along the hole due to e.g. varying salinity conditions of the borehole fluid before pumping
h_{1FW}	m.a.s.l.	Corrected hydraulic head along the hole due to e.g. varying salinity conditions of the borehole fluid during the first pumping period
h_{2FW}	m.a.s.l.	Corrected hydraulic head along the hole due to e.g. varying salinity conditions of the borehole fluid during the second pumping period
EC_w	S/m	Measured electric conductivity of the borehole fluid in the test section during difference flow logging
Te_w	ºC	Measured borehole fluid temperature in the test section during difference flow logging
EC_f	S/m	Measured fracture-specific electric conductivity of the fluid in flow anomaly during difference flow logging
Te_f	ºC	Measured fracture-specific fluid temperature in flow anomaly during difference flow logging
T_D	m^2/s	Transmissivity of section or flow anomaly based on 2D model for evaluation of formation properties of the test section based on PFL-DIFF.
T-$measl_{LT}$	m^2/s	Estimated theoretical lower measurement limit for evaluated T_D. If the estimated T_D equals T_D-measlim, the actual T_D is considered to be equal or less than T_D-measlim.
T-$measl_{LP}$	m^2/s	Estimated practical lower measurement limit for evaluated T_D. If the estimated T_D equals T_D-measlim, the actual T_D is considered to be equal or less than T_D-measlim.
T-$measl_U$	m^2/s	Estimated upper measurement limit for evaluated T_D. If the estimated T_D equals T_D-measlim, the actual T_D is considered to be equal or less than T_D-measlim.
h_i	m.a.s.l.	Calculated relative, natural freshwater head for test section or flow anomaly (undisturbed conditions)

Appendix 10

Calculation of conductive fracture frequency

Borehole ID	SecUp (m)	SecLow (m)	Number of fractures, Total	Number of fractures 10–100 (ml/h)	Number of fractures 100–1,000 (ml/h)	Number of fractures 1,000–10,000 (ml/h)	Number of fractures 10,000–100,000 (ml/h)	Number of fractures 100,000–1,000,000 (ml/h)
KLX13A	94.33	99.33	0	0	0	0	0	0
KLX13A	99.34	104.34	3	2	0	1	0	0
KLX13A	104.34	109.34	3	1	2	0	0	0
KLX13A	109.35	114.35	2	1	1	0	0	0
KLX13A	114.36	119.36	1	1	0	0	0	0
KLX13A	119.36	124.36	2	0	0	0	2	0
KLX13A	124.36	129.36	0	0	0	0	0	0
KLX13A	129.36	134.36	0	0	0	0	0	0
KLX13A	134.36	139.36	0	0	0	0	0	0
KLX13A	139.36	144.36	0	0	0	0	0	0
KLX13A	144.37	149.37	0	0	0	0	0	0
KLX13A	149.37	154.37	0	0	0	0	0	0
KLX13A	154.37	159.37	0	0	0	0	0	0
KLX13A	159.38	164.38	0	0	0	0	0	0
KLX13A	164.38	169.38	0	0	0	0	0	0
KLX13A	169.38	174.38	3	0	3	0	0	0
KLX13A	174.39	179.39	2	0	1	1	0	0
KLX13A	179.39	184.39	0	0	0	0	0	0
KLX13A	184.37	189.37	0	0	0	0	0	0
KLX13A	189.40	194.40	2	0	1	1	0	0
KLX13A	194.43	199.43	1	0	1	0	0	0
KLX13A	199.41	204.41	0	0	0	0	0	0
KLX13A	204.41	209.41	0	0	0	0	0	0
KLX13A	209.43	214.43	3	1	1	1	0	0
KLX13A	214.43	219.43	1	0	0	1	0	0
KLX13A	219.43	224.43	3	0	1	2	0	0
KLX13A	224.43	229.43	4	0	2	2	0	0
KLX13A	229.44	234.44	1	0	1	0	0	0
KLX13A	234.45	239.45	0	0	0	0	0	0
KLX13A	239.45	244.45	2	1	1	0	0	0
KLX13A	244.45	249.45	0	0	0	0	0	0
KLX13A	249.45	254.45	2	1	1	0	0	0
KLX13A	254.45	259.45	1	0	1	0	0	0
KLX13A	259.45	264.45	0	0	0	0	0	0
KLX13A	264.44	269.44	1	0	1	0	0	0
KLX13A	269.44	274.44	0	0	0	0	0	0
KLX13A	274.44	279.44	1	1	0	0	0	0
KLX13A	279.43	284.43	0	0	0	0	0	0
KLX13A	284.43	289.43	1	1	0	0	0	0
KLX13A	289.43	294.43	1	0	1	0	0	0
KLX13A	294.42	299.42	2	0	2	0	0	0
KLX13A	299.43	304.43	0	0	0	0	0	0

Borehole ID	SecUp (m)	SecLow (m)	Number of fractures, Total	Number of fractures 10–100 (ml/h)	Number of fractures 100–1,000 (ml/h)	Number of fractures 1,000–10,000 (ml/h)	Number of fractures 10,000–100,000 (ml/h)	Number of fractures 100,000–1,000,000 (ml/h)
KLX13A	304.48	309.48	0	0	0	0	0	0
KLX13A	309.48	314.48	0	0	0	0	0	0
KLX13A	314.48	319.48	1	0	0	0	1	0
KLX13A	319.50	324.50	0	0	0	0	0	0
KLX13A	324.51	329.51	0	0	0	0	0	0
KLX13A	329.52	334.52	1	1	0	0	0	0
KLX13A	334.53	339.53	0	0	0	0	0	0
KLX13A	339.54	344.54	0	0	0	0	0	0
KLX13A	344.54	349.54	1	0	0	1	0	0
KLX13A	349.55	354.55	3	1	0	2	0	0
KLX13A	354.54	359.54	0	0	0	0	0	0
KLX13A	359.55	364.55	2	0	1	1	0	0
KLX13A	364.53	369.53	3	1	1	1	0	0
KLX13A	369.54	374.54	4	2	1	1	0	0
KLX13A	374.55	379.55	3	0	3	0	0	0
KLX13A	379.54	384.54	5	0	4	1	0	0
KLX13A	384.54	389.54	7	0	4	0	3	0
KLX13A	389.54	394.54	1	1	0	0	0	0
KLX13A	394.54	399.54	0	0	0	0	0	0
KLX13A	399.53	404.53	3	1	0	2	0	0
KLX13A	404.53	409.53	1	0	0	0	1	0
KLX13A	409.53	414.53	1	0	0	1	0	0
KLX13A	414.52	419.52	3	2	0	0	1	0
KLX13A	419.52	424.52	1	1	0	0	0	0
KLX13A	424.51	429.51	2	1	1	0	0	0
KLX13A	429.51	434.51	0	0	0	0	0	0
KLX13A	434.52	439.52	1	0	1	0	0	0
KLX13A	439.51	444.51	2	0	1	1	0	0
KLX13A	444.51	449.51	0	0	0	0	0	0
KLX13A	449.51	454.51	2	0	0	1	1	0
KLX13A	454.51	459.51	3	0	2	0	1	0
KLX13A	459.51	464.51	3	0	1	2	0	0
KLX13A	464.51	469.51	5	2	2	1	0	0
KLX13A	469.51	474.51	4	1	1	2	0	0
KLX13A	474.50	479.50	7	0	4	3	0	0
KLX13A	479.51	484.51	2	0	1	1	0	0
KLX13A	484.51	489.51	4	0	2	2	0	0
KLX13A	489.51	494.51	3	1	1	1	0	0
KLX13A	494.51	499.51	2	1	1	0	0	0
KLX13A	499.52	504.52	5	1	2	2	0	0
KLX13A	504.52	509.52	0	0	0	0	0	0
KLX13A	509.52	514.52	0	0	0	0	0	0
KLX13A	514.53	519.53	1	1	0	0	0	0
KLX13A	519.54	524.54	3	0	1	2	0	0
KLX13A	524.54	529.54	1	0	1	0	0	0
KLX13A	529.54	534.54	5	0	3	2	0	0
KLX13A	534.55	539.55	1	1	0	0	0	0

Borehole ID	SecUp (m)	SecLow (m)	Number of fractures, Total	Number of fractures 10–100 (ml/h)	Number of fractures 100–1,000 (ml/h)	Number of fractures 1,000–10,000 (ml/h)	Number of fractures 10,000–100,000 (ml/h)	Number of fractures 100,000–1,000,000 (ml/h)
KLX13A	539.55	544.55	2	2	0	0	0	0
KLX13A	544.56	549.56	3	1	0	2	0	0
KLX13A	549.55	554.55	5	2	1	2	0	0
KLX13A	554.56	559.56	2	0	1	1	0	0
KLX13A	559.56	564.56	0	0	0	0	0	0
KLX13A	564.57	569.57	0	0	0	0	0	0
KLX13A	569.57	574.57	0	0	0	0	0	0
KLX13A	574.58	579.58	2	1	1	0	0	0
KLX13A	579.58	584.58	3	1	2	0	0	0
KLX13A	584.58	589.58	0	0	0	0	0	0

Appendix 11

Laxemar, borehole KLX13A
Calculation of conductive fracture frequency

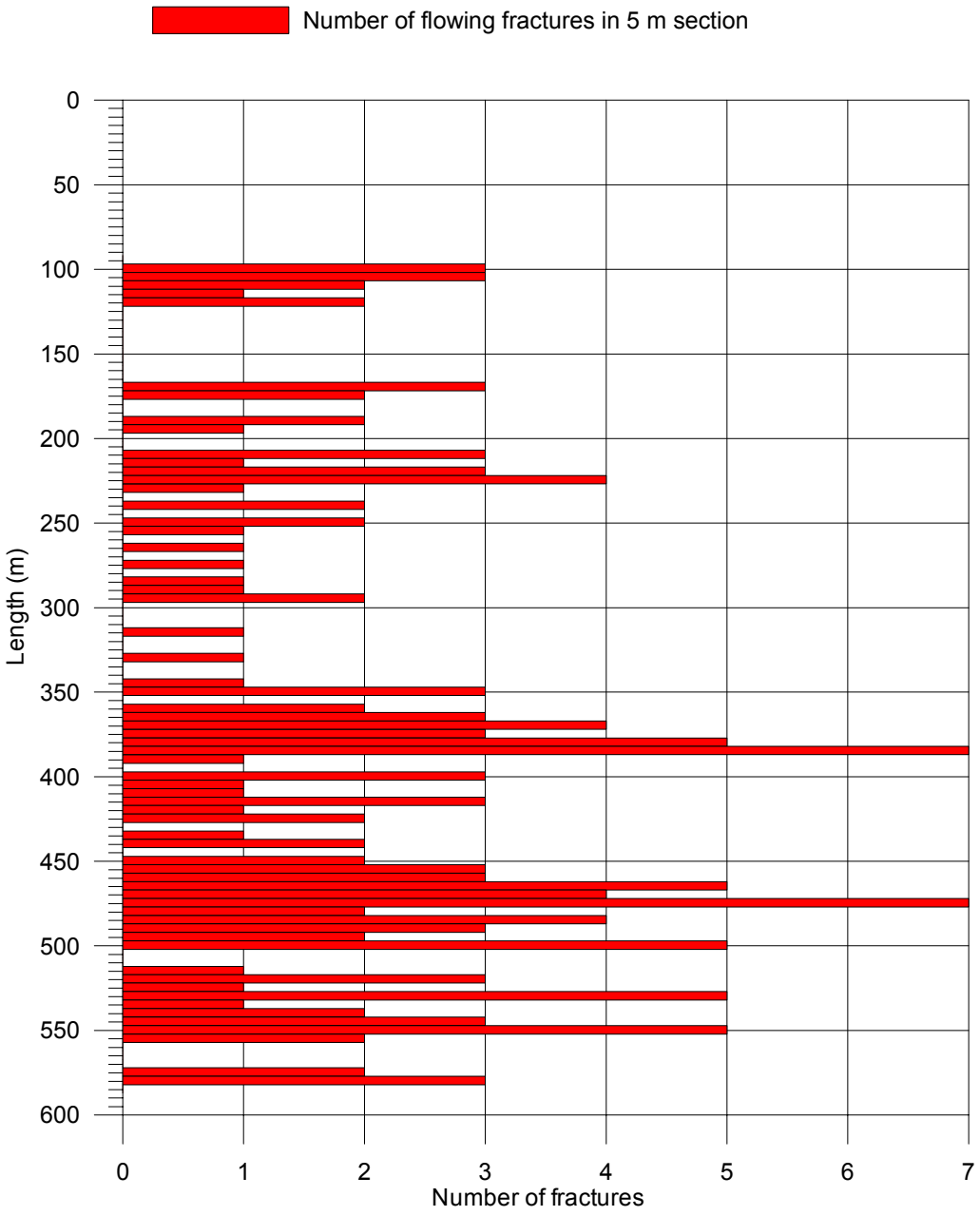

Appendix 12

Laxemar, borehole KLX13A
Comparison between section transmissivity and fracture transmissivity

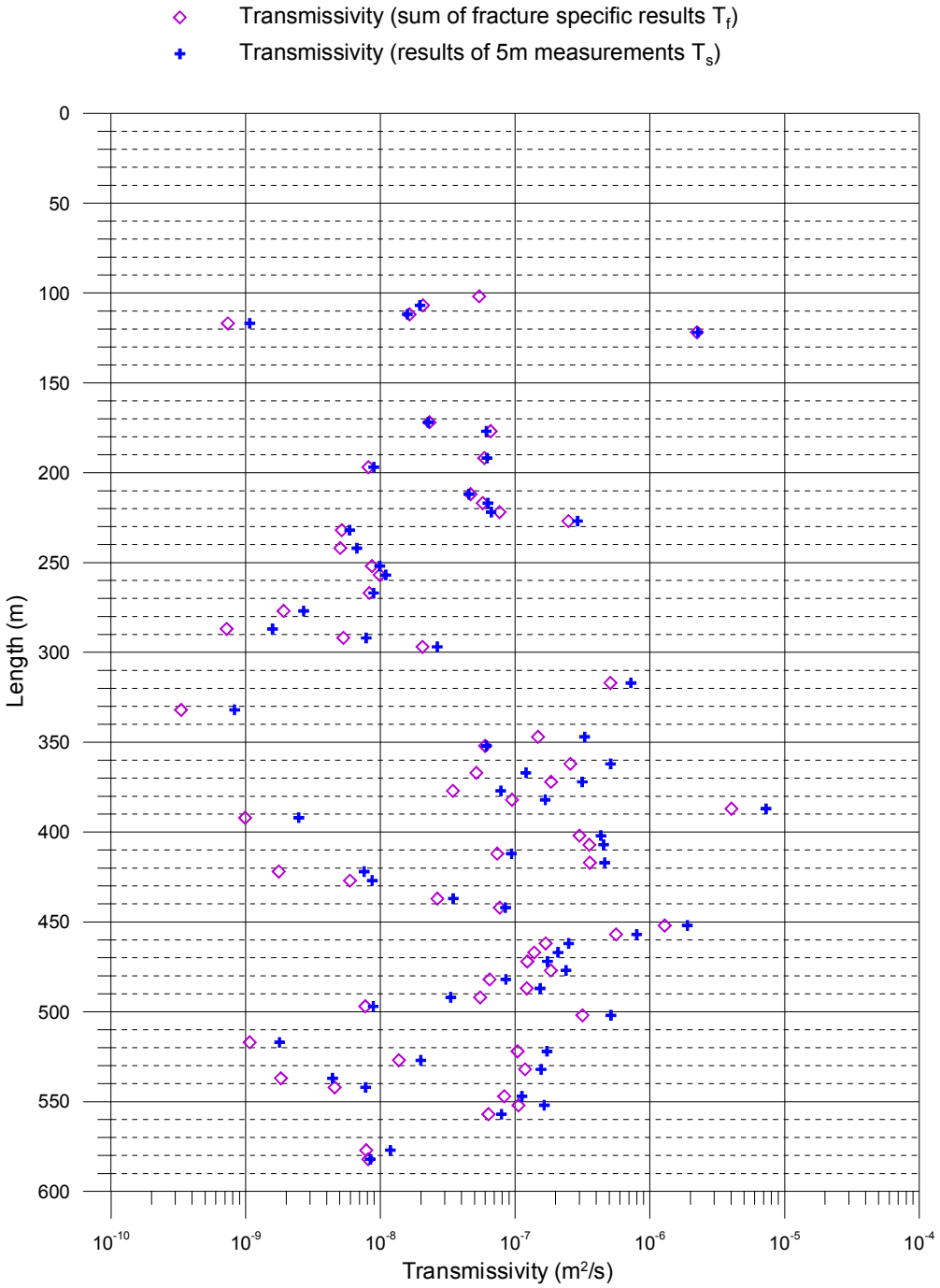

Appendix 13.1

Laxemar, borehole KLX13A
Head in the borehole during flow logging

Head(masl)= (Absolute pressure (Pa) - Airpressure (Pa) + Offset) /(1000 kg/m^3 * 9.80665 m/s^2) + Elevation (m)
Offset = 2300 Pa (Correction for absolut pressure sensor)

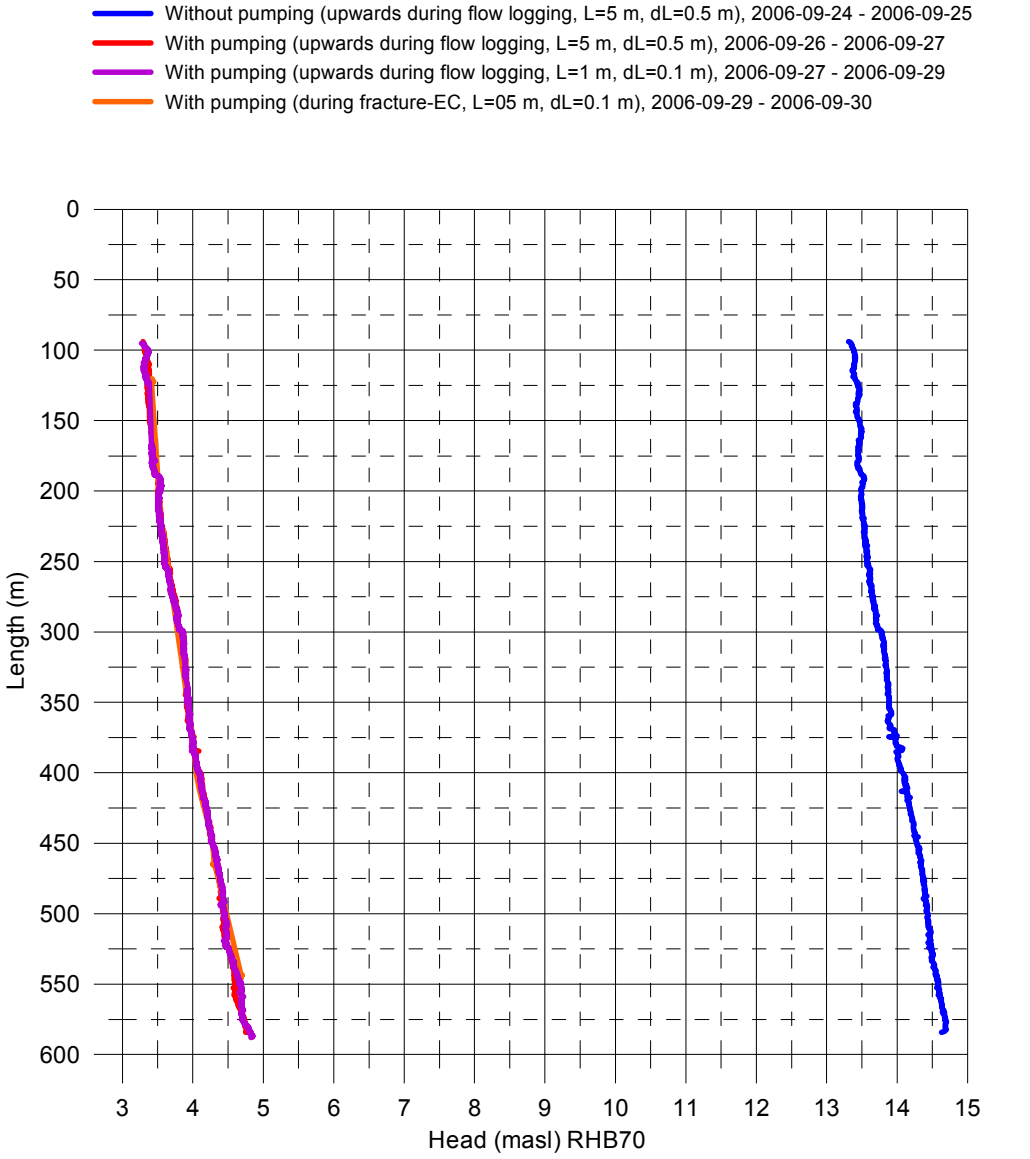

Appendix 13.2

Laxemar, borehole KLX13A
Air pressure, water level in the borehole and pumping rate during flow logging

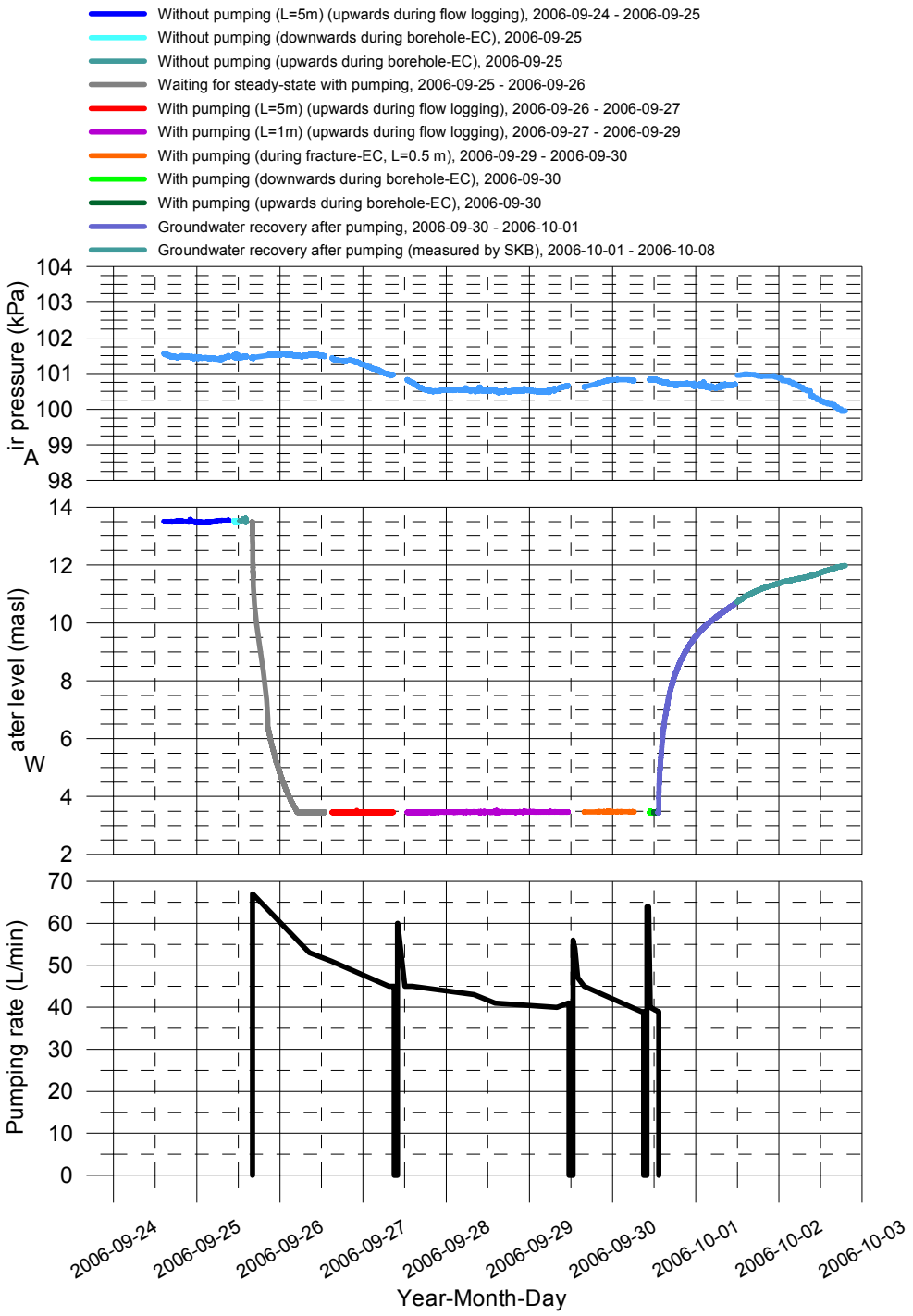

Appendix 13.3

Laxemar, borehole KLX13A
Groundwater recovery after pumping

Head(masl)= (Absolute pressure (Pa) - Airpressure (Pa) + Offset) /(1000 kg/m^3 * 9.80665 m/s^2) + Elevation (m)
Offset = 2300 Pa (Correction for absolut pressure sensor)

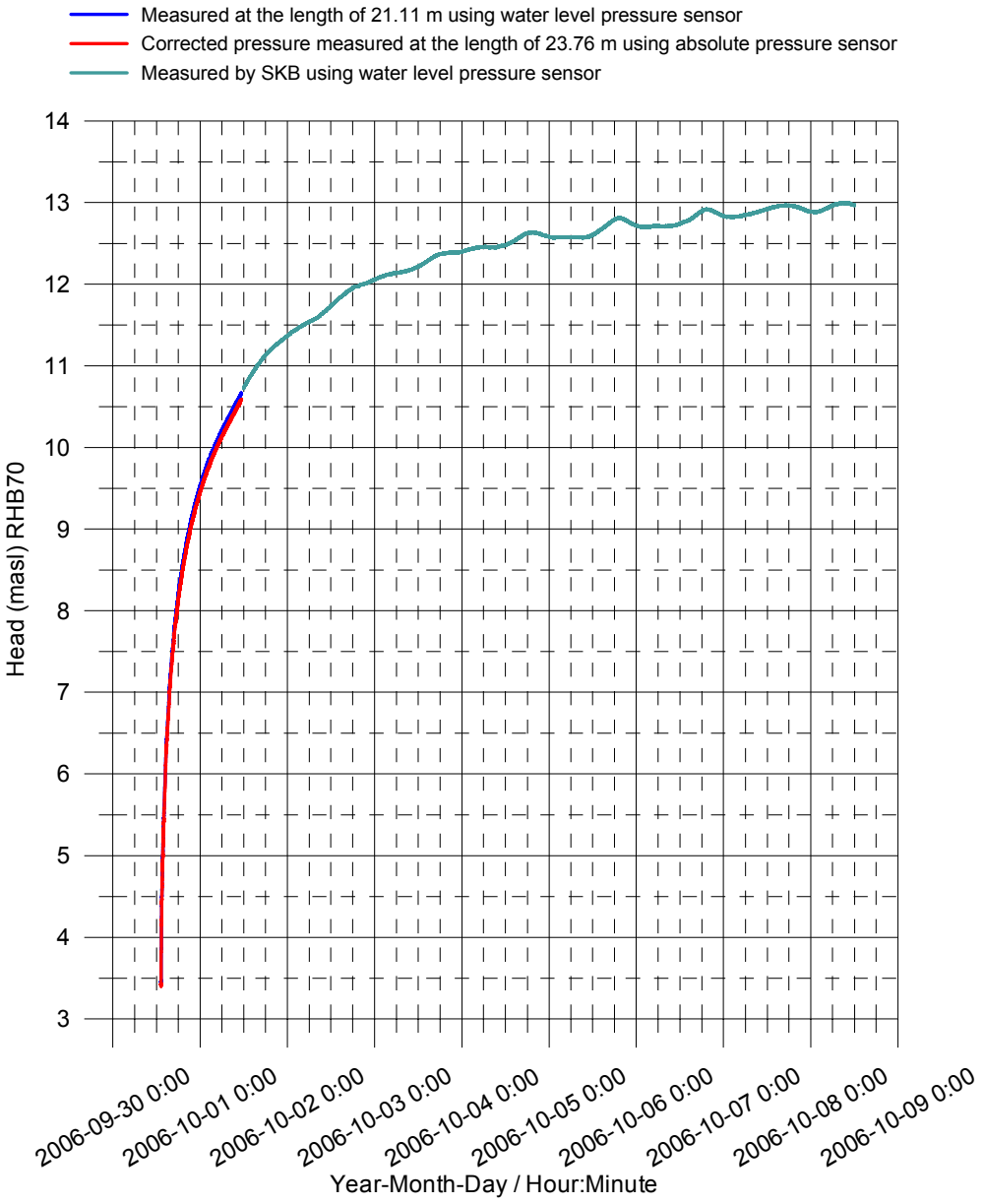

Appendix 14

Laxemar, borehole KLX13A
Fracture-specific EC results by date